Development of a Wound Dressing for Detection of Bacteria with Wound Healing Properties

Hong, Sung-Ha

Award date:
2013

Awarding institution:
University of Bath

UNIVERSITY OF BATH

Development of a wound dressing for detection of bacteria with wound healing properties

Ph.D. Thesis

Volume 1

Sung Ha Hong

Thesis for the degree of Doctor of Philosophy
University of Bath
Department of Chemistry

December 2013

To my parents

Table of Contents

Acknowledgments XIII

Abstract XV

List of Figures XVI

List of Tables XXV

Acronyms and abbreviations XXVII

1. Chapter One: Introduction 1

1.1. The clinical problem 1

1.1.1. Skin injury 2

1.1.2. Burns 2

1.1.3. Classification of burn injury 4

1.1.4. Treatment of burns 5

1.1.5. Burn infection 6

1.1.6. Toxic Shock Syndrome 6

1.1.7. Clinical diagnosis of infection 7

1.1.8. Pathogenic identification method 9

1.1. Wound dressings 10

1.1.1. Commercially available dressings 11

1.1.2. Requirements for an 'ideal' wound dressing 13

1.2. Microbiology 15

1.2.1. Bacteria 15

1.2.2. Quorum sensing 16

1.2.3. Biofilms 16

1.2.4. Commonly isolated bacterial strains 17

1.2.5. Bacterial virulence factors 21

1.3. Lipid vesicles 27
5. c Chapter 6: Prototype development 27
5.1. Introduction to prototype development 27
5.1.1. Wound Healing Process 27
5.1.2. Wound management 27
5.1.3. Collagen based biological dressing 27
6. c Chapter 6: Prototype development 27
6.1. Introduction to prototype development 27
6.1.1. Wound Healing Process 27
6.1.2. Wound management 27
6.1.3. Collagen based biological dressing 27
1.3.1. Lipid compositions of biological membranes 28
1.3.2. Phospholipids 28
1.3.3. Sterols 29
1.3.4. Principal of vesicle formation 29
1.5. References 35
2. Chapter Two: Materials, methods and instrumentation theory 43
2.1. Fluorescence 43
2.1.1. Principals of fluorescence and phosphorescence 44
2.1.3. Stokes Shift (mirror image) 45
2.1.4. Fluorescence quenching 46
2.1.5. 6(5)- Carboxyfluorescein 48
2.1.6. Fluorescence spectroscopy 50
2.2. Microscopy 51
2.2.1. Bright-field microscopy 51
2.2.2. Fluorescence microscopy 51
2.2.3. Confocal microscopy 52

2.2.4. Atomic Force Microscopy (AFM) 53
2.3. Other Instrument types used 54
2.3.1. Nanoslight (NTA) 54
2.3.2. Osmometer 55
2.4. Vesicle preparation 56
2.4.1. Materials and equipment 56
2.4.2. Preparation of aqueous solutions 57
2.4.3. Lipid stock preparation 58
2.4.4. Extrusion 61
2.4.5. Purification of vesicles 62
2.4.6. Photo-polymerisation to crosslink vesicles 63
2.5. Vesicle characterization methods 64
2.5.3. Methods for stability tests and solution preparation 65
2.5.4. pH stability assay and osmotic pressure measurement 65
2.5.5. Temperature stability assay 65
2.6. Preparation of bacterial cultures 66
2.6.1. Materials and equipment 66
2.6.2. Sterilisation 66
2.6.3. Principals of bacterial growth 66
2.6.4. Bacterial culture preparation 67
2.6.5. Bacterial supernatant preparation 68
2.7. Hydrogel and prototype preparation 69
2.7.1. Materials and equipment 69
2.7.2. Hydrogel preparation 69
2.7.3. Preparation of natural hydrogel 69
2.8. Toxicity assays 71
2.8.1. Materials and equipment 71

2.8.2. Eukaryotic keratinocyte and fibroblast Cell culture 71
2.8.3. Resazurin assay 71
2.9. Prototype preparation methods 73
2.9.1. Materials and equipment 73
2.9.2. Gel-block system 73
2.9.3. Gel coated fabric 74
2.9.4. Collagen coated prototype 74
2.9.5. Stability and sensitivity assay 74
2.9.6. Fluorescence reading 75
2.9.7. Analysis of fluorescence results 75
2.9.8. Cell attachment assays 76
2.10. References 77
3. Chapter Three: Vesicle optimisation 79
3.1. Introduction to vesicle optimisation 79
3.1.1. Vesicle naming convention 80
3.1.2. Defining vesicle stability 80
3.1.3. The Stability-response parameter 80
3.1.4. Stability issues 81
3.1.5. Thermal stability 82
3.1.6. Stabilising agents 83
3.1.7. Sensitivity of vesicles 86
3.2. Vesicle formation and characterisation 88
3.2.6. Vesicle characterisation during purification 89
3.2.7. Vesicle size characterisation 90
3.2.8. Vesicle characterisation by microscopy 91
3.2.9. Summary of vesicle characterisation 91
3.3. Vesicle stabilisation using 'stabilising agents' 92

3.3.6. Incorporation of stabilizing agents in DMPC vesicles 92
3.3.7. TCDA stabilised vesicles 92
3.3.8. Studying the stabilizing effects of DC8,9PC in DMPC vesicles 95
3.3.9. Studies of the stabilizing effects of PEG lipids in DMPC vesicles 95
3.4. Vesicle stabilisation by increasing lipid chain length 96
3.4.6. Studying the effect on stability of changing the phospholipid chain length of TCDA containing vesicles 96
3.4.7. Studying the effect of changing phospholipid chain length of TCDA-containing vesicles, on their sensitivity to bacterial supernatant 97
3.4.8. Studying the effect of changing concentration of TCDA in DSPC vesicles 99
3.5. Summary of Vesicle optimisation 100
3.5.6. pH stability of leading vesicles 101
3.5.7. Sensitivity to whole bacteria and bacterial supernatant 102
3.6. Conclusion 104
3.7. References 105
4. Chapter Four: Hydrogel and prototype dressing development 107
4.1. Introduction 107
4.2. Hydrogels 108
4.2.6. Polysaccharide gelling agents 108
4.2.7. Other hydrogels utilised in this study 110
4.2.8. Properties of gel required for use as a vesicle immobilisation matrix 112
4.3. Hydrogel fabrication and initial vesicle stability in gels 114
4.3.6. Defining stability 114
4.3.7. Stability of vesicles when embedded in hydrogels 114
4.3.8. Studying the initial stability of vesicles 115

4.4. Vesicle sensitivity in gel matrixes 116
4.4.6. Fmoc FF 116
4.4.7. Polyacrylamide 117
4.4.8. Gelatin 119
4.4.9. Hypromellose 120
4.4.10. Agar and agarose 121
4.5. Systematic study of vesicle stability in gels 123
4.5.7. Detailed vesicle stability in Agarose gel 125
4.5.8. Summary of vesicle stability in gel matrixes 126
4.6. Fmoc FF –Agarose gel multi-layer assembly 127
4.6.6. Preparation of FmocFF/agarose gel multi-layer assembly 127
4.6.7. Testing the response of gels 128
4.6.8. Protease assay 128
4.6.9. Breakdown of FmocFF gel on addition of protease 129
4.6.10. Stability and sensitivity of the FmocFF multi-layer assembly system. 129
4.6.11. Response of vesicles in agarose with the additional pure-agarose layer to bacterial supernatant 130
4.6.12. Response of the gel multi-layer assembly to bacterial supernatant in the presence of protease 131
4.6.13. Microbial Logic gate 133
4.7. Conclusions 135
4.8. References 136
5. Chapter Five: *In vitro* cytotoxicity 139
5.1. Introduction 139
5.1.1. Eukaryotic Cells 140
5.1.2. Use of Keratinocyte cell lines in *in vitro* assays 140

5.1.3. Use of Fibroblasts cell lines in *in vitro* assays 141
5.1.4. Cell viability assessment 141
5.2. Methods and materials used for cytotoxicity assays 142
5.2.1. HaCaT and EA.hy926 Cell culture for cytotoxicity 142
5.2.2. HaCaT and EA.hy926 Cell culture for supernatant assays 142
5.2.3. Viability measurement 143
5.3. Results and discussion of cytotoxicity results 144
5.3.1. Initial the calibration curve 144
5.3.2. Initial cytotoxicity analysis 145
5.3.3. Stability of vesicles in the presence of eukaryotic cells 146
5.3.4. Cytotoxicity of vesicles tested in well plates over 24, 48 and 72h 147
5.3.5. Confocal images of cell incubated in media containing vesicles 148
5.3.6. Cellular response to vesicles in conjunction with bacterial supernatant 148
5.3.7. Cytotoxicity of gels in suspension 151
5.4. Conclusions 152
5.5. References 153
6. Chapter 6: Prototype development 155
6.1. Introduction to prototype development 155
6.1.1. Wound Healing Process 155
6.1.2. Wound management 157
6.1.3. Summary 157
6.2. Gel-block type wound dressing 159
6.2.1. Stability and sensitivity of Gelatin based gel-block type wound dressing160
6.2.2. Stability and sensitivity of Agar and Agarose based gel-block type wound dressing 161

6.2.3. Confocal imaging 162
6.2.4. Limitations of the gel-block systems 164
6.2.5. Summary of the gel-block system 165
6.3. Gel coated fabric wound dressing 167
6.3.1. Choice of Fabric 167
6.3.2. Hypromellose coated fabric 168
6.3.3. Agarose/Hypromellose gel coated fabric 169
6.3.4. Agarose coated fabric 170
6.3.5. Summary of gel-coated fabric system 171
6.4. First Generation Prototype (FGP) wound dressing 172
6.4.1. Improving visual response 172
6.4.2. Studying the stability of FGP for storage 174
6.4.3. FGP on *ex vivo* skin model 175
6.5. Second generation prototype (SGP) wound dressing 178
6.5.1. Collagen based biological dressing 178
6.5.2. Proposed mechanism of wound healing enhancement by SGP 179
6.5.3. Experimental results of cell growth on SGP 179
6.6. Conclusion 181
6.7. References 182
7. Chapter Seven: Post project development 183
7.1. Conclusions and Future work 183
7.2. Demand for new methods to combat/prevent infections 185
7.2.1. Infections and Antimicrobial resistance 185
7.2.2. Economics of development of new antibiotics 185
7.3. Health-economics of development of a new dressing 186
7.3.1. Cost involved in treatment of burns 186
7.4. The proposed solution: commercialisation of the prototype dressing 188

7.4.1. Clinical trials 188
7.5. Summary 191
7.6. References 192

Publications

Marshall, S. E., Hong, S. H., Tun, T. N., & Jenkins, A. T. A. (2013). The effect of lipid and fatty acid composition of phospholipid vesicles on long term stability and their response to Staphylococcus aureus and Pseudomonas aeruginosa supernatants. *Langmuir*.

Marshall, S. E., Jenkins, A. T. A., Al-Bataineh, S. A., Short, R. D., Hong, S. H., Thet, N. T., ... & Szili, E. J. (2013). Studying the cytolytic activity of gas plasma with self-signalling phospholipid vesicles dispersed within a gelatin matrix. *Journal of Physics D: Applied Physics*, *46*(18), 185401.

Thet, N. T., Hong, S. H., Marshall, S., Laabei, M., Toby, A., & Jenkins, A. (2012). Visible, colorimetric dissemination between pathogenic strains of Staphylococcus aureus and Pseudomonas aeruginosa using fluorescent dye containing lipid vesicles. *Biosensors and Bioelectronics*.

Jenkins, A. T. A., Thet, N. T., Zhou, J., Hong, S. H., & Marshall, S. (2011). O7. 2 A microbiologically sensitive "intelligent" burns dressing concept. *Burns*, *37*, S5.

Zhou, J., Tun, T. N., Hong, S. H., Mercer-Chalmers, J. D., Laabei, M., Young, A. E., & Jenkins, A. T. A. (2011). Development of a prototype wound dressing technology which can detect and report colonization by pathogenic bacteria. *Biosensors and Bioelectronics*, *30*(1), 67-72.

Presentations

Bacteriosafe conferences every 6 months in various counties including Austria, Germany, Singapore and Ireland.

Bio-nano Summer School, Austria

Poster Presentation, EU-Korea Conference on Science and Technology 2013, Brighton, UK

Seminar, DongA University, 2013, Seoul, Korea

Poster Presentation, the 1st International Paediatric Wound Symposium 2011, Rome, Italy

Acknowledgments

First of all I would like to thank my supervisor Dr. Toby Jenkins, Department of Chemistry, University of Bath, UK. Without his supervision and guidance this research work would not have been possible.

I would also like to thank my colleagues within the Toby Jenkin's group as well as those who have left the group: Charby, June, Serena, Jess, Thet, David, Maisem, Diana, Hollie as well as all of the members of bacteriosafe. I would also like to express my gratitude towards Dr. Finbarr O'Sulivan, Dr. Endre Szili and Maisem for their guidance and support in achieving the biological side of the project. I would also like to express my gratitude towards June, Jude, Jess and Hollie for their editing skills. Acknowledgements of results figures 3.11 and 3.12 to Jin and figure 6.20 to David and Maisem where I prepared the prototypes being tested.

Finally, I am indebted to all of my family and friends for all of their support throughout my studies. My parents and my two sisters for supporting me throughout my entire studies, especially Sung Ju for everything she has done for me. I would like to express my special thanks to Geon Hwan and Yeon Soo, for supporting me when it was most needed.

This research work was performed at the Department of Chemistry, University of Bath, financially supported by the Bacteriosafe project funded by the EC 7th framework Bacteriosafe program.

Abstract

There has been a significant increase in children's burns in the past several years and figures indicate that children suffer more burns compared to any other age groups. The main concern following a burn is the possibility of infections. The aim of this project is to construct a unique wound dressing, which enhances healing and stimulates wound closure by incorporation of collagen, as well as signalling the presence of pathogenic bacteria on colonisation.

The process of signalling bacterial colonisation was achieved by incorporation of a phospholipid based nanocapsule, with a colourimetric response and a mechanism for release of a dye. This research invested into finding the optimum phospholipid composition to obtain a stable and sensitive system. The signalling device uses the biomimetic aspect of vesicles to signal the presence of pathogenic bacteria via the effect of secreted toxins on the sensor interface. The modified phospholipid based sensors were immobilised into gel matrices and further developed to produce prototype dressings. The healing enhancing property was achieved by a thin layer of collagen coating.

This work presents the results obtained from the initial modification process of the sensor, to incorporation of the vesicles into gel matrices through to development of First and Second Generation Prototype dressings. Verification of stability and sensitivity of the vesicles was carried out following each stage of development, using clinically isolated strains of pathogenic bacteria. Initial cytotoxicity and verification of the wound healing property was achieved by in vitro cell assays.

List of Figures

Figure 1.1: Graph showing burn injury locality of children. Indicating that most injuries occur in own homes, most often in the kitchen. 3

Figure 1.2: Histological overview of the different classifications of burns in terms of the depth of the injury[21] 4

Figure 1.3: A. Rule of nines. B. Lund-Browder diagram, taken from the U.S. Department of Health & Human Services (http://chemm.nlm.nih.gov/burns.htm). 5

Figure 1.4: Flow chart followed by clinicians at Frenchay Hospital in Bristol in diagnosing infections in paediatric patients with burns of any size and depth. Chart supplied by Dr. Amber Young (Frenchay Hospital) and Dr. Toby Jenkins (University of Bath). 8

Figure 1.5: Silver surfphadiazine 11

Figure 1.6: Patients with partial thickness scald injury treated using Biobrane™: **A.** No removal of dressing; **B.** Dressing removed. (Images supplied by Dr. Amber Young, Burns unit, Frenchay Hospital, Bristol, UK.) 12

Figure 1.7: Structure of a prokaryotic cell. Image obtained from Bacterial structure, Growth and Metabolism by Richard A. et al.[53] 15

Figure 1.8: Stages of Biofilm formation [57] 17

Figure 1.9: Scanning electron micrograph of Staphylococcus aureus x9560magnification (image source: Source: Carr J. H., in MRSA_PHIL #10046, Public Health Image Library.) 18

Figure 1.10: Scanning electron microscopy pictures of P. aeruginosa PAO1 (bar = 1 μm)[63] 19

Figure 1.11: False colour SEM (x6836) of *E. coli* 0157:H7 (image source: Source: Carr J. H., in PHIL #10068, Public Health Image Library.) 20

Figure 1.12: Blood agar plate showing S. aureus (MSSA 476) and P. aeruginosa (PAO1) secrete toxins that break red blood cells and that E. coli (DH5α) does not secrete these toxins. Acknowledgment: J.Zhou Ph.D. Thesis 2011 21

Figure 1.13: Diagram showing the mode of action of α-haemolysin. This toxin creates pores within the bilayer membrane, disrupting the cell. This diagram was modified from an image from Exotoxins of *Staphylococcus aureus*, 2000. [69] 22

Figure 1.14: Mode of action of delta toxin[70] 23
Figure 1.15: Diagram showing site of cleavage of phospholipid by phospholipase C. This toxin breaks down phospholipid membranes damaging the polar head group. This cleavage site remains the same in other phospholipids [72]. 24
Figure 1.16: Cartoon representation of regulation of virulence genes by S. aureus[79] 24
Figure 1.17: Accessory gene regulatory system. Acknowledgement: Dr. Toby Jenkins, University of Bath. 25
Figure 1.18: showing schematic representation of lysis of vesicle upon contact with bacterial toxin 27
Figure 1.19: Chemical structure of Cholesterol 29
Figure 1.20: Lipid angle diagram - A: Shape parameter (S)>1.2; B: S=1; C: S<0.6. 30
Figure 1.21: Self-assembly of lipids into different shapes as concentration increases[91] 32
Figure 2.1: The Jablonski diagram, illustrating the excitation of a fluophore to the higher energy level and emission of fluorescence and phosphorescence as the fluophore moves back down to the ground state. 44
Figure 2.2.: Spectra illustrating the Stokes' shift. Acknowledgement: J. Zhou Ph.D. Thesis 2011. 46
Figure 2.3: Showing excitation and emissionspectrum of 6(5)- Carboxyfluorescein, indicating excitation wavelength of 480nm and emission wavelength of 530nm (left), and the chemical structure of 6(5)- Carboxyfluorescein (right)[2] 48
Figure 2.4: A: The colour change observed in solution as the concentration of 6(5)- Carboxyfluorescein is increased under white-light. B: The colour change observed in solution as the concentration of 6(5)- Carboxyfluorescein is increased under UV-light. C: A plot of the self-quenching effect as the concentration of 6(5)-Carboxyfluorescein is increased. Images and graph acknowledgement: W.D. Jamieson, Ph.D. Thesis 2013, University of Bath. 49
Figure 2.5: Schematic of light microscope. Image Acknowledgment: J.Zhou, Ph.D. Thesis 2011, University of Bath. 51
Figure 2.6: The NTA instrument used to measure the size and stability of nanoparticles at different temperatures 54
Figure 2.7: The Liposofast ™® extruder 61

Figure 2.8. Representation of TCDA crosslinking, initiated by formation of radicals of **A** irradiated TCDA to from **B** the crosslinked product. Acknowledgment of scheme to Serena Marshall PhD. candidate at the University of Bath. 63
Figure 2.9: Schematic of the NTA system 64
Figure 2.10: The stages of bacterial growth. A: initial lag phase, B: exponential growth phase, C: stationary phase, D: logarithmic decline phase. 67
Figure 2.11. Structure of **A** resazurin and **B** resorufin[11]. 71
Figure 2.12: Cartoon representation of gel block system 73
Figure 2.13: Diagrammatic representation of prototype layout in each well of a 12 well plate, with two layers of coated fabric 74
Figure 2.14: Illustration of measurement site (middle of the well) 75
Figure 3.1: Representation of the transition temperatures of various lipids. The peak of each curve indicates the 'melting temperature' of the lipids from gel to liquid- crystalline states. The plot indicates that as the lipid chain length increases, the transition temperature increases[1]. 82
Figure 3.2: Structure of 10,12-Tricosadiynoic acid (TCDA) 84
Figure 3.3. A Representing the colour profiles associated with different dilutions of TCDA. As well as representation of TCDA crosslinking, initiated by formation of radicals of **B** irradiated TCDA to from **C** the crosslinked product. Acknowledgment of scheme to Serena Marshall PhD. candidate at the University of Bath. Image acknowledgement to Jin Zhou Ph.D. thesus 2011. 84
Figure 3.4: Chemical structure of 1,2-bis(10,12-tricosadiynoyl)-*sn*-glycero-3-phosphocholine, (DC8,9PC) 85
Figure 3.5: the transitions between liquid-crystalline and gel-crystalline phase of a lipid bilayer. 86
Figure 3.6: Structure of cholesterol 87
Figure 3.7: A. Aqueous solution containing lipid mixture: opaque before extrusion **B.** The opaque solution becomes transparent following extrusion (x3 at 60°C). 88
Figure 3.8: Fluorescence intensity of eluent using NAP-25 column. Acknowledgment: Jessica Bean Ph.D. candidate, Department of Chemistry, University of Bath. 89
Figure 3.9: A. Plot of the size and population of DPPC vesicles in HEPES (red) and in Triton solution (orange). The decrease in population of 100nm vesicles is clearly

visible,as the detergent is introduced. **B**. Showing the capture of the video taken for analysis of vesicles in HEPES. **C**. Showing the capture of the video taken for analysis of vesicles on addition of Triton. 90
Figure 3.10: ATM of vesicles on Maleic anhydride coated glass slides. **A.** shows a forward amplitude scan zoomed in at frame size of 5μm. **B.** shows a backwards Topography scan zoomed at frame size of 254nm. 91
Figure 3.11: Stability measurements of TCDA-DM systems with varying concentrations of TCDA. Study performed by Jin Zhou, University of Bath[13]. 92
Figure 3.12: Toxin tests on vesicles with TCDA concentrations varying from 0% to 40%.; illustrating the optimum TCDA concentration (high sensitivity and stability) may be between 20% and 30%. Study performed by Jin Zhou, University of Bath.93
Figure 3.13: Effect of TCDA concentration on sensitivity of DMPC vesicles to purified toxins. Fluorescence intensity values were converted to SR-parameter values to aid analysis of results....94
Figure 3.14: Effect of TCDA concentration on sensitivity of DMPC to bacterial supernatant. Fluorescence intensity values were converted to SR-parameter values to aid analysis of result.s....94
Figure 3.15: SR-parameters calculated following overnight incubation at 37°C. The SR-parameter of the 25% TCDA-DP system is more than double that of the 25% TCDA-DM system, indicating improved stability by incorporation of TCDA in place of the DMPC in the DPPC system. 96
Figure 3.16: A: Overnight response curves of the 25% TCDA-DP and the 25% TCDA-DS systems tested against bacterial supernatants. **B:** SR-parameters of the fluorescence intensities. 97
Figure 3.17: Crosslinked 25% TCDA-DS vesicles. Upon crosslinking, some solutions turned green and a precipitate was observed, whilst other solutions showed no difference.- suggesting that incorporation of TCDA into the vesicle system makes the system more difficult to standardise. 98
Figure 3.18: Overnight stability and sensitivity at 37°C of TCDA-DS vesicles with varying concentrations of TCDA. General trend observed: sensitivity increases with increasing concentration of TCDA, while stability decreases. 99

Figure 3.19: Vesicle response to bacterial supernatant after 100 mins of exposure: (1) Triton-X100,(2) *S. aureus* RN4282, (3) *P. aeruginosa* PAO1, (4) *E. coli* DH5α, (5) HEPES buffer.....102
Figure 4.1: Chemical structure of Hypromellose 110
Figure 4.2: Structure of Fmoc-diphenylalanine (FmocFF).....111
Figure 4.3: Instability of vesicles when added to 2mg mL^{-1} FmoFF gel compared to when added to HEPES buffer.....116
Figure 4.4: images taken under day-light and under UV-lamp at 254nm, indicating lysed, fluorescent vesicles.....117
Figure 4.5: Response of vesicles to addition of Triton X-100 and HEPES buffer. **A**: original ingredient of gel **B**: 1mL of water replaced with vesicle solution from the original recipe **C:** total water content of the original recipe replaced with HEPES with additional vesicle solution **D**: vesicle diluted with HEPES to yield the same dilution as in gel mixtures. 118
Figure 4.6: The overnight response of vesicles dispersed in 2% hypromellose gel to bacterial supernatant at 37°C. Vesicles were dispersed into the gel and incubated overnight with supernatant of *P. aeruginosa* PAO1, *S. aureus* MSSA476 and *E. coli* DH5α, as well as Triton X-100 as a positive control and HEPES as a negative control.....119
Figure 4.7: Response of vesicles immobilised in hypromellose. Upon incubation with supernatant of *P. aeruginosa* PAO1 and *S. aureus* MSSA476, a fluorescence increase can be observed, along with a slight increase in fluoresce when incubated with *E. coli* DH5α due to passive leakage. Triton X-100 and HEPES were used as controls. 120
Figure 4.8: The overnight response of vesicles in **(A)** agar gel matrix and (B) in agarose gel matrix, upon incubation at 37°C with bacterial supernatant; lysis of vesicles shown by *P. aeruginosa* PAO1, *S. aureus* MSSA476 and the positive control, Triton X-100. Vesicles show stability in negative control, HEPES, however slight instability is indicated by incubation with *E. coli* DH5α. Images on the right of each graph show the visual response on incubation with Triton X-100 (T), *S. aureus* MSSA476 (M), *P. aeruginosa* PAO1 (P), *E. coli* DH5α(D) and HEPES (H). 121
Figure 4.9: The effect of hydrogel matrices containing the three leading vesicle. Vesicles dispersed in each gel formulations were stored at 37 °C for 14 days,

followed by addition of *S. aureus* RN4282 supernatant to obtain a value of F_f, or HEPES as a negative control. 124
Figure 4.10: Change in fluorescence of three lead vesicle types in agarose gel at 37 °C over 14 days, and response to lytic supernatant from an overnight culture of *S. aureus* RN 4282 at 14 days. 125
Figure 4.11: Diagram of gel multi-layer assembly 128
Figure 4.12: Image showing breakdown of FmocFF gel on addition of Protease using water as a control. 129
Figure 4.13: Stability response Parameter, SR, calculated and graphed for time points; T=2 h and T=18 h, following initial incubation of agarose/vesicle layer with the additional pure agarose layer (without the FmocFF gel layer) with water (a) and protease (b) for 1 h followed by 18 h incubation with bacterial supernatant at 37°C. 130
Figure 4.14: Stability response Parameter, SR, calculated and graphed at T=2 h and T=18 h following initial incubation of complete gel multi-layer assembly system with protease for 1 h, followed by 18 h incubation with bacterial supernatant at 37°C. 131
Figure 4.15: Stability response Parameter, SR, calculated and plotted at T=2 h and T=18 h following initial incubation of the complete gel multi-layer assembly system with water for 1 h, followed by 18 h incubation with bacterial supernatant at 37°C. **Error! Bookmark not defined.**
Figure 4.16: 10% milk BHI agar plate incubated with supernatant of *P. aeruginosa* PAO1, *S. aureus* MSSA476 and *E. coli* DH5α and protease as a positive control and broth solutions as negative controls, overnight at 37°C. 133
Figure 5.1: Calibration curves for HaCaT and EA.hy926 cell lines 144
Figure 5.2: results of cytotoxicity assay, showing non-cytotoxic effects of vesicles as well as lysed vesicles compared to the HEPES and pure media control to both types of cell lines. 145
Figure 5.3: Stability of vesicles on incubation with HaCaT (top plot) and EA.hy926 cells (bottom plot). Following 24 h exposure to eukaryotic cells, stability was assessed by fluorescence intensity measurements on addition of Trion X-100 and HEPES. 146

Figure 5.4: Shows the viability of HaCat cells when exposed to media containing vesicles over a period of 24, 48 and 72h. Alamar blue assay was used to study the viability of cells. 147
Figure 5.5: Confocal images of HaCat cells (A) vesicles incubated with HaCat cells (B) over a period of 24h. Stained with neutral red solution at X40 magnification. 148
Figure 5.6: Showing response of vesicles to bacterial supernatant in a eukaryotic cell environment.....149
Figure 5.7: Vesicle lysis using serial dilution of pure δ-toxin.....150
Figure 5.9: Response of eukaryotic cells to hydrogels dissolved in cell growth media over a period of 24h at 37°C and 5% CO_2. The viability of vesicles was measured using the resazurin assay.....151
Figure 6.1: Diagram showing the different stages of wound healing process following an injury.....156
Figure 6.2: A: Cartoon representation of the structure of the gel-block type wound dressing. **B:** Photographic image of the gel-block system under day light (left) and under UV-light (right) 159
Figure 6.3: Overnight stability and sensitivity study of vesicles in gel-block system. The fluorescence of a 12 well plate was measure in an overnight study. Plot shows responsive vesicles in toxin producing bacterial supernatant, and stable vesicles in HEPES and *E. coli* DH5α.....160
Figure 6.4: Average well scans of before addition of supernatant and after addition of supernatant and incubation at 37°C on agar gel-block systems.....161
Figure 6.5: Average well scans of before addition of supernatant and after addition of supernatant and incubation at 37°C on agar gel-block systems.....162
Figure 6.6: Cross section image of Z-stack of a thin layer of agarose gel-block system with vesicles of an approximate concentration of $1x10^8$ particles mL^{-1}....162
Figure 6.7: Thin layer of 15% TCDA-DS vesicles immobilised in agarose gel matrix confocal images of TCDA-DS vesicles immobilised in agarose gel on glass slide was imaged using confocal. **Top row:** effect of AGR- stain of *S. aureus* RN6911 supernatant on vesicles in gel matrix captured over time, showing no increase in background fluorescence over a 00, 60 and 120s time period. **Middle row:** effect of AGR+ stain of *S. aureus* RN6390B supernatant on vesicles in gel matrix over time,

showing increase in background fluorescence within the first 60s. **Bottom row:** effect of *S. aureus* USA300 supernatant on vesicles in gel matrix over time, showing increase in background fluorescence within the first 60s. The scale bar represents 10μm. 163
Figure 6.8. The effect of the thickness of gels on the diffusion of toxins from supernatant for lysis of vesicles. The thickness of the gel was measured to be approximately 3mm thick. 164
Figure 6.9: Image showing the effect of dehydration of gel on stability of vesicles. Top three images were taken under day light and the bottom three images were taken under UV-light. 165
Figure 6.10: Diagram of the gel coated fabric system 167
Figure 6.11: Light microscope image of untreated polypropylene fabric. Image acknowledgements: Neil Poulter, University of Bath Ph.D. Thesis, 2010. 167
Figure 6.12: Showing average well scans of before addition of supernatant and after addition of supernatant and overnight incubation at 37°C on hypromellose coated systems. 168
Figure 6.13: Showing average well scans of before addition of supernatant and after addition of supernatant and overnight incubation at 37°C on agarose/hypromellose gel coated systems. 169
Figure 6.14: Showing average well scans of before addition of overnight bacterial culture and after overnight incubation at 37°C on agarose gel coated systems. Vesicles on the agarose system were shown to be responsive. 170
Figure 6.15: Average well scans before addition of overnight bacterial culture and after 18hr of overnight incubation with shaking at 37°C. Vesicles show both fluorescence increase and visible colour change following incubation with AGR+ stain of S. aureus. 171
Figure 6.16: Image of prototype dressing with addition of AGR +/- *S. aureus* supernatant on porcine skin 172
Figure 6.17: A: agarose coated dressing with lower concentration of vesicles, approximately $1x10^{12}$. **B:** agarose coated dressing with higher concentration of vesicles, approximately $1x10^{36}$ (first generation prototype dressing) 173

Figure 6.18: Average of well scan following overnight incubation with bacterial culture. Results show responsive and stable vesicles even when a higher concentration of vesicles was incorporated. 173
Figure 6.19: Average of well scans on Day 1, Day 21 and following addition of Triton X100 on Day 21. SR-parameter of 13.2 ±0.222 174
Figure 6.20: image of before incubation and after incubation of FGP dressing on tissue injected with overnight bacterial culture. Acknowledgment: W.D. Jamieson and Maisem Labbei, University of Bath. 175
Figure 6.21: image of before incubation and after incubation of FGP dressing on tissue injected with overnight bacterial culture. 176
Figure 6.22: Cartoon representation of the prototype dressing 178
Figure 6.23: Representation of wound healing being promoted by second generation dressing (collagen dressing) 179
Figure 6.24: Eukaryotic cell growth on black surface (non-adherent to cells), agarose coated fabric and collagen coated agarose coated fabric normalised against maximum cell growth of tissue culture plate. Both HaCaT and Eayh926 cell lines show improved attachment on collagen coated dressing compared to simple agarose coated fabric. 180
Figure 7.1: Histological features of human and porcine skin. Sections were taken through comparable portions of the dermis of both tissue samples. Images modified from article by Sullivan et al. [14] 190

List of Tables

Table 2.1: All of the components in the table above were dissolved in 100mL of purified water. And the pH was measured and adjusted to pH 7.4. 57
Table 2.2: The components shown in the table 2.1 were dissolved in 13mL of purified MiliQ water, and the pH was measured and adjusted to pH 7.4. Then the vial containing the solution was sealed and kept in a dark environment at 4°C..... 57
Table 2.3: Stock 1 solution, in which each component was dissolved in 1mL of chloroform..... 58
Table 2.4: Summary of composition of vesicles without crosslinker incorporated. Components were all dissolved in 1mL of chloroform prior to evaporation by nitrogen gas. 59
Table 2.5: The components were all dissolved in 1mL of Chloroform. Any variation of TCDA concentration was made by varying the concentration of main phosphodicholine 60
Table 2.6: A summary of the composition of DC8, 9PC containing vesicles..... 60
Table 2.7: Showing the transition temperature and the extrusion temperature of different lipid systems used in this investigation 62
Table 3.1: Summary of stability of vesicles of various compositions with stability – response parameter values, following long-term stability studies. *No increase in fluorescence on addition of Triton.[14] 100
Table 3.2: The effect of pH changes on the stability of the three leading vesicles. The effect was monitored over a 14 day period. The SR-parameter values were calculated following 14 day storage at 37 °C and lysis using Triton X-100. 101
Table 3.3: SR-parameter values following overnight incubation with pathogenic bacteria cells (*S. aureus* RN4282 and *P. aeruginosa* PAO1 and relative non-response from HEPES buffer, *E. coli* DH5α, LB broth, TS Broth (TSB) and Triton X-100 was the positive control. 103
Table 4.1: Gels prepared using HEPES Buffer..... 112
Table 4.2: Vesicle stability was assessed by observing for immediate appearance of the fluorescence on addition of vesicle solution to gel. 'Stable' in this case indicates that fluorescence increase upon addition of vesicle solution to gel was

not immediate. Unstable indicates that the solution appeared fluorescent immediately after addition of vesicle solution to gel. 115
Table 4.3: The osmolality and pH of the FmocFF gel as well as the vesicle solution. This work was carried out by Charlotte Spencer, MChem student at the University of Bath, UK[17] 117
Table 4.4: The osmolality ratio values were calculated based on the ratio of the osmotic pressure (mOsm/kg H_2O) of each vesicle type against each solution. A value close to 1 is optimal. This table has been modified from the original obtained from Marshall et. al. *Langmuir* 2013. 123
Table 4.5: Representation of logic gate 134
Table 5.1: Image showing the structure of a human Eukaryotic cell[1] 140
Table 6.1: SR-values and colony forming units 177
Table 7.1: Shows the average breakdown of costs involved in treatment of a minor burn injury. 186

Acronyms and abbreviations

°C	Degrees centigrade
µm	micrometre
5(6)-CF	5(6)-carboxyfluorescein
AFM	Atomic Force Microscopy
AGR	Accessory gene regulator
C981	carbopol gel
CBT	Children's Burns Trust
CF	6(5)- Carboxyfluorescein
CF50	50mM 6(5)- Carboxyfluorescein
CFU	Colony forming units
CHO	Cholesterol
CMC	Critical micelle concentration
CO_2	Carbon Dioxide
DC8,9PC	1,2-bis(tricosa-10,12-diynoil)-sn-glycero-3-phosphocholine
DH5α	An attenuated strain of nono-pathogenic *E. coli*
DM	Dimyristoyl
DMEM	Dulbecco's Modified Eagle Medium
DMSO	Dimethylsulfoxide
DNA	Deoxyribonucleic acid
DO	Dioleoyl
DP	dipalmitoyl
DS	distearoyl
E. coli	*Escherichia coli*
EDTA	Ethylenediaminetetraacetic acid
F	Fluorophore
FBS	fetal bovine serum

FDA	Food and Drug Administration
F_f	Final vesicle fluorescence value after addition of a lytic agent
FGP	First Generation Prototype
F_i	Initial vesicle fluorescence value
FmocFF	Fmoc-diphenylalanine
F_o	Unquenched Fluorophore
g	Gram
GUV	Giant unilamellar vesicles
h	Hours
HEPES	4-(2-hydroxyethyl)-1-piperazineethanesulfonic acid
HM	Hydroxypropylmethylcellulose
Hz	Hertz
kg	Kilogram
K_Q	bimolecular quenching rate coefficient
K_s	Stern-Volmer quenching constant
LasR	autoinducer
LB	Luria broth
LC_{50}	Median lethal dose
LUV	Large unilamellar vesicles
L_α	Liquid crystalline phase
L_β	Liquid gel phase
mg	milligram
mg	Milligrams
min	minute
mL	millilitre
mm	millimetre
mM	Mili molar
mOsm	milliosmoles
MRSA	methicillin resistant *staphylococcus aureus*
MSSA	Methicillin susceptible *staphylococcus*

	aureus
NaCl	Sodium chloride
NaOH	Sodium hydroxide
nm	nanometre
NTA	Nanosight instrument
P. aeruginosa	*Pseudomonas aeruginosa*
PAO1	A common lab strain of *P. aeruginosa*
PBS	Phosphate Saline buffer
PC	Phosphatidylcholine
PCR	Polymerised Chain Reaction
PDA	Polyduacetylenes
PE	Phosphatidylethanolamine
PE	phosphatidylethanolamine
PEG	Polyethylene glycol
Phos A2	Phospholipase A2
PL	Glycerophospholipids
PMN	Polymophonuclear leukocytes
PSG	Penicillin, Streptomycin and Glutamine
PSM	Phenol soluble modulin
QS	Quorum sensing
RN4282	Clinical strain of *S. aureus*
RN6390B	AGR positive strain of *S. aureus*
RN6911	AGR negative strain of *S. aureus*
RNAIII	RNA which regulated toxin production
rpm	Rotations per minute
s	Seconds
S	Shape parameter
S. aureus	*Staphylococcus aureus*
S.epidermis	*Staphylococcus epidermis*
S_0	Singlet ground state
S_1 and S_2	Singlet excited state
SEM	Scanning electron microscopy
SGP	Second Generation Prototype

SR	Stability-Response parameter
SUV	Small unilamellar vesicles
t	Time
T	Temperature
T_1	Triplet excited state
TBSA	Total body surface area
TCDA	10,12-tricosadiyanoic acid
T_m	Phase transition temperature
triton	Triton X-100™
TSA	Tryptic soy agar
TSB	Tryptic soy broth
TSS	Toxic shock syndrome
TSST	Toxic shock syndrome toxin
UV	Ultraviolet
v	Volume
V_{50}	Median lethal dose in terms of vesicle lysis
w/v	Wight to volume ratio
α	Alpha
β	Beta
δ	Delta
τ_o	Unquenched lifetime

Chapter One: Introduction

1.1. The clinical problem

One of the major problems following a skin injury is infection[1], especially if the patient in question has a compromised immune system or if the infection is hard to detect. Examples illustrating this situation are paediatric scalds. When a child suffers from a scald, their body reacts to the burn by presenting with increased body temperature, which is much like the symptoms of children with infected wound sites. As a result, a swab of the wound site is necessary to prove the existence of an infection before administering antibiotics. This process of swabbing requires the removal of any dressing, which can increase chances of scarring, infection, or delay the healing process. Furthermore, during the process

of testing the child for infection, the condition of the child may deteriorate, with potentially fatal consequences. [3]

In order to treat these wounds more effectively and more efficiently, this study aims to develop a device which can sense and signal the presence of pathogenic bacteria. The 'intelligent wound dressing' developed in this study contains a bacterial 'toxin sensor', which can signal infection without having to swab the wound and grow a culture in order to determine the presence or absence of infection in the wound.

1.1.1. Skin injury

Skin is the largest organ in the human anatomy, representing 16% of the body weight and measuring between 0.2 and 0.3m^2 in adults[5]. Skin is mainly composed of the epidermis and the dermis, with the dermis layer being much thicker than the epidermis layer[7]. The skin of newborns and young children is thin; gradual thickening of the skin occurs, before a slow thinning of the skin takes place with age. The main role of the skin is to serve as a protective barrier against the surrounding environment [8]. Upon occurrence of a skin injury, this barrier is broken, leading to major disabilities and infections that can result in death. All wound injuries are at risk of infection, however some patients are more susceptible, and some are more severely affected by, wound infections than others. Some infections are harder to detect while others are harder to provide treat. In order to effectively treat wound injury infections, early detection is crucial. Physicians state that an infection of a burn injury is harder to diagnose, especially when dealing with paediatric burn injuries[3]. As a result, development of such a key clinical diagnostic tool within a bacterial infection-signalling device for paediatric burns was the focus of this study.

1.1.2. Burns

Burn injuries are a major cause of morbidity and mortality in children[10]. Each year in the USA, over 440 000 children with burn injuries are taken into hospitals[12], of which approximately 1100 die from related illnesses, causing burn related injuries to be one of the most common causes of paediatric death[14]. The severity of

paediatric burns was recognised, and by implementation of effective precautions and treatment methods, there had been a decline in the number of deaths due to burn-related-injuries[15]. However, young children under the age of 5 remain part of a high risk group, accounting for approximately 18% of all patients with burns[16]. In the past several years in the UK, there has been a significant increase in paediatric burn injuries. According to the Children's Burns Trust (CBT), in 2010 there was an average of 10 children under the age of 5 admitted to hospital with burn injuries every day. The majority of these injuries were scalds caused by hot liquids and most occurred within the vicinity of their own homes, typically in the kitchen; Figure 1.1 illustrates the injury locations concerning children under the age of 5 [17].

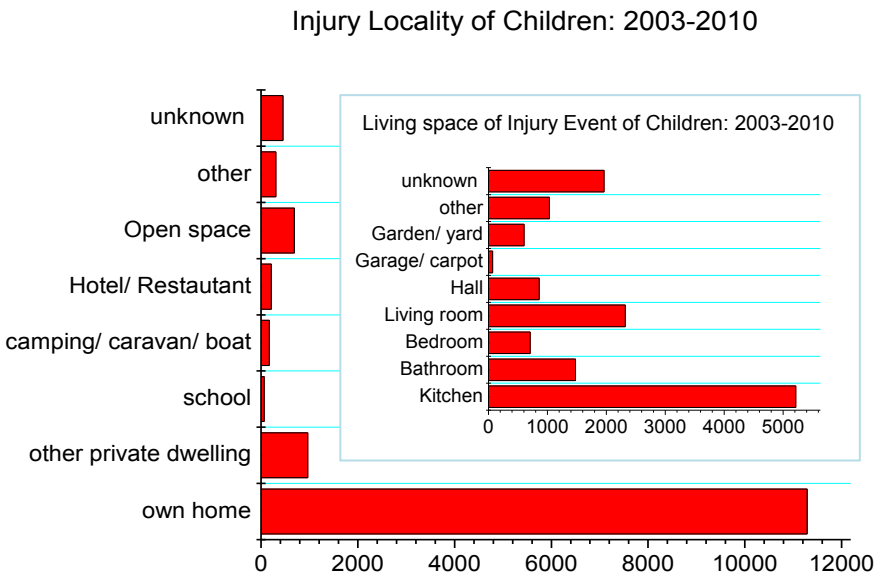

Figure 1.1: Graph showing burn injury locality of children. Indicating that most injuries occur in own homes, most often in the kitchen.

The increase incidents of paediatric burns is not only a problem occurring in the USA and in Europe, but also in Asian countries, where the diet involves various hot soup-based meals, steamed meals and boiled rice. Hangang Sacred Heart Hospital, a South Korean hospital, which incorporates Asia's largest burn unit, reported an increase in paediatric scald injuries from 72% in 2005 to 87% in 2009, with most of these scalds being caused by hot liquid spills. This translates into an increase of 15% within 4 years in paediatric scalds due to hot liquids [18,19].

The damage caused by scalds does not only involve the pain that the children suffer, but also the possibility of scar development, other physical and emotional trauma, and even social problems, especially in children under the age of 5.[20]

1.1.3. Classification of burn injury

Burn injuries can be categorised into four different classifications depending on the depth and the intensity of the burn. Figure 1.2 below shows the histological overview of the different degrees relating to the depth of a burn injury.

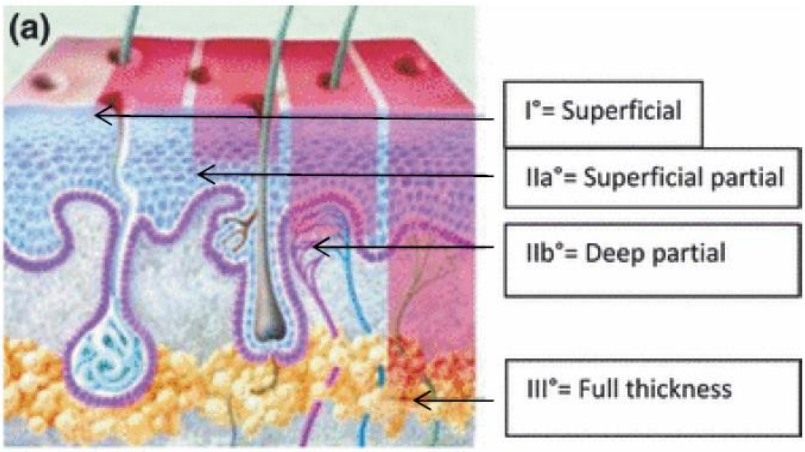

Figure 1.2: Histological overview of the different classifications of burns in terms of the depth of the injury[21]

The first is the superficial burn, which is also known as a first degree burn. This only involves the outer layer of epidermis and healing occurs fairly rapidly, usually without scarring. This type of injury can be caused by exposure to the sun and hot liquids. The next is a partial thickness burn, also known as second degree burn. These burns can be further divided into two groups, the superficial partial thickness and the deep partial thickness. As the name suggests, the deep partial thickness burn involves a deeper wound site where more than 50% of the dermis is damaged. Treatment may involve skin grafting. The superficial partial thickness burn is less severe and healing can occur with minimal scarring. Both types of partial thickness burns are often caused by hot liquids, flames and chemicals. A full thickness burn, also known as a, third degree burn, is more damaging compared to

superficial and partial thickness burns, and may involve destruction of nerve fibres and underlying structures of the skin[22,23,24].

As well as the classifications described above, burns can be described in terms of Total Body Surface Area (TBSA)[25]. This is a measure used to assess the severity of the burn as a percentage. In adults, the 'rule of nine' is used to established the extent of the burn injury, whereas in children the 'Lund-Browder' diagram, as shown in figure 1.3 below, is used to establish the severity of the burn.

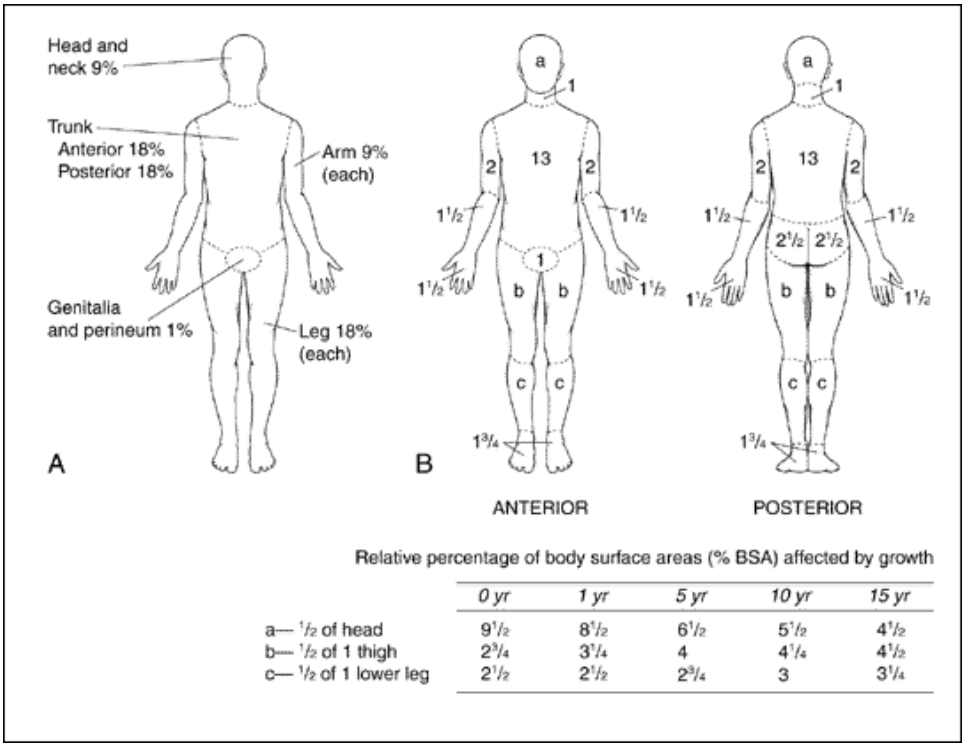

Figure 1.3: A. Rule of nines. B. Lund-Browder diagram, taken from the U.S. Department of Health & Human Services (http://chemm.nlm.nih.gov/burns.htm)

1.1.4. Treatment of burns

The standard medical advice for a scald is to cool the affected area with water for 10-30 mins and cover the area with cling film. Depending on the severity of the injury, the patient may be hospitalised to minimise infection. Upon hospitalisation, the injured area is cleaned, the dead tissue removed, the area disinfected and a dressing is applied.[26].

1.1.5. Burn infection

The survival of patients through the critical care stage, without the interference of infections, is the major hurdle arising from a burn injury. Infection of burn injuries can delay healing, increase pain levels, increase chances of scarring and may even lead to death. Due to the moist nature, elevated temperature, and nutrient rich environment of a burn wound, burns provide an ideal environment for growth of bacteria [27].Infections are known to occur more commonly in young children and the elderly patients[28]. Rapid diagnosis and appropriate treatment is necessary when an infection occurs[29]. However, the major concern when faced with an infected burn is that the infection is hard to diagnose. The symptoms related to burn injuries, hyperthermia, tachycardia and hyperventilation, are also common to patients with infected wound sites. The similarity in symptoms displayed, make diagnosis of an infection much more difficult[27].

The most common pathogens isolated from burn wounds are *Staphylococcus aureus* and *Pseudomonas aeruginosa*, others may include *Streptococcus pyogenes* and *Acinetobacter baumanni*i [3, 30, 31]. *S. aureus*, which is most commonly associated with smaller burns, produces several virulence factors such as proteinases and collagenases, a variety of exotoxins, such as toxic shock syndrome toxin-1 (TSST-1) as well as a range of endotoxins.

1.1.6. Toxic Shock Syndrome

Toxic shock syndrome is caused by infection and colonisation by a TSST-1 producing strain of bacteria, most commonly arising from a toxin-producing strain of *S. aureus*. TSST-1 is a superantigen which results in over-stimulation of the immune system[32]. Early detection of an infection caused by a TSST-1 producing strain is vital, however the early symptoms are very closely related to the early symptoms of infection of non-toxin producing stains, which in turn are very similar to the symptoms arising from the pre-existing burn injury[32].

In summary, early diagnosis of infection of burn injuries is vital in reducing the mortality rate[33].

1.1.7. Clinical diagnosis of infection

Wound infection includes regular monitoring of the patient's blood work and vital signs, as well as an inspection of the entire wound. The indications clinicians look for include conversion of classification of the burn (from partial-thickness to full-thickness), tissue necrosis and a rapid spread of cellulitis into surrounding healthy tissue[3].

Clinicians at the paediatric burn unit at Frenchay Hospital in Bristol follow strict guidelines to prevent misdiagnosis. Misdiagnosis of an infection that is present can cause death, and misdiagnosis of a non-existent infection can cause a broad cascade of issues including those linked with overuse of antibiotics, adding to the global concern of antibiotic resistance. Clinicians at the burn unit in Frenchay utilise the flow chart in Figure 1.4 when a child with a burn of any size and depth presents with any of the following symptoms: temperature above 39°C; capillary refill time of below 3.4 seconds; development of any type of rash, unexplained tachycardia or tachyponea; low white blood cell count.

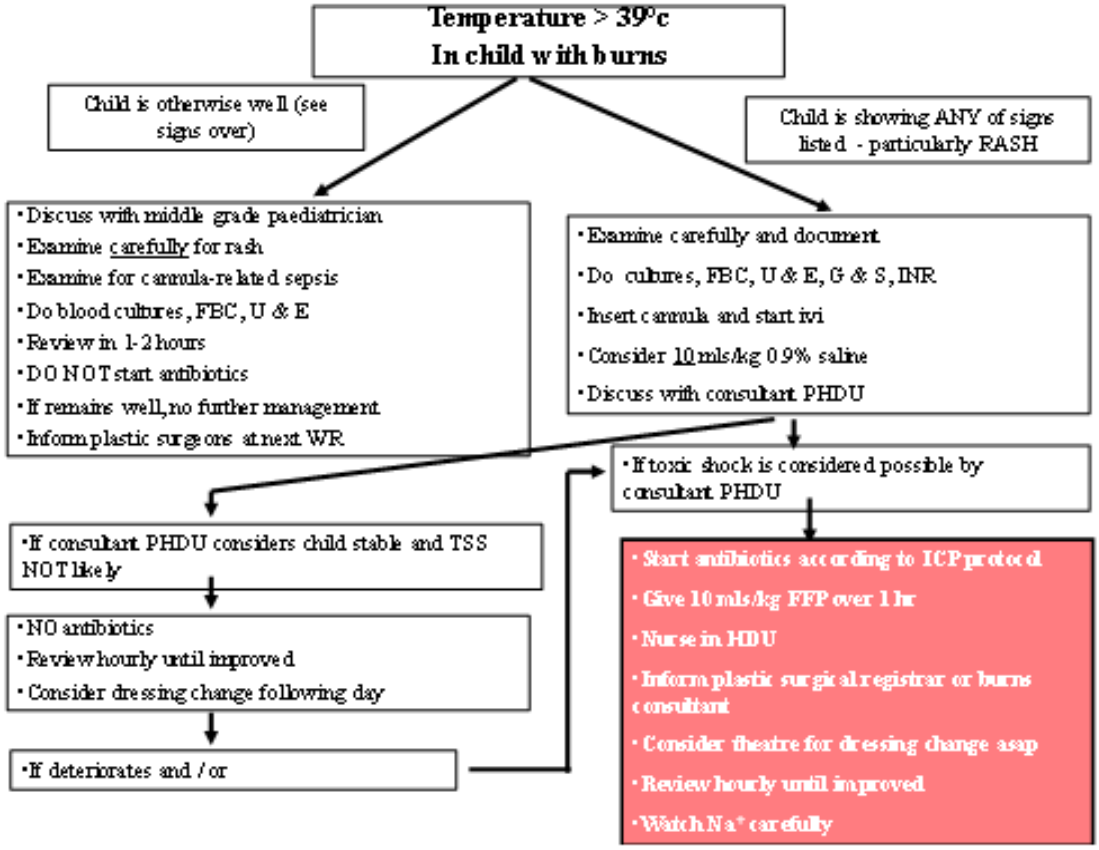

Figure 1.4: Flow chart followed by clinicians at Frenchay Hospital in Bristol in diagnosing infections in paediatric patients with burns of any size and depth. Chart supplied by Dr. Amber Young (Frenchay Hospital) and Dr. Toby Jenkins (University of Bath).

Most clinical microbiology laboratories globally rely on culturing a sample collected by swab of the surface of the skin or a tissue biopsy of the sample, and correlating the culture results to the clinical data to identify the infection type as well as the strain responsible for the infection. A detailed method of this procedure has been reported by Church et al[7].

1.1.8. Pathogenic identification method

Upon successful swabbing of the wound surface, quantitative counts may be carried out to obtain the bacterial counts per cm^2 of the wound surface. This method provides the identification of the pathogen as well as the exact count per cm^2. However, the process requires swabbing and culturing, which is time consuming[7].

Other methods include biochemical analysis, searching for known virulence factors or genes coding for specific mechanisms. Recent discoveries of molecular diagnostic tools for infectious diseases, such as the use of polymerase chain reaction (PCR), have led to a faster identification of the genotypic characteristics of the cause of infections. A major advantage of PCR is that the detection of genetic material does not require the labour intensive and time consuming process of culturing the infective organisms[34,35].

1.1. Wound dressings

Wound dressings can be defined as material(s) used as wound coverings. Dressings have been used since 2010 BC, where mixtures of herbs, ointments and oils were incorporated into occlusive bandages[36]. In the mid-20th century, the importance of maintaining a moist healing environment was determined, leading to the development of moisture-retentive dressings, such as hydrogel-based dressings, which are used extensively in the present-day.

Moisture-retentive dressings are known to not only provide a moist wound environment, but also to be beneficial in the healing process of the wound. A moisture-rich environment is thought to promote migration of keratinocytes by supporting the movement of cells and maintaining the electrical gradient[37,38,39].

Whilst it is important to develop a wound dressing that can detect bacterial infection, it is also key to encourage wound healing.

1.1.1. Commercially available dressings

Most commercially available burn wound dressings are hydrogel based; some incorporate biological matter as well as incorporation of antimicrobial factors. The most commonly used burn wound dressings include silver sulphadiazine dressings, which incorporate antimicrobial properties due to the silver, and Biobrane ™, which has wound healing enhancing properties due to the incorporation of collagen derivatives[11].

1.1.1.1. Wound dressings containing silver

The antimicrobial properties of silver-containing compounds have been exploited from as early as 1000 B.C., and due to their antimicrobial properties, silver compounds have been developed for use in medicine for centuries[40].

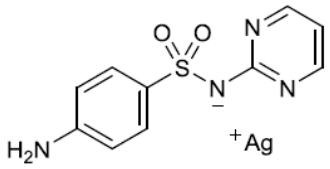

Figure 1.5: Silver surfphadiazine

Silver sulphadiazine dressings (Flammazine® and Silvadene®) were one of the first, and are still amongst the most commonly used, dressings for the treatment of burn wounds[41,42]. Despite studies revealing the disadvantages and side effects caused by the use of silver sulphadiazine dressings[43], it is still used as the reference dressing in studies that involve wound dressings comparisons[44]. Furthermore, a recent Cochrane review on dressings incorporating silver has concluded that there is insufficient evidence to show the wound healing promotion and wound infection prevention effects of dressings containing silver[45]. Alternative wound dressings containing silver were developed to minimise the side effects of silver sulphadiazine[46].

1.1.1.2. Biobrane ™

A **B**

Figure 1.6: Patients with partial thickness scald injury treated using Biobrane™: **A.** No removal of dressing; **B.** Dressing removed. (Images supplied by Dr. Amber Young, Burns unit, Frenchay Hospital, Bristol, UK.)

Biobrane™ is a biosynthetic membrane skin dressing designed to be used on superficial and partial-thickness burn wounds. It is composed of a nylon mesh with silicone membrane on which peptides derived from porcine type I collagen are bonded to, to create a dressing which can temporarily perform the actions of the epidermis layer lost due to the injury. As the wound heals and re-epithelisation occurs, the dressing lifts off revealing healed skin beneath the dressing. The dressing is designed to provide increased mobility, speed of healing and rate of epithelialisation as well as decreasing pain and length of patient hospital stay[47].

Biobrane™ has been shown to be successful in decreasing the length of hospital stays. However limitations of Biobrane™ involve steric hindrance of out flow of exudate due to the irregularity of pores and crosslinked collagen peptides. Figure 1.6 above shows images of two patients treated with Biobrane™. The patient on the left (A) was successfully treated using Biobrane™. Despite a suspected infection, the dressing was left on, and the patient made full recovery with no scar formation. The patient on the right (B) was admitted with 22% TBSA partial thickness burns and was treated with Biobrane™. The dressing was removed due to a wound site infection. The infection was treated, but the removal of the dressing left the patient with permanent scars. These two cases indicate the importance of a diagnosis of infection for effective treatment with a low risk of scar formation.

1.1.2. Requirements for an 'ideal' wound dressing

In order to develop an efficient burn wound dressing, the criteria for an 'ideal' wound dressing have to be met. Several surveys [48,42]have been conducted involving medical practitioners across the globe in order to create guidelines for an 'ideal' dressing for treatment of burns. These include elements such as the ability for a dressing to restore and act as a skin barrier, the ability to absorb excess exudate and fluid secreted by the wound, the adherence of tissue, as well as wound healing and the antimicrobial properties of a dressing.

1.1.2.1. Restoring skin barrier and wound healing

The primary and one of the most important roles of any wound dressing is to restore the broken barrier, by addition of a protective layer over the breeched area, for thermal insulation as well as for infection control[49].

In addition to a dressing which provides a provisional skin barrier, a dressing which can aid the process of wound healing, and promote the growth of cells to provide a permanent skin barrier, would be beneficial. Epithelialisation is promoted when the oxygen level in the tissue is increased, thus a dressing which allows gaseous exchange would be valuable to aiding wound healing. Moreover, addition of growth factors, such as collagen have been shown to speed up the process of epithelialisation[9,13].

1.1.2.2. Tissue adherence

Recent studies showed that dressings, which are easily removable with minimum pain, would be ideal. A study on pain management of burns showed that patients with burns suffer a significantly prolonged persistent pain due to frequent dressing changes when compared to patients with chronic wounds [50]. Furthermore, according to a globally distributed survey carried out among burn care specialists, the most important burn wound dressing characteristic is a 'non-adherent, non-traumatic wound interface'[48].

1.1.2.3. Absorbency

The absorbency of a dressing was found to be an essential property as dressings with the ability to absorb large amounts of fluid can be used to manage the exudate and wound fluids. Commercially available dressings are able to manage the fluid produced by the wound, but there has not been any evidence to show improvement in wound healing. As a result the combination of absorbency with addition of growth factors may be advantageous[51].

1.1.2.4. Antimicrobial activity

According to an online survey conducted among clinicians, the antimicrobial properties of wound dressings are essential[48]. This result is further supported by a similar survey carried out on the treatment methods chosen for partial thickness burns – silver sulphadiazine dressings are the most commonly used dressings for treatment of burns[42].

To summarise, according to global surveys involving medical professionals, the properties of an "ideal" burn wound dressing for the effective treatment of paediatric burns include low tissue adherence, absorbency, and promotion of wound healing and antimicrobial properties.

1.2. Microbiology

1.2.1. Bacteria

Bacteria are prokaryotic, unicellular microorganisms with free flowing cyclic genetic material, unbound by a membrane. Bacterial cells can be found in various different shapes such as spheres, rods, spirals and other less common shapes with size ranges of a few microns[52].

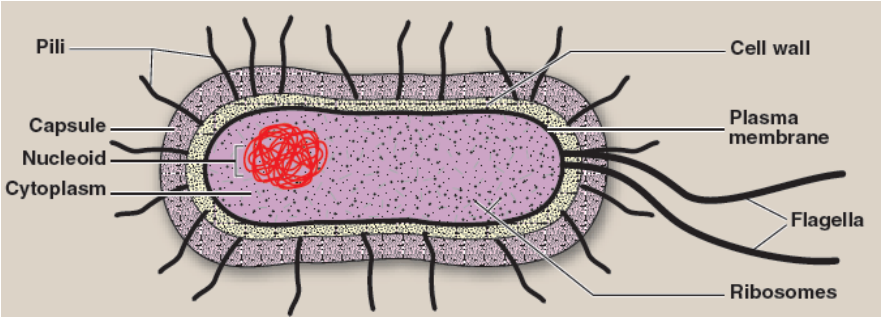

Figure 1.7: Structure of a prokaryotic cell. Image obtained from Bacterial structure, Growth and Metabolism by Richard A. et al.[53]

Pathogenic bacteria can be broken down into two main groups; opportunistic and primary pathogens. Opportunistic pathogens mainly cause disease in individuals with compromised or impaired immune systems. An example would be *Staphylococcus epidermidis*; an opportunistic pathogen and one of the most important causes of nosocomial infections. By contrast, primary pathogens can cause disease in healthy individuals with intact immunological defenses.

Bacterial infections of a burn injury are the main problems faced during treatment which can increase pain, delay the healing process and of particular concern in children, can also cause toxic shock syndrome (TSS), as stated in the previous section. The major pathogenic bacteria involved with burns infections are *Staphylococcus aureus (S. aureus)* and *Pseudomonas aeruginosa (P. aeruginosa)*. According to a study carried out in Hallym University, Hangang Sacred Heart Hospital in South Korea, the most frequently isolated bacteria from a burn patient was *P. aeruginosa* followed by *S. aureus.* The same study showed that the majority

of these isolated bacteria displayed high antibiotic resistance[19,18].

In this investigation, clinically isolated and fully sequenced strains of *S. aureus* and *P. aeruginosa* were used as highly infectious models.

1.2.2. Quorum sensing

Quorum sensing can be described as being the communication pathway used by both gram-positive and gram-negative bacteria to control cell- density dependent gene expression. This process regulates a variety of physiological functions, including the regulation of virulence factors and biofilm formation. The quorum sensing mechanism involves the production and detection of small extracellular molecules known as autoinducers, which trigger mechanisms for the expression of certain genes [54].

1.2.3. Biofilms

Bacteria in nature can exist as single cells in the planktonic phase as well as being attached to a surface in communities called biofilms. Biofilms in nature can be comprised of a single species as well as multiple species, with a predominance of single species biofilms in infected wounds or surfaces of medical instruments, and a predominance of multispecies biofilms in the environment. The most widely studied biofilm forming bacteria include *P. aeruginosa* as the gram-negative example and *S. aureus* as the gram-positive bacteria. Extensive studies of biofilm formations suggest that biofilms are a stable phase in their biological cycle which involves multiple steps from formation to dissolution of the biofilm. The formation of biofilms often involves communication; in *P. aeruginosa* it is thought to involve cell-to-cell communication[55].

The formation of a biofilm follows several stages, as displayed in Figure 1.8. Firstly bacteria attach to a surface; the cells then proliferate and form colonies, followed by the final stages of biofilm maturation and detachment of cells. The initial attachments of the cells occur by an adsorption process followed by an irreversible attachments of cells occurring though the production of adhesins[56]. The final

stages in biofilm growth are the maturation and detachment of cells.

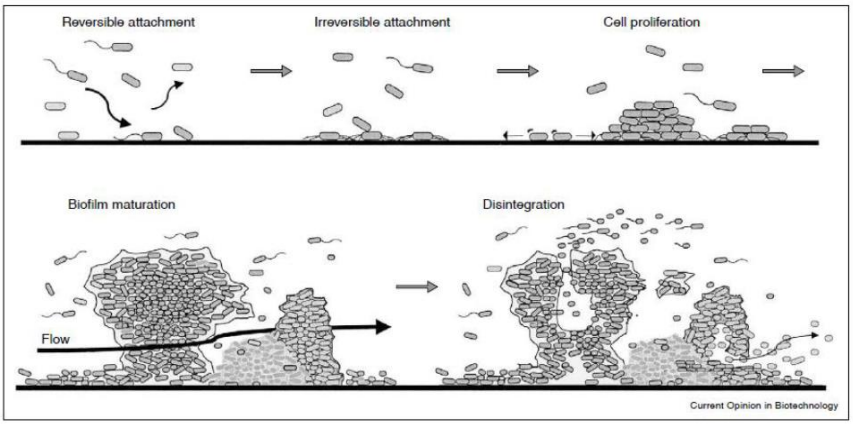

Figure 1.8: Stages of Biofilm formation [57]

Biofilms haven been known for their predominance in medical device-related infections[58], however recent studies have shown the importance of biofilm in pathogenesis of burn wound infections [59].

1.2.4. Commonly isolated bacterial strains

As discussed in a previous section of Chapter 1, the most commonly isolated bacteria from infected burn wounds include *Streptococcus pyogenes, Acinetobacter baumannii, Staphylococcus aureus* and *Pseudomonas aeruginosa*, with predominance by the latter two species.

1.2.4.1. Staphylococcus aureus

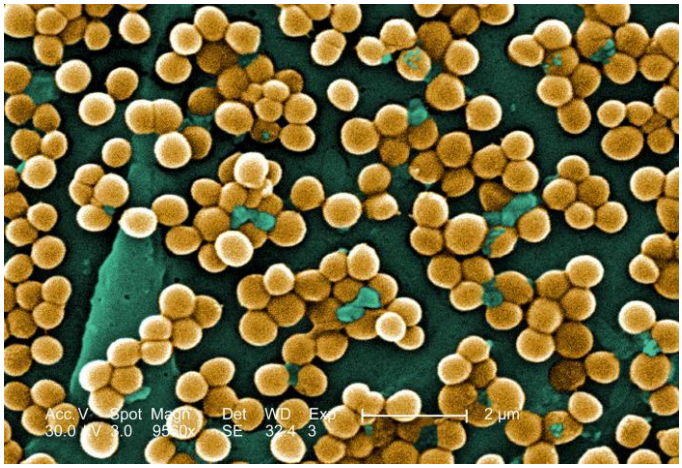

Figure 1.9: Scanning electron micrograph of Staphylococcus aureus x9560magnification (image source: Source: Carr J. H., in MRSA_PHIL #10046, Public Health Image Library.)

Staphylococcus aureus (*S. aureus*) is a gram positive bacterium (Figure 1.9). It is a human pathogen and is frequently found in human hair and skin, and yet it is one of the most common causes of skin infections[60] . Approximately 80% of the population are carriers of *S. aureus* with 20% being persistent carriers and 60% irregular carriers[61]. 30-50% of healthy adults are nasal carriers, 20% are facial carriers and 5-10% of adults are skin carriers of this type of bacteria. It can easily be spread by means of contaminated wounds and droplets to the surrounding environment[62]. Most importantly, burn site wound infections are commonly caused by this type of bacteria, with higher percentages of isolated strains being resistant to antibiotics when compared to those isolated from non-burn patients[30]. *S. aureus* is also commonly isolated from chronic wounds. In children, *S. aureus* infections can cause toxic shock syndrome, requiring more complex treatment methods.

In this investigation clinically isolated strains of *S. aureus* were used. Specifically: a strain with complete genome sequence, MSSA 476, a TSST-1 positive stain, RN4282 as well as AGR positive and negative strains, RN6390B and RN6911 respectively.

1.2.4.2. Pseudomonas aeruginosa

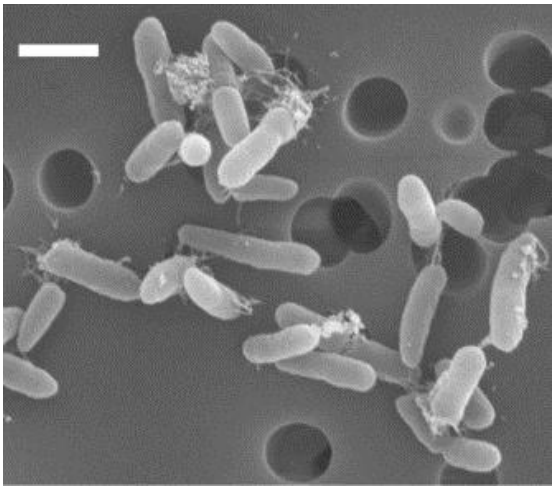

Figure 1.10: Scanning electron microscopy pictures of *P. aeruginosa* PAO1 (bar = 1 μm)[63]

Pseudomonas aeruginosa,(*P. aeruginosa*), is a rod-shaped, Gram negative and opportunistic bacterium, which can grow in a wide range of temperatures (including as high as 42°C), with optimum growth temperature of 37°C. The bacterium is typically found in water and soil as well as on plant surfaces in the planktonic form or in the form of a biofilm, if attached to a surface (Figure 1.10).

P. aeruginosa is one of the main causes of nosocomial infections with increasing incidence of antibiotic resistance[64]. A recent study performed in Turkey showed that 58 out of 170 patients with *P. aeruginosa* were patients in intensive care units, of which 57% had surgical site infection and 13% had catheter related infections [65]. A major concern is the increase in antibiotic resistance of this bacterium, including most penicillins along with a number of other antibiotics. The antibiotic resistance is often caused by rapid biofilm formation in a wound environment. As a result, any attempt to prevent bacteria from growing needs to be done prior to biofilm formation, thus by implication: as soon as a wound is caused[66]. Bacteria can also gain resistance to antibiotics by genetic mutation and horizontal gene transfer. *P. aeruginosa* is also one of the most commonly isolated pathogens in a burn infection. The origin of the infection is usually in the human gastrointestinal tract, but

colonisation occurs in sites with a compromised immune system, such as a burn wound site[62].

In this study, a clinically isolated strain of *P. aeruginosa* with complete genome sequence[64], PAO1, was used as a gram-negative and highly infectious model.

1.2.4.3. Escherichia coli

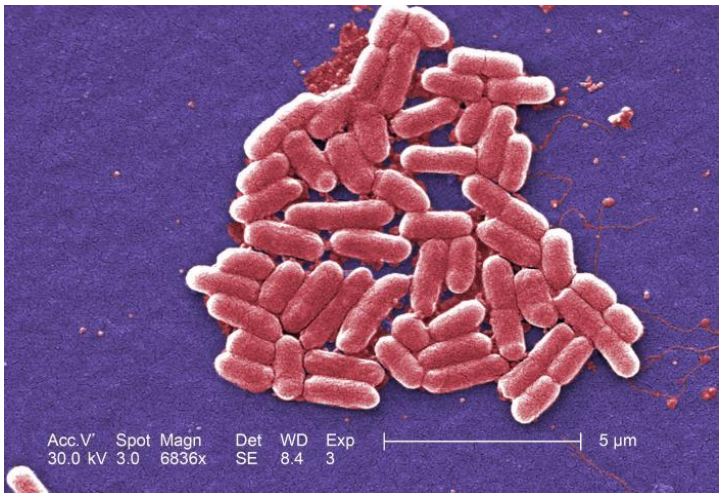

Figure 1.11: False colour SEM (x6836) of *E. coli* 0157:H7 (image source: Source: Carr J. H., in PHIL #10068, Public Health Image Library.)

Escherichia coli (*E. coli)* are rod-shaped Gram-negative bacteria ranging from 2 to 5 µm in size[67] (Figure 1.11). Generally, the majorities of *E. coli* strains are non-pathogenic and harmLess; they are found naturally in the gut flora to protect against opportunistic pathogens. Some remain pathogenic and can cause common infections such as urinary tract, and gastrointestinal tract infections[62].

In this study, a non-pathogenic strain, DH5α, was chosen as the negative control organism. All of the virulence factors have been removed; it is a strain that is often used in biological studies to produce certain proteins by genetic modification[68].

1.2.5. Bacterial virulence factors

Bacterial toxins are substances which affect the host cells in various ways. Bacteria secrete two different types of toxins; endotoxins and exotoxins. Endotoxins are often embedded within the outer layer of gram-negative bacteria, and can be released upon the decomposition of the cell wall following cell death. [52] Exotoxins are those which can be secreted by all types of pathogenic bacteria into the surrounding environment.

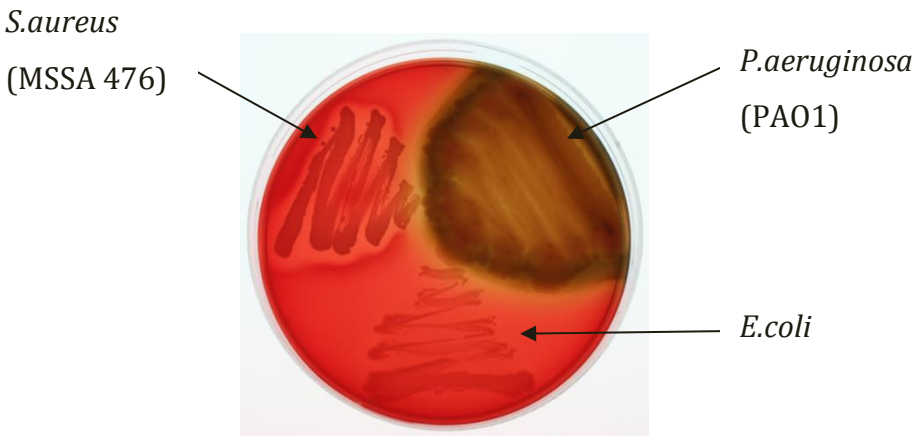

Figure 1.12: Blood agar plate showing *S .aureus* (MSSA 476) and *P. aeruginosa* (PAO1) secrete toxins that break red blood cells and that *E. coli* (DH5α) does not secrete these toxins. Acknowledgment: J.Zhou Ph.D. Thesis 2011

There are three different ways in which toxins can interfere with eukaryotic cells. Some toxins damage the cell membrane by creating pores within the membrane or by dissolving the cell membrane; an example of this would be the α-toxin secreted by strains of *S. aureus.* Other methods involve inhibiting the process of protein synthesis or disrupting ion concentration within the cell. The production of haemolytic proteins by *S. aureus* and *P. aeruginosa* is shown by means of a blood agar plate; Figure 1.12.

1.2.5.1. Exoproteins produced by *Staphylococcus aureus*

S. aureus is known to produce a wide range of toxins and exoproteins which interfere with human cells, in order to aid the colonisation process. The toxins and proteins secreted include lipases, four different types of haemolysin along with other types of proteases. There are also exoproteins which are only secreted by certain strains such as toxic shock syndrome toxins and leukocidin, and are also known as superantigens [69].

There are four types of haemolysin; Alpha, Beta, Gamma and Delta. Alpha-haemolysin, also known as alpha toxin, is produced by a wide range of *S. aureus* strains. The mechanism of action is through the formation of pores and lysis of eukaryotic cells by these pores within the cell membrane (Figure 1.13).

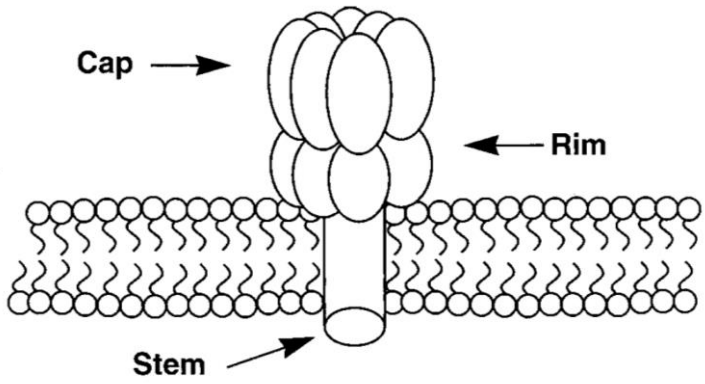

Figure 1.13: Diagram showing the mode of action of α-haemolysin. This toxin creates pores within the bilayer membrane, disrupting the cell. Modified from an image from Exotoxins of *S. aureus*, 2000. [69]

More importantly, delta-toxin is one of the main causes of cell death due to damage to the cell membrane. Delta-toxin is a very small protein, consisting of a 26-amino acid peptide (Figure 1.14), however it is able to cause total disintegration of eukaryotic cells. Its mode of action and degree of damage to the cell depends on the concentration of the protein released. At lower concentrations, the toxin is adsorbed into the membrane and causes disruption in a circular manner. As the concentration increases, the toxins aggregate and disrupt the membrane further. Upon further increase of the protein concentration, the toxin acts like a surfactant and solubilises the membrane into micelles [69].

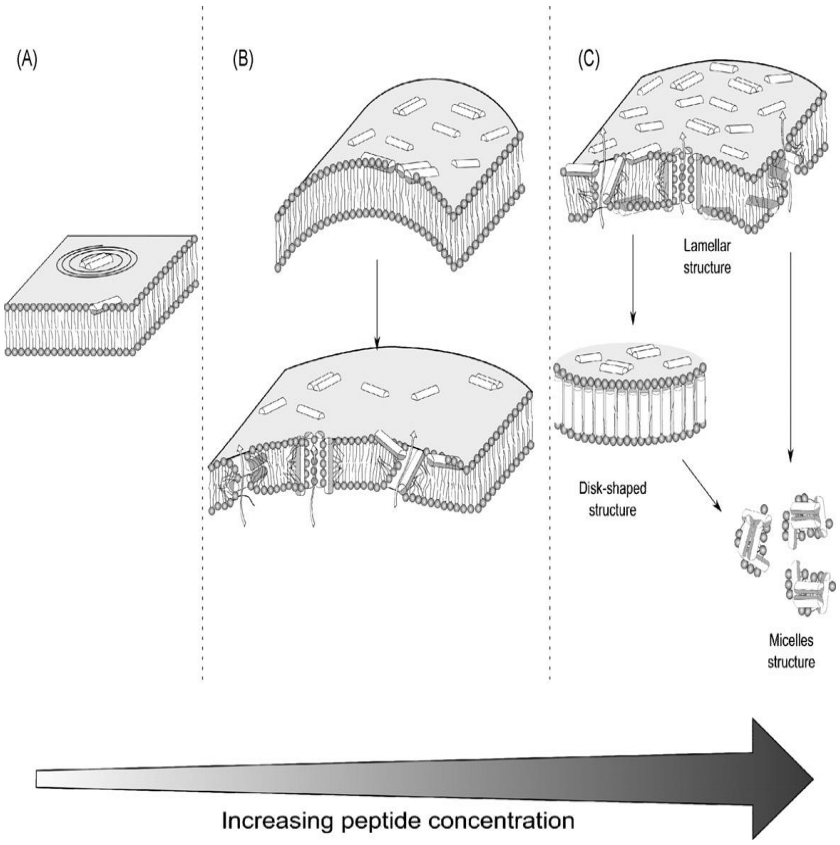

Figure 1.14: Mode of action of delta toxin[70]

Other than haemolysin, some strains of *S. aureus* are also known to secrete superantigens such as toxic shock syndrome toxins (TSST). As mentioned in Section 1.1.5, upon infection by TSST-producing bacteria in a paediatric scald injury, this toxin can cause serious damage to the child. TSS is potentially fatal and immediate treatment is required. However, the symptoms caused by this toxin are hard to distinguish from the symptoms of a scald injury, especially in a child[69].

1.2.5.2. Exoproteins produced by *Pseudomonas aeruginosa*

P. aeruginosa produces lipases such as phospholipase C, another class of membrane damaging protein. Its mode of action is to cleave phospholipids in a membrane bilayer[71,72,73]. This type of protein hydrolyses the polar head group of a phospholipid; the cleavage site is shown in the diagram below (Figure 1.15)

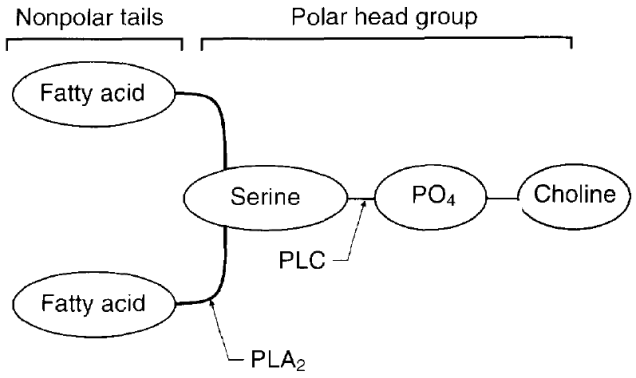

Figure 1.15: Diagram showing site of cleavage of phospholipid by phospholipase C. This toxin breaks down phospholipid membranes damaging the polar head group. This cleavage site remains the same in other phospholipids [72].

Rhamnolipids are a type of bio-surfactant produced by *P. aeruginosa*. They have been known to inhibit microbial growth by lysing cells[74] or causing alteration to the membrane structure by acting on the lipid or the surface proteins of the cell[75]. Results from studies have demonstrated the antimicrobial properties of these rhamnolipids against gram-positive bacteria[76]. As a result of these mechanisms, rhamnolipids are also thought to be one of the lipid membrane damaging agents.

1.2.5.3. Regulation of virulence factors

In the case of *S. aureus*, certain virulence factors, especially those of interest in this study, the exoproteins, are regulated by the quorum sensing system. Quorum sensing is a system controlled by the population density of bacteria and thus stimulates and regulates processes depending on the population density[77].

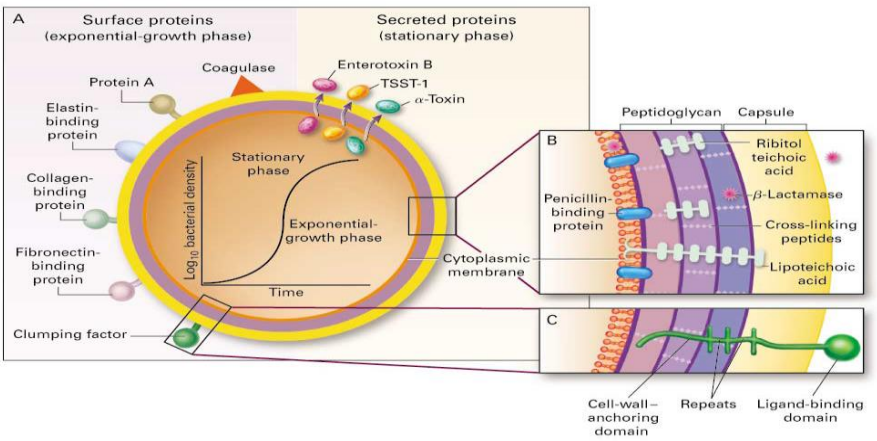

Figure 1.16: Regulation of virulence genes by *S. aureus*[79]

During the early growth stage of bacteria, the gene encoding for surface adhesion for formation of biofilm is stimulated. As the bacterial population density increases and the growth stage reaches its exponential phase, the expression of the adhesion gene decreases, and the expression of the gene coding for exoproteins production is stimulated[78]. Figure 1.16 illustrates the secretion of virulent proteins such as TSST-1 and α-toxin at the stationary phase following the exponential growth phase of a bacterial population.

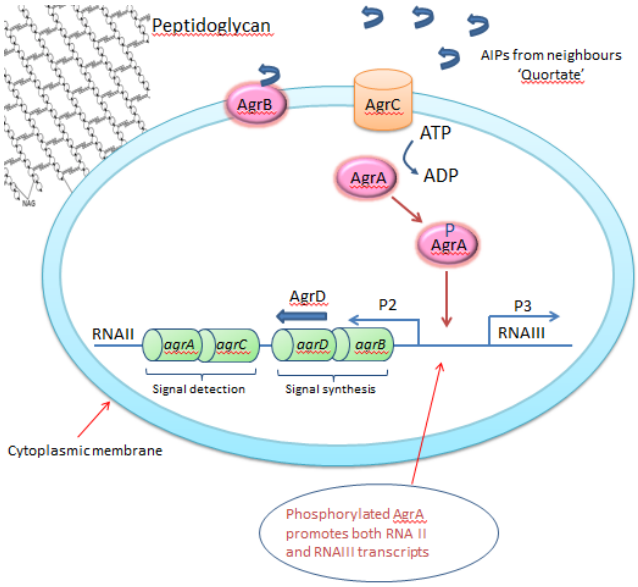

Figure 1.17: Accessory gene regulatory system. Acknowledgement: Dr. Toby Jenkins, University of Bath.

The accessory gene regulatory (AGR) system is the process that directly controls the up-regulation and down-regulation of toxins and virulence factors. The processes which occur are illustrated in the diagram in Figure 1.17. The expression of AGR gene is stimulated by the binding of Sar A protein to sequences which are upstream of the AGR gene. The stimulation of the AGR gene causes the production of AGR A, B, C. AGR B is a cytoplasmic membrane protein, which is cleaved to form AGR D –derived cyclic peptides, also known as thiolactone. As the concentration of thiolactone increases outside the cell, phosphorylation of AGR C, a cytoplasmic membrane sensor, is stimulated. The phosphorylated form of AGR C subsequently phosphorylates AGR A, which activates the production of RNA III. The activation of RNAIII causes an up-regulation of toxin production[80].

As a result, an increased bacterial population increases the concentration of AGR D-derived cyclic peptide, which promotes phosphorylation of AGR C and AGR A, resulting in activation of RNAIII and thus up-regulation of toxin production.

Up-regulation of this system results in the production and secretion of the membrane-damaging proteins. Down-regulation of this process, however, results in minimal or no production, and thus no secretion of these proteins[80,81].

Various different strains of *S. aureus* were investigated for use as the gram-positive model. The investigated strains include MSSA 476 (generic clinical isolate), RN3282 (TSST positive) USA300 (LAC) RN6390B (AGR+) RN6911 (genetic modification to obtain AGR-).

1.2.5.4. Regulation of virulence factors in *P. aeruginosa*

Along with S. aureus, the virulence factors of *P. aeruginosa* are also governed by the quorum sensing mechanism. *P. aeruginosa* produces autoinducer - signal molecules used for cell- to-cell communication, a key requirement for activation of virulence factors and genes such as *LasR* and *lab*[82]. The autoinducers bind to the regulatory proteins on the surface of the cells and induce stimulation of gene expression. This promotes the production of exoproteins such as rhamnolipids, which have been found to be one of the main proteins responsible for damage of lipid bilayer membranes. As well as stimulating the production of exoproteins, the binding of autoinducers increases the production of further autoinducers. As a result, a high density of cells in a localized area gives rise to a high concentration of these autoinducers in the localized area, which in turn causes further stimulation of virulence genes and thus an increased production of virulence factors.[78]

1.3. Lipid vesicles

The biocompatibility and biomimicry exhibited by lipid vesicles has enabled their development for a wide range of uses such as cellular models and drug delivery vehicles. In addition, their ability to encapsulate both hydrophilic and hydrophobic drugs lead to the development of vaccines, arthritis treatments and hormone replacement therapies[83].

Recent advances have focused on the development of stimuli-sensitive vesicles, which lyse upon a specific environmental trigger, allowing controlled and monitored delivery of bioactive ingredients to target sites. Targeted drug delivery using vesicles has been studied using various different environmental triggers such as pH, light, temperature, ultrasonic waves and biological and chemical agents[84].

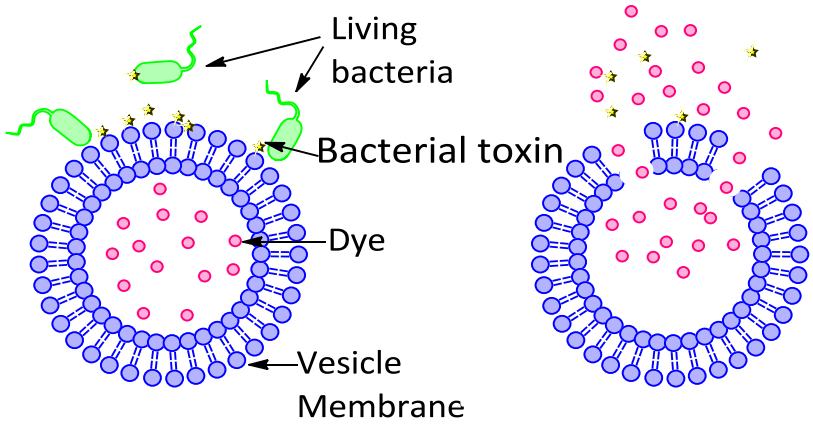

Figure 1.18: showing schematic representation of lysis of vesicle upon contact with bacterial toxin

Previous research conducted by this group focused on biological-enzyme-triggered lysis of vesicles, utilising the principal that vesicles can be designed to mimic eukaryotic cells[85]. Certain pathogenic bacteria produce and secrete membrane damaging proteins such as exotoxins, which aids bacterial colonisation by inducing cell death due to the lysis of eukaryotic cell membranes. As vesicles can be

designed to mimic eukaryotic cell membranes, vesicles can also be designed to mimic this process and lyse upon contact with bacterial membrane-damaging proteins.

This study aimed to develop a eukaryotic cell mimicking biosensor, which can detect and lyse upon contact with membrane damaging proteins secreted by pathogenic bacteria. Figure 1.18 depicts a schematic of the project concept.

1.3.1. Lipid compositions of biological membranes

The majority of biological membranes are composed of proteins and lipids. The major lipid components found in bio-membranes include glycerophospholipids (also known as phospholipids), spingolipids and sterols[86].

1.3.2. Phospholipids

Glycerophospholipids (PL) are molecules derived from glycerol molecules. Lipids with the backbone composed of sn-glycerol 3-phosphate and fatty acid alcyl chains form the basis of phospholipids such as phosphatidylcholine (PC), phosphatidylethanolamine (PE) and phosphatidylglycerol (PG). The carbon chain length of lipids ranges from 14 to 22, with predominance of 16 and 18 found in biological membranes.

Phospholipids are amphiphilic molecules and thus contain a polar hydrophilic head group, and a long fatty acid hydrocarbon tail group. In solution, these molecules align with all head groups facing the same direction, in order to minimize the energy of repulsion. Above a critical concentration, the lipids aggregate to form micelles and lipid vesicles. This critical concentration is known as the critical micelle concentration (CMC).

PCs are one of the most abundant lipid types in eukaryotic cells and are the most readily available; PCs were used as the main constituent of the vesicles developed during this study.

1.3.3. Sterols

Sterols include lipids such as cholesterol, which are major and essential components of eukaryotic cell membranes. The cholesterol concentration of a eukaryotic membrane is variable within a 0~25% cholesterol concentration range.

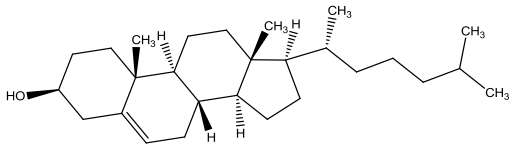

Figure 1.19: Chemical structure of Cholesterol

Cholesterol depletion studies in eukaryotic cells showed that many of the cellular functions involved the presence of cholesterol within the membrane. Cholesterol is also thought to play a major role in the bacterial virulence, as it can act as binding sites for certain proteins produced by bacteria[87].

1.3.4. Principal of vesicle formation

In 1925 Gorter and Grendel reported that lipid membranes of eukaryotic cells were arranged in a bilayer, with the hydrophobic tailgroups facing the core of the membrane and the hydrophilic headgroups facing the aqueous layer. This can be easily achieved by using the correct lipid compositions above a critical concentration[88].

1.3.4.1. Lipid polymorphism

Due to the amphiphilic nature of lipids, spontaneous micelles can be formed, as well as bilayers and lipid vesicles in aqueous solutions. The driving force of this process is minimization of energy due to unfavourable non- polar and polar interactions, as well as the maximisation of polar-polar interactions between the hydrophilic, polar head groups and water molecules[89].

Depending on the nature of the lipids, different structures can be formulated. This is due to the differences in the shape parameter of lipids. Figure 1.20 shows the different shapes of aggregates formed using lipids of various shapes.

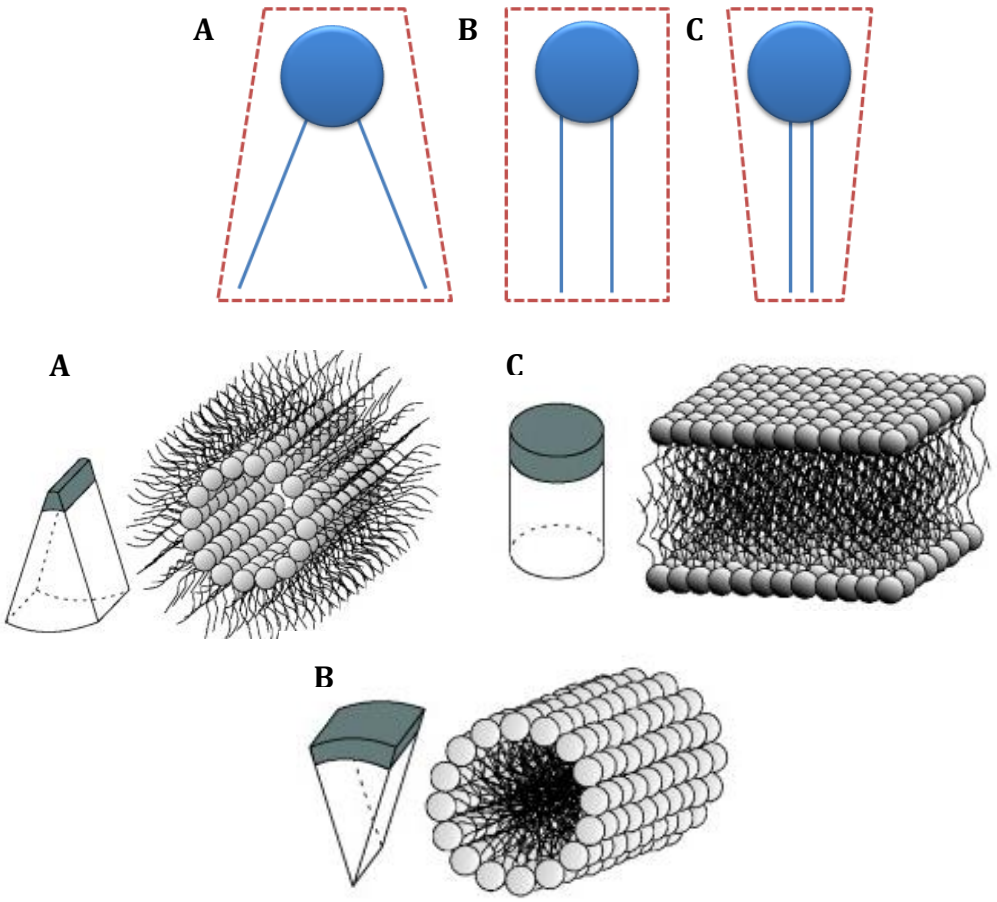

Figure 1.20: Lipid angle diagram - A: Shape parameter (S), S>1.2; B: S=1; C: S<0.6

As previous stated, the shape of the lipid aggregates is determined by the shape parameter of the lipid, which is the ratio of the volume of the lipid to the product of the area of the polar head group and the length. This is defined by the equation below, where S is the shape parameter, v is the volume, a is the area of the polar headgroup and l is the maximum length of the acyl chain.

$$S = \frac{v}{al}$$

PCs have a shape parameter of approximately 1, thus, according to Figure 1.20, they are cylindrical in shape, and can form bilayers with lamellar aggregates.

However, the shape parameter can only be used to predict and define the shapes formation of single-phospholipid structures. In order to predict the shape formation of a lipid mixture, the average shape parameter (P) can be used:

$$\mathrm{P} = \frac{N_x v_x + N_y v_y}{(N_x a_x + N_y a_y)h} = \frac{v_x + R_e v_y}{(a_x + R_e a_y)h}$$

Where v_x and v_y are the volume of the two lipids used, a_x and a_y are the polar head group areas, R_e is the molar ratio (N_y/N_x) and h is the average thickness of the mixed monolayer. When P-parameter value equals one, the average cross sectional area of the acyl chain equals the average cross sectional area of the head groups, thus formation of a cylindrical, planar bilayer, formation.

The planar bilayers follow a so-called self-assembly principal to form closed bilayer systems such as vesicles, to minimise the energy cost [90].

1.3.4.2. Principals of lipid self-assembly

The formation of vesicles from planar bilayer structures depends on the energy barrier trade-off. The planer bilayer system can be 'opened', with the end acyl chain groups exposed to the surrounding, or 'closed' by bending the bilayer system, to obtain a system with no exposed acyl chain.

In an 'opened' planar bilayer, the spacing between the molecules will be thermodynamically favoured over the 'closed' bilayer, where the close packing of the molecules will change the molecular spacing, requiring more energy to maintain the structure. However in an aqueous media, the interaction of the aqueous phase with the 'opened' bilayer will be thermodynamically unfavourable, compared to the interaction of the aqueous phase with the 'closed' bilayer. Thus, depending on the surrounding media, the bilayer will exist as the more thermodynamically favourable state. And the formation of vesicles is due to the overall lower energy cost.

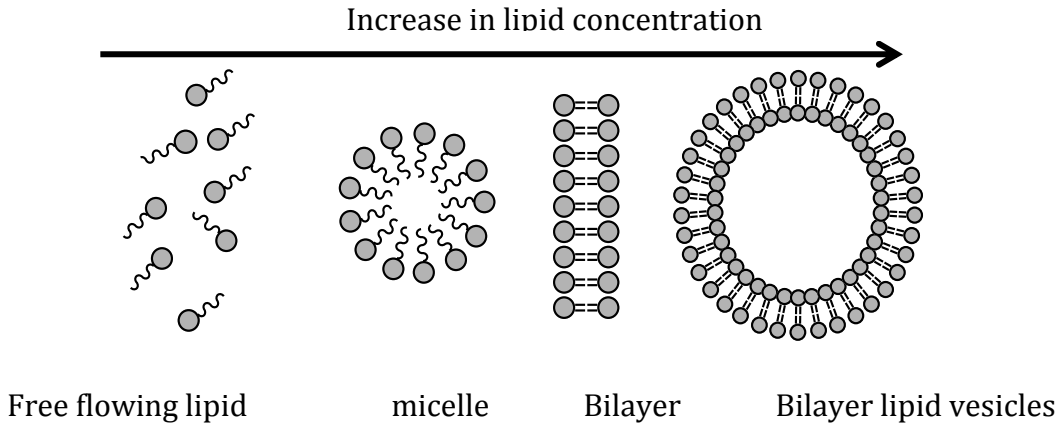

Figure 1.21: Self-assembly of lipids into different shapes as concentration increases[91]

Lipids can self-assemble to form vesicles of various sizes. These can be divided into four main categories, small unilamellar vesicles (SUV), large unilamellar vesicles (LUV), giant unilamellar vesicles (GUV) and multilamellar vesicles (MLV). SUVs are approximately 20-50nm in diameter, consist of a single lipid bilayer and are thermodynamically unstable due to their small size.

LUVs have diameters ranging between 100nm up to 5μm. These can be made by free-thawing methods, which induce fusion of SUVs, followed by extrusion through polycarbonate filters that produce uniform LUVs.

GUVs are approximately 5 to 300 μm in diameter. These are large liposomes which can be viewed with optical microscopy. The size of these giant liposomes bares a closer resemblance to eukaryotic in comparison to other liposomes. As such, they can be viewed as excellent candidates for use as cell models, however, due to their large diameter, they hold large internal volumes, rendering them fragile[92].

As the name suggests, MLVs are multi-compartmental vesicles and thus consist of more than one bilayer vesicle. These vary greatly in size, and are relatively easily formed[89,58].

1.3.4.3. Lamellar phases

As mentioned above, phospholipids are cylindrical in shape, and therefore form lamellar aggregates. Within the aggregate, and depending on the lipid chain length, temperature and pressure, lipid aggregates can be in different lamellar phases[93]. Typically there are two major phases:

- L_{α}– lamellar liquid-crystalline phase
- L_{β}– lamellar gel phase

The lamellar gel phase is when the bilayer is at a 'solid' state and the lamellar liquid-crystalline phase is when the bilayer is at the 'liquid' state. The transition between the lamellar gel phase and lamellar liquid-crystalline phase is often referred to as 'melting'. This melting temperature is also known as the transition temperature (T_m).

The greater the transition temperature, the more stable the vesicles would be at higher temperatures. This can be applied to the vesicles being investigated in this study. Previous studies have been conducted using DMPC as the bulk lipid with transition temperature being 23˚C, much lower than the testing temperature (37˚C)[94]. As a result, lipids with higher transition temperatures (DPPC, DHPC and DSPC) were used in this study and their effect on stability was observed.

1.4. Aims and Objectives

The overall aim of this project was to develop a wound dressing which incorporates a pathogenic bacterial toxin sensing element as well as an element for enhancing wound healing for the management of paediatric burns.

The primary objective of this research was to improve the pre-existing bacterial sensor component. The pre-existing sensor consisted of mainly DMPC and TCDA s showing response to pathogenic bacteria and minimal stability. This system was improved through altering the composition of the sensor element as well as incorporation of various other stabilising agents.

On successful improvement of the sensor, the secondary objective was to incorporate the phospholipid based sensors were incorporated into a hydrogel matrix, where a range of gels were screened to identify the optimum gel composition with minimum interference to the action of the sensor whist protecting and retaining hydrated environment.

The final objective was to produce a prototype dressing, with the capability of sensing the presence of pathogenic bacteria. Vesicles were embedded in a hydrogel matrix to produce gel-block type prototype as well as a gel-coated fabric prototype which used non-woven polypropylene as a scaffold. A final collagen I coating was used to add a wound healing enhancement element to the prototype. Individual components of the end prototype were tested for their cytotoxic activity using eukaryotic cell lines.

1.5. References

1. Pruitt, J. B. A.; McManus, A. T.; Kim, S. H.; Goodwin, C. W., Burn Wound Infections: Current Status. *World Journal of Surgery* **1998,** *22* (2), 135-145.

2. Schultz, G., Molecular regulation of wound healing. *Acute and chronic wounds: Nursing management. 2nd edition. St. Louis, MO: Mosby* **1999**, 413-429.

3. Jenkins, A. T. A.; Young, A., Smart dressings for the prevention of infection in pediatric burns patients. *Expert Review of Anti-infective Therapy* **2010,** *8* (10), 1063-1065.

4. Martin, P., Wound healing--aiming for perfect skin regeneration. *Science* **1997,** *276* (5309), 75-81.

5. Goldsmith, L. A., My organ is bigger than your organ. *Archives of dermatology* **1990,** *126* (3), 301.

6. Sai K, P.; Babu, M., Collagen based dressings—a review. *Burns* **2000,** *26* (1), 54-62.

7. Church D, Burn wound infections. *Clin Microbiol Rev* **2006,** *19* (2), 403–434.

8. Ian Hymes, W. B., Belinda Prescott, *Thermal radiation: physiological and pathological effects* Rugby: Institution of Chemical Engineers: 1996.

9. Boateng, J. S.; Matthews, K. H.; Stevens, H. N. E.; Eccleston, G. M., Wound healing dressings and drug delivery systems: A review. *Journal of Pharmaceutical Sciences* **2008,** *97* (8), 2892-2923.

10. Sharma, R. K.; Parashar, A., Special considerations in paediatric burn patients. *Indian journal of plastic surgery: official publication of the Association of Plastic Surgeons of India* **2010,** *43* (Suppl), S43.

11. Mathangi Ramakrishnan, K.; Babu, M.; Mathivanan, J. V.; Shankar, J., Advantages of collagen based biological dressungs in the management og superficial and and superficial partial thickness burns in children, *Ann Burns Fire Disasters* **2013**, 26(2), 98-104

12. Palmieri, Topical Treatment of Pediatric Patients with Burns: A Practical Guide. *American journal of clinical dermatology* **2002,** *3* (8), 529-534.

13. Yang HT, Y. H., Cho YS, Kim D, Hur J, Chun W, Kim JH, Seo CH, Lee BC, Koh JH, Treatment of Deep Second Degree Burn Wound using Heterogenic Type I Collagen Dressing. *J Korean Burn Soc* **2010,** *13* (2), 3.

14. Nelson, K. J.; Beierle, E. A., Exhaust system burn injuries in children. *Journal of Pediatric Surgery* **2005,** *40* (4), 43-46.

15. Gauglitz, G.; Jeschke, M., Acute treatment of severely burned pediatric patients. In *Handbook of Burns*, Jeschke, M.; Kamolz, L.-P.; Sjöberg, F.; Wolf, S., Eds. Springer Vienna: **2012**; 241-257.

16. Bronstein, A. C.; Spyker, D. A.; Cantilena JR, M., PhD, Louis R; Green, J. L.; Rumack, B. H.; Giffin, S. L., 2009 annual report of the American association of poison control centers' national poison data system (NPDS): 27th annual report. *Clinical Toxicology* **2010,** *48* (10), 979-1178.

17. Dunn, K. *UK burn injury data 1986-2007*; International Bur Injury Database: **2008**.

18. DC Kim, D. N., Epidemiology of Burns in Korea. *Journal of Korean Burn Society* **2011,** *14* (1), 6-11.

19. Chun, W., Burns in South Korea. Hong, S.-H., Ed. Seoul South korea **2011**.

20. Chung JA, J. Y., Kim MC, Ko JH, Lee JW, Oh SJ, Seo DK, Analysis of 2759 Pesiatric Burn Patients: 2000-2004. *J Korean Soc Plast Reconstr Surg* **2006,** *33* (5), 581-586.

21. Evers, L. H.; Bhavsar, D.; Mailänder, P., The biology of burn injury. *Experimental Dermatology* **2010,** *19* (9), 777-783.

22. Reed, J. L.; Pomerantz, W. J., Emergency Management of Pediatric Burns. *Pediatric Emergency Care* **2005,** *21* (2), 118-129.

23. Sheridan, R. L., Sepsis in pediatric burn patients. *Pediatric Critical Care Medicine* **2005,** *6* (3), S112-119.

24. Joffe, M. Emergency care of moderate and severe thermal burns in children. http://www.uptodate.com/contents/emergency-care-of-moderate-and-severe-thermal-burns-in-children.

25. Duffy, B. J.; McLaughlin, P. M.; Eichelberger, M. R., Assessment, triage, and early management of burns in children. *Clinical Pediatric Emergency Medicine* **2006,** *7* (2), 82-93.

26. NHS, Treating burns and scalds. **2012**.

27. Edwards-Jones, V.; Greenwood, J. E., What's new in burn microbiology?: James Laing Memorial Prize Essay 2000. *Burns* **2003,** *29* (1), 15-24.

28. Pruitt, B., The diagnosis and treatment of infection in the burn patient. *Burns* **1984,** *11* (2), 79-91.

29. Farroha, A.; Frew, Q.; Jabir, S.; Dziewulski, P., Staphylococcal scalded skin syndrome due to burn wound infection. *Annals of burns and fire disasters* **2012,** *25* (3), 140-142.

30. Song, W.; Lee, K. M.; Kang, H. J.; Shin, D. H.; Kim, D. K., Microbiologic aspects of predominant bacteria isolated from the burn patients in Korea. *Burns* **2001,** *27* (2), 136-139.

31. LAWRENCE, J., Burn bacteriology during the last 50 years. *Burns* **1992,** *18*, S23-S29.

32. Laabei, M.; Young, A.; A. Jenkins, A. T., In Vitro Studies of Toxic Shock Toxin-1–secreting Staphylococcus aureus and Implications for Burn Care in Children. *The Pediatric infectious disease journal* **2012,** *31* (5), 73-77

33. (a) McAllister, R. M. R.; Mercer, N. S. G.; Morgan, B. D. G.; Sanders, R., Early diagnosis of staphylococcal toxaemia in burned children. *Burns* **1993,** *19* (1), 22-25; (b) White, M.; White, K.; Thornton, A. E. R.; Young, Early diagnosis and treatment of toxic shock syndrome in paediatric burns. *Burns* **2005,** *31* (2), 193-197.

34. Steiner, I.; Steiner, E.; Schmutzhard, J.; Sellner, A.; Chaudhuri, P. G. E.; Kennedy, EFNS-ENS guidelines for the use of PCR technology for the diagnosis of infections of the nervous system. *European journal of neurology* **2012,** *19* (10), 1278-1291.

35. Bhatnagar, J.; Bhatnagar, D. M.; Blau, W. J.; Shieh, C. D.; Paddock, C.; Drew, L.; Liu, T.; Jones, M.; Patel, S. R.; Zaki, Molecular Detection and Typing of Dengue Viruses from Archived Tissues of Fatal Cases by RT-PCR and Sequencing: Diagnostic and Epidemiologic Implications. *The American journal of tropical medicine and hygiene* **2012,** *86* (2), 335-340.

36. Dow, G.; Browne, A.; Sibbald, R. G., Infection in chronic wounds: controversies in diagnosis and treatment. *Ostomy/wound management* **1999,** *45* (8), 23-7, 29-40

37. Clark, R. A. F., Fibronectin Matrix Deposition and Fibronectin Receptor Expression in Healing and Normal Skin. *Journal of investigative dermatology* **1990,** *94* (s6), S128-134.

38. Larjava, H.; Larjava, T.; Salo, K.; Haapasalmi, R. H.; Kramer, J.; Heino, Expression of integrins and basement membrane components by wound keratinocytes. *The Journal of clinical investigation* **1993,** *92* (3), 1425-1435.

39. Gabbiani, G.; Gabbiani, Cytoplasmic filaments and gap junctions in epithelial cells and myofibroblasts during wound healing. *The Journal of cell biology* **1978,** *76* (3), 561-568.

40. Russell, A. D.; Hugo, W. B., 7 Antimicrobial Activity and Action of Silver. In *Progress in Medicinal Chemistry*, Ellis, G. P.; Luscombe, D. K., Eds. Elsevier: **1994**; (31), 351-370.

41. Fox, C. L., Silver sulfadiazine—a new topical therapy for pseudomonas in burns: Therapy of pseudomonas infection in burns. *Archives of Surgery* **1968,** *96* (2), 184-188.

42. Hermans, M. H. E., Results of an Internet Survey on the Treatment of Partial Thickness Burns, Full Thickness Burns, and Donor Sites. *Journal of Burn Care & Research* **2007,** *28* (6), 835-847 10.1097/BCR.0b013e3181599b88.

43. Fuller, F. W., The Side Effects of Silver Sulfadiazine. *Journal of Burn Care & Research* **2009,** *30* (3), 464-470

44. Singer, A.; Dagum, Current Management of Acute Cutaneous Wounds. *The New England journal of medicine* **2008,** *359* (10), 1037-1046.

45. Storm-Versloot, M.; Vos, C.; Ubbink, D.; Vermeulen, H., Topical silver for preventing wound infection. *Cochrane Database Syst Rev,* (3), **2010**

46. Aziz, Z.; Aziz, S. F.; Abu, N. J.; Chong, A systematic review of silver-containing dressings and topical silver agents (used with dressings) for burn wounds. *Burns* **2012,** *38* (3), 307-318.

47. Greenwood JE, C. J., Kavanagh S., Experience with biobrane: uses and caveats for success. *Eplasty.* **2009,** *9*, 25 -25

48. Selig, H.; Selig, D.; Lumenta, M.; Giretzlehner, M.; Jeschke, D.; Upton, L.; Kamolz, The properties of an "ideal" burn wound dressing – What do we need in daily clinical practice? Results of a worldwide online survey among burn care specialists. *Burns* **2012,** *38* (7), 960-966.

49. Salas Campos L, F. M. M., Martínez de la Chica AM., Topical chemotherapy for the treatment of burns. *Rev Enferm.* **2005,** *28* (5), 67-70.

50. Browne, A.; Browne, R.; Andrews, S.; Schug, F.; Wood, Persistent Pain Outcomes and Patient Satisfaction With Pain Management After Burn Injury. *The Clinical journal of pain* **2011,** *27* (2), 136-145.

51. Selig, H. F.; Lumenta, D. B.; Giretzlehner, M.; Jeschke, M. G.; Upton, D.; Kamolz, L. P., The properties of an "ideal" burn wound dressing – What do we need in daily clinical practice? Results of a worldwide online survey among burn care specialists. *Burns* **2012,** *38* (7), 960-966.

52. Richard V. Goering, P. D., *Medical Microbiology*. Morsby: **2008**.

53. Harvey, R. A.; Champe, P. C.; Fisher, B. D., Lippincott's illustrated reviews: microbiology. *Lippincott Williams & Wilkins, Philadelphia* **2007**.

54. Bassler, B.; Miller, M., Quorum Sensing. In *The Prokaryotes*, Rosenberg, E.; DeLong, E.; Lory, S.; Stackebrandt, E.; Thompson, F., Eds. Springer Berlin Heidelberg: **2013**; 495-509.

55. (a) Davies, D. G.; Davies, The Involvement of Cell-to-Cell Signals in the Development of a Bacterial Biofilm. *Science* **1998,** *280* (5361), 295-298; (b) O'Toole, G.; O'Toole, H.; Kaplan, R.; Kolter, BIOFILMFORMATION ASMICROBIALDEVELOPMENT. *Annual review of microbiology* **2000,** *54* (1), 49-79.

56. Stoodley, P.; Sauer, K.; Davies, D.; Costerton, J. W., Biofilms as complex differentiated communities. *Annual Reviews in Microbiology* **2002,** *56* (1), 187-209.

57. Molin, S.; Tolker-Nielsen, T., Gene transfer occurs with enhanced efficiency in biofilms and induces enhanced stabilisation of the biofilm structure. *Current opinion in biotechnology* **2003,** *14* (3), 255-261.

58. Tamilvanan, S.; Venkateshan, N.; Ludwig, A., The potential of lipid- and polymer-based drug delivery carriers for eradicating biofilm consortia on device-related nosocomial infections. *Journal of Controlled Release* **2008,** *128* (1), 2-22.

59. Trafny, E. A., Susceptibility of adherent organisms from Pseudomonas aeruginosa and Staphylococcus aureus strains isolated from burn wounds to antimicrobial agents. *International journal of antimicrobial agents* **1998,** *10* (3), 223-228.

60. Chen, S.; Chen, S.; Jiang, S.; Xiong, M.; Luo, J.; Tang, J.; Ge, Z., Environmentally Friendly Antibacterial Cotton Textiles Finished with Siloxane Sulfopropylbetaine. *ACS Applied Materials & Interfaces, 3* (4), **2011,** 1154-1162,

61. Kluytmans, J., Nasal carriage of Staphylococcus aureus: epidemiology, underlying mechanisms, and associated risks. *Clinical microbiology reviews* **1997,** *10* (3), 505.

62. Tom Elliott, T. W., Husam Osman and Martin Gill, *Lecture Notes: Medical Microbiology*. 4th ed.; Blackwell Publishing Ltd: 2007.

63. Sun, X.; Danumah, C.; Liu, Y.; Boluk, Y., Flocculation of bacteria by depletion interactions due to rod-shaped cellulose nanocrystals. *Chemical Engineering Journal* **2012,** *198–199* (0), 476-481.

64. Stover, C. K.; Olson, Complete genome sequence of Pseudomonas aeruginosa PAO1, an opportunistic pathogen. *Nature,* **2000,** *406* (6799), 959.

65. Onguru, P., Imipenem-resistant Pseudomonas aeruginosa: risk factors for nosocomial infections. *Journal of Korean Medical Science* **2008,** *23* (6), 982.

66. HarrisonBalestra, C.; Harrison, B., A Wound Isolated Pseudomonas aeruginosa Grows a Biofilm In Vitro Within 10 Hours and Is Visualized by Light Microscopy. *Dermatologic surgery* **2003,** *29* (6), 631.

67. Kubitschek, H. E., Cell volume increase in Escherichia coli after shifts to richer media. *J Bacteriol.* **1990,** *1* (172), 94-101.

68. Chart, H.; Smith, H.; La Ragione, R.; Woodward, M. J., An investigation into the pathogenic properties of Escherichia coli strains BLR, BL21, DH5α and EQ1. *Journal of applied microbiology* **2000,** *89* (6), 1048-1058.

69. Dinges, M. M., Exotoxins of Staphylococcus aureus. *Clinical microbiology reviews* **2000,** *13* (1), 16.

70. Verdon, J., [delta]-hemolysin, an update on a membrane-interacting peptide. *Peptides* **2009,** *30* (4), 817.

71. Blackwell, G. J., Inhibition of phospholipase. *British Medical Bulletin* **1983,** *39* (3), 260.

72. Songer, J. G., Bacterial phospholipases and their role in virulence. *Trends in Microbiology* **1997,** *5* (4), 156-161.

73. Titball, R. W., Bacterial phospholipases C. *Microbiol. Mol. Biol. Rev.* **1993,** *57* (2), 347-366.

74. Cameotra, S. S.; Makkar, R. S., Recent applications of biosurfactants as biological and immunological molecules. *Current Opinion in Microbiology* **2004,** *7* (3), 262-266.

75. Sotirova, A.; Spasova, D.; Vasileva-Tonkova, E.; Galabova, D., Effects of rhamnolipid-biosurfactant on cell surface of Pseudomonas aeruginosa. *Microbiological Research* **2009,** *164* (3), 297-303.

76. Bharali, P.; Saikia, J. P.; Ray, A.; Konwar, B. K., Rhamnolipid (RL) from Pseudomonas aeruginosa OBP1: A novel chemotaxis and antibacterial agent. *Colloids and Surfaces B: Biointerfaces* **2013,** *103* (0), 502-509.

77. Williams, P.; Williams, Quorum sensing, communication and cross-kingdom signalling in the bacterial world. *Microbiology* **2007,** *153* (12), 3923-3938.

78. Wilson, B. A.; Salyers, A. A.; Whitt, D. D.; Winkler, M. E., *Bacterial pathogenesis: A molecular approach*. American Society for Microbiology (ASM): 2011.

79. Lowy, F. D., Staphylococcus aureus infections. *New England Journal of Medicine* **1998,** *339* (8), 520-532.

80. Yarwood, J.; Yarwood, P.; Schlievert, Quorum sensing in Staphylococcus infections. *The Journal of clinical investigation* **2003,** *112* (11), 1620-1625.

81. Abdelnour, A.; Arvidson, S.; Bremell, T.; Ryden, C.; Tarkowski, A., The accessory gene regulator (agr) controls Staphylococcus aureus virulence in a murine arthritis model. *Infection and immunity* **1993,** *61* (9), 3879-3885.

82. Pearson, J. P.; Gray, K. M.; Passador, L.; Tucker, K. D.; Eberhard, A.; Iglewski, B. H.; Greenberg, E., Structure of the autoinducer required for expression of Pseudomonas aeruginosa virulence genes. *Proceedings of the National Academy of Sciences* **1994,** *91* (1), 197-201.

83. Limayem Blouza, I.; Charcosset, C.; Sfar, S.; Fessi, H., Preparation and characterization of spironolactone-loaded nanocapsules for paediatric use. *International Journal of Pharmaceutics* **2006,** *325* (1–2), 124-131.

84. Mufamadi, M. S.; Pillay, V.; Choonara, Y. E.; Du Toit, L. C.; Modi, G.; Naidoo, D.; Ndesendo, V. M. K., A Review on Composite Liposomal Technologies for Specialized Drug Delivery. *Journal of Drug Delivery* **2011,** *2011*.

85. Zhou, J.; Loftus, A. L.; Mulley, G.; Jenkins, A. T. A., A Thin Film Detection/Response System for Pathogenic Bacteria. *Journal of the American Chemical Society* **2010,** *132* (18), 6566-6570.

86. Yeagle, P. L., *The Structure of Biological Membranes*. 2011.

87. Thet, N. T.; Hong, S. H.; Marshall, S.; Laabei, M.; Toby, A.; Jenkins, A., Visible, colorimetric dissemination between pathogenic strains of Staphylococcus aureus and Pseudomonas aeruginosa using fluorescent dye containing lipid vesicles. *Biosensors and Bioelectronics* **2012,** *41* (0), 538-543.

88. Gorter, E.; Gorter, ON BIMOLECULAR LAYERS OF LIPOIDS ON THE CHROMOCYTES OF THE BLOOD. *The Journal of experimental medicine* **1925,** *41* (4), 439-443.

89. Luckey, M., *Membrane structural biology : with biochemical and biophysical foundations*. Cambridge University Press: Cambridge, 2008.

90. Antonietti, M.; Förster, S., Vesicles and Liposomes: A Self-Assembly Principle Beyond Lipids. *Advanced Materials* **2003,** *15* (16), 1323-1333.

91. Edler, D. K., 2nd Year Lecture notes. University of Bath: 2008.

92. Moscho, A.; Orwar, O.; Chiu, D. T.; Modi, B. P.; Zare, R. N., Rapid preparation of giant unilamellar vesicles. *Proceedings of the National Academy of Sciences* **1996,** *93* (21), 11443-11447.

93. Luzzati, V.; Tardieu, A.; Luzzati, A., Lipid Phases: Structure and Structural Transitions. *Annual review of physical chemistry* **1974,** *25* (1), 79-94.

94. Keough, K. M. W., Gel to liquid-crystalline phase transitions in water dispersions of saturated mixed-acid phosphatidylcholines. *Biochemistry* **1979,** *18* (8), 1453.

Chapter Two: Materials, methods and instrumentation theory

2.1. Fluorescence

The use of fluorescence has broadened extensively, not only in fluorescence spectroscopy and time resolved fluorescence but also in application for biological sciences. Its use has been extended to environmental monitoring as well as genetic analysis and DNA sequencing[1].

Fluorescence is one of two categories of luminescence. Luminescence is the emission of light from a substance from an electronically excited state. Depending

on the nature of the excited state, the luminescence can be divided into the two categories, fluorescence and phosphorescence[1].

2.1.1. Principals of fluorescence and phosphorescence

Fluorescence and phosphorescence, as described above, can be defined as being the emission of light by a substance that has absorbed energy through a light source or other electromagnetic radiation.

Fluorescence involves the transitions of electrons from an electronically excited state to the ground state. In a singlet exited state the excited electron has the opposite spin to the electron on the ground state orbital, therefore the transition is spin allowed. As a result, the transition occurs rapidly. The Jablonski diagram (figure 2.1) shows the difference pathways of electrons when excited and relaxed due to absorption and emission of energy.

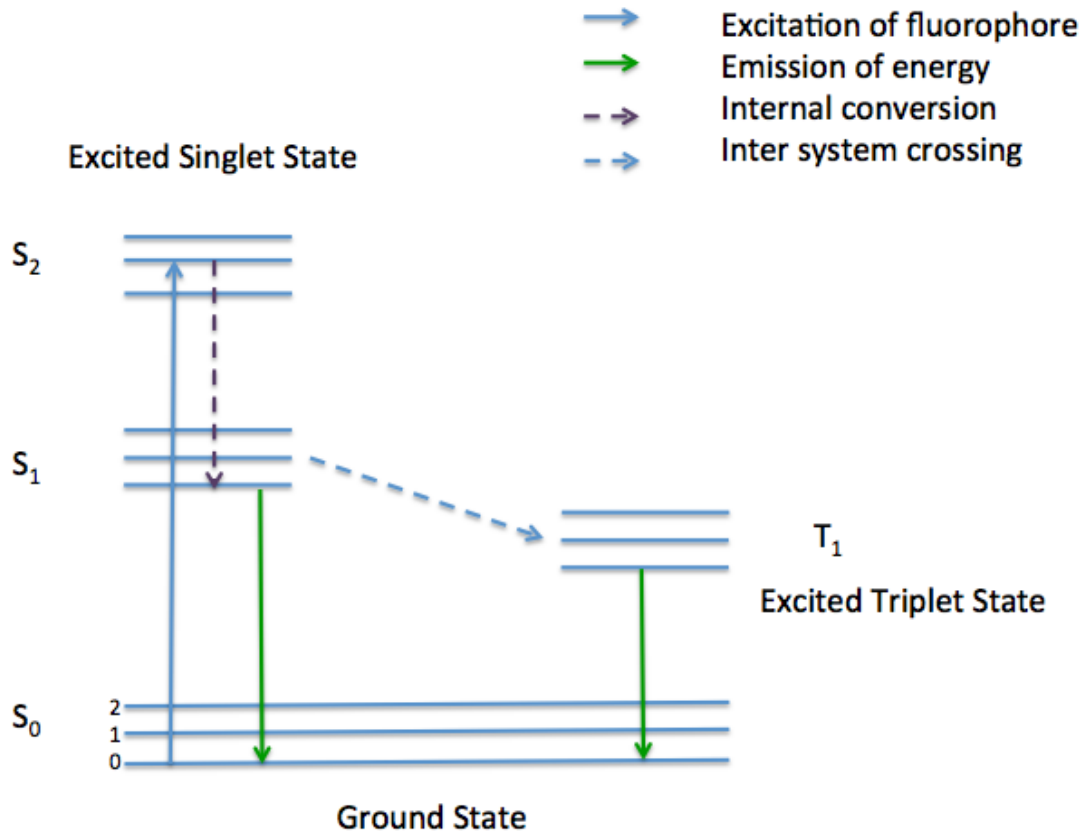

Figure 2.1: The Jablonski diagram, illustrating the excitation of a fluophore to the higher energy level and emission of fluorescence and phosphorescence as the fluophore moves back down to the ground state.

The Jablonski diagram above illustrates the process which occurs between absorption and emission of light. The diagram displays different electronic states, the singlet (S) and the triplet (T). In a singlet state, all of the electrons in the molecules have paired electrons and in a triplet state, only one set of electrons is unpaired. At room temperature, all electrons are assumed to be at the lowest energy level, the ground state (0).

When light energy is absorbed by a fluorophore, the electron is excited to a higher vibrational level of a higher state (S_1 or S_2) from the ground state (S_0). Fluorescence is the energy emitted when the excited fluorophore is relaxed back to its original ground state (S_0) from the excited state. The timescale of this process is approximately 10^{12} s^{-1}

Phosphorescence is the emission of light from a triplet-excited state. In this case the electron of the higher excited state has the same spin as the electron on the ground state, therefore transitions are forbidden, which slows down the rate of emission.

2.1.3. Stokes Shift (mirror image)

The absorption spectrum of the fluorophore is often the mirror image of the emission spectrum. This is due to reasons described by the Franck-Condon principle, which states that the electronic transitions are vertical and do not affect distances, which in turn means that the nucleus does not move and thus the vibrational levels of the excited state resemble the vibrational state of the ground state. Some of these transitions are favourable for both absorption and emission.

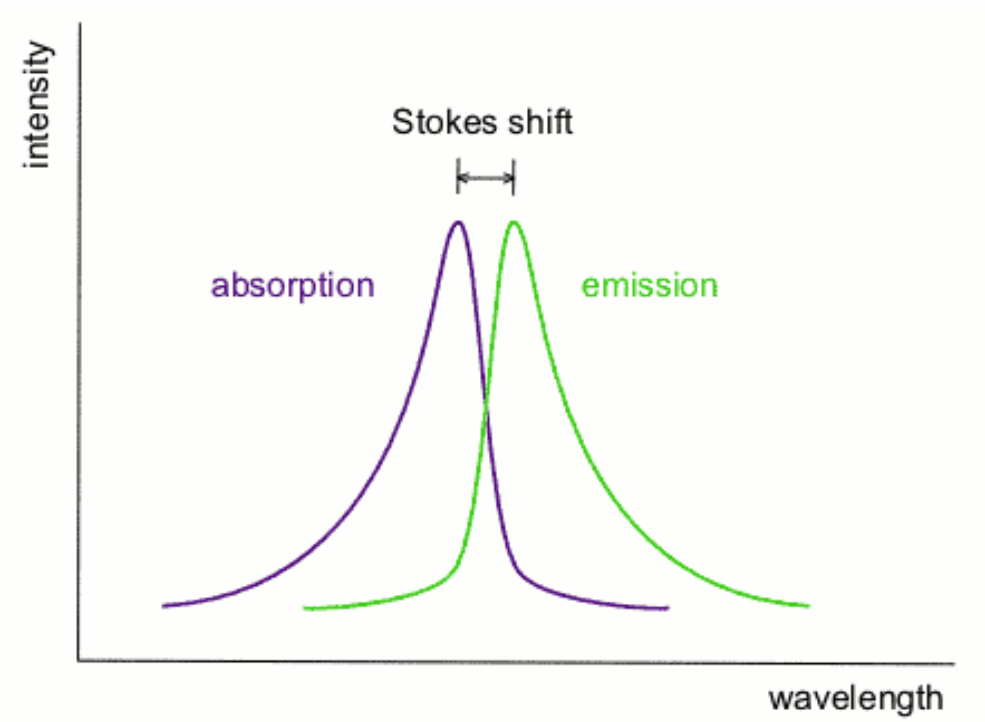

Figure 2.2.: Spectra illustrating the Stokes' shift. Acknowledgement: J. Zhou Ph.D. Thesis 2011.

2.1.4. Fluorescence quenching

The fluorescence intensity can be reduced by a number of processes, of which quenching is one. The energy that has been absorbed can be dissipated, without any occurrence of fluorescence. This process can occur though a number of mechanisms. An excited – state fluorophore can be deactivated though contact with other molecules within the solution, this type of molecule is called a quencher and the process is called collisional quenching. The quencher can bind to the fluorophore to form a non-fluorenscent complex; this process is called static quenching. The decrease in the fluorescence intensity can be described by the Stern-Volmer equation:

$$\frac{F_o}{F} = 1 + K_{sv}[Q] = 1 + K_Q \tau_o [Q] \qquad (1)$$

Where F_o is the unquenched fluorophore, F is the fluorophore, K_{sv} is the Stern-Volmer quenching constant, K_Q is the bimolecular quenching rate coefficient, τ_o is the unquenched lifetime.

If the quencher forms a non-fluorescent complex when associated with the fluophore, static quenching is achieved can be achieved. This can be described by deriving the above equation (1).the derived equation (2) is displayed below, where K_s is the constant derived from the association of the quencher and fluorophore.

$$\frac{F_o}{F} = 1 + K_s\,[Q] \qquad (2)$$

The equations below represent the rate relating the process of fluorescence quenching. A is the fluorophore, A^* is the fluorophore in its excited state and k_Q represents the quenching rate constant.

$A + h\upsilon \rightarrow A^*$ Rate = $k_a\,[A]$

$A^* \rightarrow A + h\upsilon$ Rate = $k_f\,[A^*]$

$A^* + Q \rightarrow A + Q^*$ Rate = $k_Q\,[A^*]\,[Q]$

Under steady state: $$[A^*] = \frac{k_a\,[A]}{K_f + k_q\,[Q]}$$

The intensity of fluorescence in the absence and the presence of the quencher are given below;

$I_f(0) = k_a\,[A]$ Absence of quencher

$I_f(Q) = k_f\,[A^*]$ Presence of quencher

Combining the two equations gives rise to the resulting equation;

$$\frac{I_f\,(0)}{I_f\,(Q)} = 1 + \frac{k_a}{k_f}\,[Q]$$

Plotting of $I_f\,(0)$ / $I_f(Q)$ versus [Q] gives a linear relationship, where the gradient is equal to Stern-Volmer constant K_{sv}, hence;

$$K_{sv} = \frac{k_a}{k_f}$$

This principal of fluorescence and fluorescence quenching was used within this project as the signalling indicator of stable vesicles and responsive vesicles. This system was also used as the signalling device of the prototype dressing developed.

2.1.5. 6(5)- Carboxyfluorescein

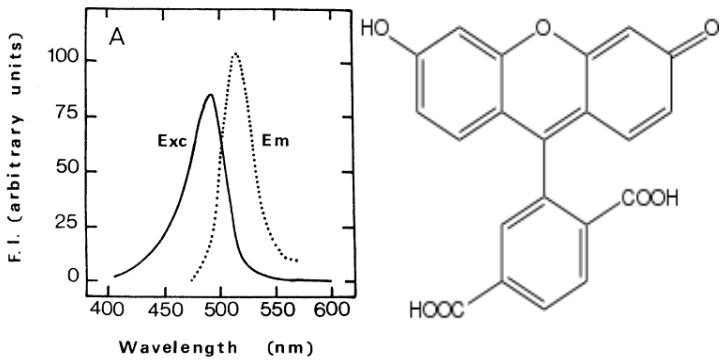

Figure 2.3: Showing excitation and emissionspectrum of 6(5)- Carboxyfluorescein, indicating excitation wavelength of 480nm and emission wavelength of 530nm (left), and the chemical structure of 6(5)- Carboxyfluorescein (right)[2]

6(5)- Carboxyfluorescein is the fluoresce marker used throughout this project. It is one of the most commonly used fluorescence marker used to assess leakage and stability of vesicles. The excitation and emission profile (figure2.3) indicates that it can be excited at 480nm and the emission wavelength is at 530nm. 6(5)-Carboxyfluorescein is a molecule that dimerises at high concentrations, which quenches the fluorescence, as depicted in Figure 2.4.

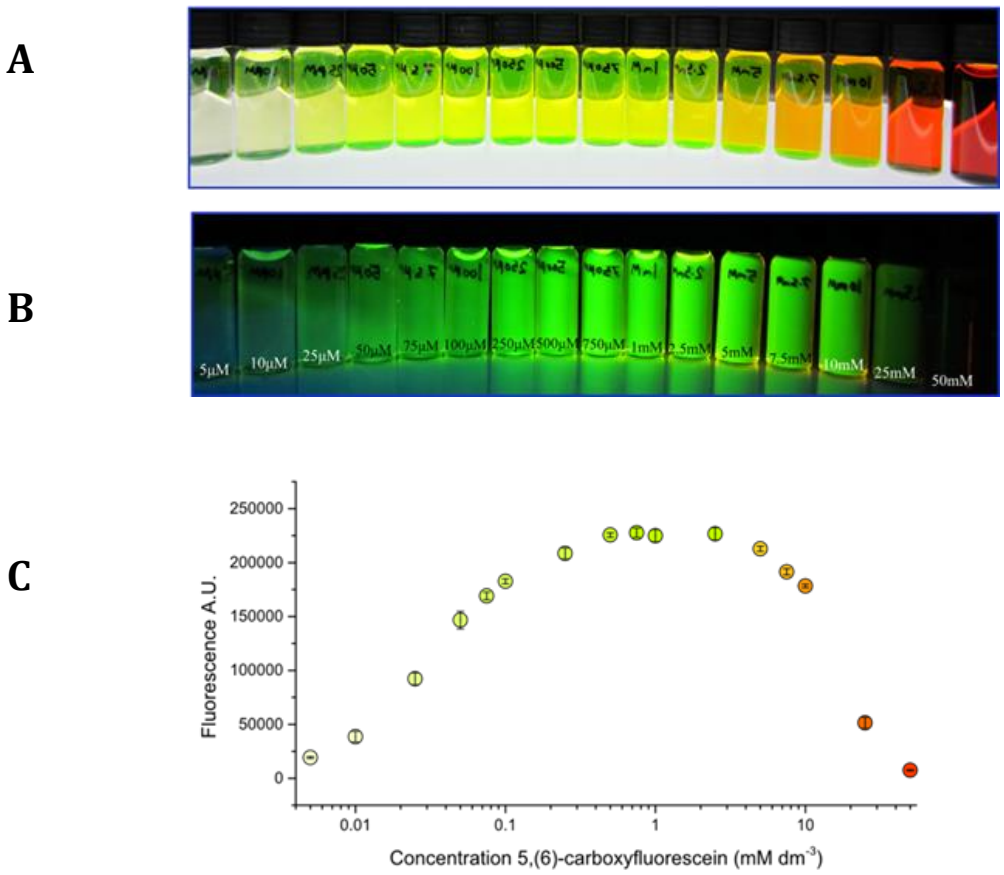

Figure 2.4: A: The colour change observed in solution as the concentration of 6(5)- Carboxyfluorescein is increased under white-light. B: The colour change observed in solution as the concentration of 6(5)- Carboxyfluorescein is increased under UV-light. C: A plot of the self-quenching effect as the concentration of 6(5)-Carboxyfluorescein is increased. Images and graph acknowledgement: W.D. Jamieson, Ph.D. Thesis 2013, University of Bath.

From the results of the colour profile associated with the concentration of 6(5)-Carboxyfluorescein, a 50mM concentration was thought to give rise to a quenched fluorescence system.

2.1.6. Fluorescence spectroscopy

A fluorometer is an instrument that measures the parameters of fluorescence: its intensity and wavelength distribution of emission spectrum after excitation by a specific spectrum of light[3]. The sample is irradiated by monochromatic light of a defined wavelength emitted by a laser lamp. The fluorophore in the sample are exited and the emission of fluorescence is detected and recorded as the intensity versus the wavelength, as emission spectra[1]. The measurements acquired cannot be associated with absolute units; as a result the units involved were depicted as arbitrary units (au).

The spectrometer used in this work is a FLUOstar Omega microplate reader supplied by BMG labtech ltd. The plate reader covers a wide range of excitation and emission wavelengths. The increase in fluorescence intensity was measured to determine vesicle lysis using this instrument. For fluorescence intensity measures of vesicles , excitation and emission filters of 485 ± 12 nm and 520 nm were used, with a gain of 650.

The instrument was used for both fluorescence and UV/Vis absorbance microscopy. UV/Vis absorbance was used to follow bacterial growth during the study of vesicle response to whole bacteria. These measurements were carried out at 600 nm (Optical Density, OD_{600}).

2.2. Microscopy

Microscopy was used to capture images of vesicles immobilised on surfaces and in gel matrixes. Fluorescence microscopy as well as light microscopy was used to capture images of cell growth, as well as gel dispersion, on tissue culture plates in media containing vesicles.

2.2.1. Bright-field microscopy

Bright-field microscopy has been used for a number of years to view cells using visible light to illuminate a sample on a stage. The image can be magnified up to 1000 times by the objective lenses. This technique is often used during eukaryotic cell culture techniques to obtain cell counts for calculating cell densities and viewing the general health of a culture. This methodology was used for basic cell culture work as well as viewing cell attachment on prototype dressings, prior to more quantitative assessments.

2.2.2. Fluorescence microscopy

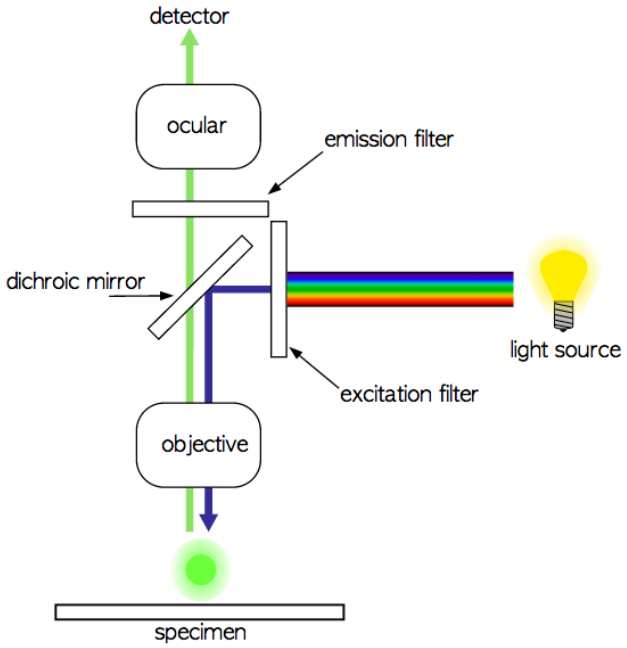

Figure 2.5: Schematic of light microscope. Image Acknowledgment: J.Zhou, Ph.D. Thesis 2011, University of Bath.

Light microscopy can be adapted to use fluorescence in order to give a visual representation of fluorescent vesicles, and fluorescently tagged and stained samples. Fluorescence microscopy uses an ultraviolet light source to excite fluorophores - the emitted photons can then be detected and viewed optically. In the case of inverted microscopes, the light source is passed through the objective and onto the sample. The emitted light from the fluorescence of the sample is focused by the same objective used as that used for the initial excitation. The light is then passed through a filter, to screen out the excitation light, before it passes through to the detector[4]. This method was used to image vesicles in solution as well as vesicles immobilized on a surface.

A Nikon eclipse TE2000-S epi-fluorescence microscope was used to view vesicles in solution and immobilised on glass surface before and after lysis of vesicles by Triton X100 and bacterial supernatant. The method was also used to view vesicle interaction with eukaryotic cell lines.

2.2.3. Confocal microscopy

Confocal Microscopy uses similar principals to the conventional fluorescence microscopy, but allows imaging in three dimensions. The sample can be scanned in the x, y and z direction.

Two different confocal microscope systems were used within this study. For the analysis involving interaction of eukaryotic cells with vesicles, a Nikon A1-R Microscope, equipped with a 488 nm DAPI laser and a 10x CFI Plan Fluor DL objective, was used. And for analysis of vesicles in gel, the images were acquired using a Leica SP3 AOBS confocal. Samples were excited at 488nm and collected at 504-548nm. The time course was acquired with a 30 second cycle time. Post-acquisition, time course images were processed using auto-deblur.

2.2.4. Atomic Force Microscopy (AFM)

The atomic force microscope was developed in 1986, in order to image the surface morphology of a wide range of materials. This type of microscopy enables the atomic scale feature detection of polymers, ceramic materials as well as biological samples. Atomic force microscopy involves the use of a tip which is moved along the sample in the x, y and z direction and either the repulsive force between the tip and the sample, or the tip deflection is recorded and converted into an image representing the surface of the sample[5]. There are two main modes: contact and tapping mode. The contact mode involves dragging the tip along the sample and measuring the forces between the tip and the surface; the tapping mode involves using an oscillating tip which oscillates along the surface of the material. As the tip oscillates along the surface, it experiences the attractive and repulsive forces. A laser beam aimed at the back of the assembly of the tip is reflected off the surface to a split photodiode. This detects the small deflections and generated as a topographical image representing the surface structure[6].

A digital Instruments Nanoscope IIIA AFM was used for visualisation of vesicles on treated glass surfaces.

2.3. Other Instrument types used

2.3.1. Nanoslight (NTA)

Figure 2.6: The NTA instrument used to measure the size and stability of nanoparticles at different temperatures

Nanosight (Figure 2.6) is a technology that involves the tracking of the Brownian motion of individual particles in a liquid suspension of nanoparticles. This motion is first captured by a video and analysed by tracking the movement of individual particle. This instrument tracks individual particles; therefore, the size and intensity of particles can be determined. Hence the number of particles in a given solution can be calculated.

2.3.2. Osmometer

Osmolality is a technique used to measure the number of moles/kg of solvent present in a given aqueous solution. The osmolality can be measured from finding the freezing point depression of a sample. The measured freezing point depression of a sample can be compared against the measure of pure water to give a value of osmotic concentration. Using equation 2.1 below, the osmolality of a given sample can be calculated, where **ξ** is the osmolality of the sample. This equation assumes that the freezing point of an ideal, undissociated aqueous solution with osmolality of 1 osmol/kg is -1.858°C

$$\boldsymbol{\xi} = \frac{\Delta \boldsymbol{T}\ (\boldsymbol{°C}) \boldsymbol{x}\ \mathbf{1000}\ (\boldsymbol{mosm})}{\mathbf{1.858}\ (\boldsymbol{°C})}$$

A Löser Micro-Osmometer Type 15 was used to carry out osmolality measurements of vesicles and hydrogel matrices. 50µl samples were measured in 1mL eppindorf tubes, using deionised H_20 to calibrate the instrument. Osmolality values were obtained with units of mosm/kg H_20.

2.4. Vesicle preparation

2.4.1. Materials and equipment

TritonX-100 (#T8787), 10,12-Tricosadiynoic acid, TCDA (#91445), Cholesterol (#C8667), maleic anhydride (#M625), Ethylenediaminetetraacetic acid, EDTA (#EDS), sodium chloride, NaCl (#S7653), 5(6)-Carboxyfluorescein (#21877), 1,2-Distearoyl-sn-glycero-3-phosphoethanolamine (#P3531), 1,2-Distearoyl-sn-glycero-3-phosphocholine (#P1138) and gelatine from porcine skin (#271616) were obtained from Sigma-Aldrich (UK). 1,2-dimyristoyl-sn-glycero-3-phosphocholine (#850345P) and 1,2-dimyristoyl-sn-glycero-3-phosphoethanolamine(#850745P), 1,2-dipalmitoyl-*sn*-glycero-3-phosphocholine (#850355), 1,2-dihexadecanoyl-sn-glycero-3-phosphoethanolamine (#110633) and 1,2-bis(10,12-tricosadiynoyl)-sn-glycero-3-phosphocholine (#870016) were obtained from Avanti Polar Lipids (USA). Sephadex™ G25 columns were obtained from GE Healthcare (UK). FLUOstar Omega plate reader was purchased from BMG Labtech. UVP CL 1000 Crosslinker was purchased from Fischer Scientific (UK).

2.4.2. Preparation of aqueous solutions

2.4.2.1. Preparation of HEPES buffer solution (pH 7.4)

HEPES buffer was prepared at a pH of 7.4 and was used for cleaning of equipment and in the purification step of vesicles. The table below shows the composition of the buffer solution (Table 2.1)

Table 2.1: All of the components in the table above were dissolved in 100mL of purified water. And the pH was measured and adjusted to pH 7.4.

Component	*Concentration (mM)*	*Mass (mg)*
NaCl	107	624
NaOH	5.6	22.4
HEPES	10	238.3
EDTA	1	29.22

2.4.2.2. Preparation of Carboxyfluorescein solution (pH 7.4)

Self-quenched carboxyfluorescein solution was used as the signalling dye encapsulated inside the vesicles. The table below shows the components of the dye solution (Table2.2).

Table 2.2: The components shown in the table 2.1 were dissolved in 13mL of purified MiliQ water, and the pH was measured and adjusted to pH 7.4. Then the vial containing the solution was sealed and kept in a dark environment at 4°C

Component	*Concentration (mM)*	*Mass (mg)*
NaCl	10	7.6
NaOH	135	70.2
HEPES	10	31
EDTA	1	3.7
Carboxyfluorescein	50	244

2.4.3. Lipid stock preparation

Two different types of lipid stock solutions were made. Stock 1 solution consisted of each of the lipid components dissolved in 1mL of Chloroform at a concentration of 0.01mM. The lipid stock 2 solutions were then made using different percentage concentrations of each lipid stock 1 solutions.

Stock 1:

Table 2.3: Stock 1 solution, in which each component was dissolved in 1mL of chloroform

Component	*Mass (mg)*
TCDA	35
DCPC	91
DMPC	68
DMPE	64
DPPC	73
DPPE	69
DSPC	79
DSPE	75
CHO	39

Stock 2:

Type A: lipid Vesicle

Table 2.4: Summary of composition of vesicles without crosslinker incorporated. Components were all dissolved in 1mL of chloroform prior to evaporation by nitrogen gas.

Component	*Mole Percentage (%)*	*Mass (mg)*	*Amount in 100μL (μL)*
DMPE/DPPE/DSPE	73	49.6/53.6/57.7	73
DMPE/DPPE/DSPE	2	1.28/1.38/1.5	2
CHO	20	7.8	20

100 μL of the stock 2 solution was dissolved in 1mL of chloroform, in a glass vial. The solvent was then evaporated off under nitrogen, until a thin film was formed at the bottom of the glass vial. The thin film of lipid was then re-suspended in 5mL of CF50 solution and heated to 75° C in a water bath for 10 mins. Once the lipid suspension had fully dissolved in CF50 solution, a series of freeze and thaw cycles enhanced encapsulation of vesicles. This process was repeated three times. Following on from this, the vesicle solution was extruded three times through two polycarbonate membranes at the corresponding temperature depending on the bulk lipid used and purified using Nap-25 columns. The purified vesicles solution was then kept at 4 °C.

Type B: TCDA containing Vesicle Synthesis

Table 2.5: The components were all dissolved in 1mL of Chloroform. Any variation of TCDA concentration was made by varying the concentration of main phosphodicholine

Component	*Mole Percentage (%)*	*Mass (mg)*	*Amount taken from stock solution 1 for 100 µL of stock solution 2 (µL)*
TCDA	25	8.75	25
DMPC/DPPC/DSPC	53	36.0/38.7/41.9	53
DMPE/DPPE/DSPE	2	1.28/1.38/1.5	2
CHO	20	7.80	20

Type B vesicles were made following the same method as the lipid vesicles (type A), however, the purified vesicle solution was kept at 4 °C overnight and crosslinked the next morning using a UV Crosslinker at 254nm[7].

Type C: DC8, 9PC containing Vesicle Synthesis

Table 2.6: A summary of the composition of DC8, 9PC containing vesicles

Component	*Mole Percentage (%)*	*Mass (mg)*	*Amount taken from stock solution 1 for 100 µL of stock solution 2 (µL)*
DC8,9PC	30	26.8	30
DMPC	40	27.4	40
CHO	30	11.61	30

Type C vesicles were made using the same method as the vesicles containing TCDA (Type B) apart from the samples being cross-linked immediately following purification (and **not** left at 4°C overnight).

2.4.4. Extrusion

Figure 2.7: The Liposofast ™® extruder

Following re-suspension of lipid film into the CF50 buffer solution, a series of freeze-thaw processes was carried out in order to enhance encapsulation of the surrounding solution into the vesicle. This process was then followed by extrusion of vesicles through a filter. The extrusion of vesicles was carried out using a Liposofast ™® extruder (Figure 2.7) and passed through two 0.1micron polycarbonate filters. During this process, the extruder was heated to at least 10°C higher than the transition temperature of the lipid [8]. The table below shows a summary of the different conditions used for individual vesicle type.

Table 2.7: Showing the transition temperature and the extrusion temperature of different lipid systems used in this investigation

Lipid	*Transition Temperature (°C)*	*Extrusion Temperature (°C)*
DMPC	23	33
DPPC	45	55
DSPC	55	65

2.4.5. Purification of vesicles

The separation of vesicles with un-encapsulated CF50 dye was carried out using GE healthcare NAP-25 sephadex columns. The column storage solution was drained and equilibrated with excess HEPES buffer. Once the buffer solution had passed through the column, 2mL of the sample was loaded on the column. When the sample was loaded onto the column, 1mL of HEPES buffer was loaded and left to drain. Following this, a further 2mL of the buffer was loaded and the purified sample was collected. The vesicles were then stored at 4°C overnight.

2.4.6. Photo-polymerisation to crosslink vesicles

Vesicles containing TCDA were crosslinked using UV light (λ = 254 nm). A 1mL aliquot of the vesicle solution was loaded into a 1.4mL quartz cuvette and placed into the middle of the UV crosslinker (230V, 30Hz, 254nm), supplied by Ultra Violet Products. The crosslinking of TCDA occurred at timer setting 1 (Approx. 6 seconds). The crosslinking mechanism is shown by Figure 2.8, section 3.1.6.1. displays a more detailed explanation of TCDA stabilisation.

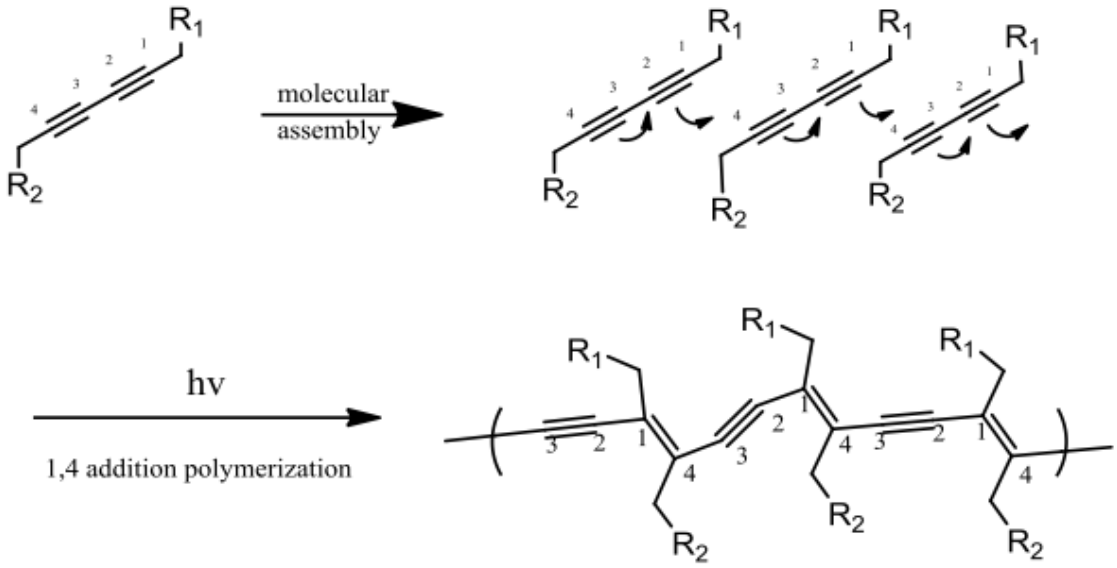

Figure 2.8: Representation of TCDA polymerisation, though UV irradiation. Acknowledgment of scheme to Dr. JZhou, University of Bath.

2.5. Vesicle characterization methods

Following preparation, vesicles were characterised to ensure initial formation, encapsulation of self-quenched dye, the size characterisation as well as uniform of distribution particles.

2.5.1. Vesicle characterisation during purification

Vesicle characterisation during the purification stage was carried out by collecting four drops of eluent from the NAP-25 column into each well of a 96 well plate (Figure 2.8). The fluorescence intensity was measured using a FLUOstar BMG Labtech microplate reader.

2.5.2. Using the NTA system

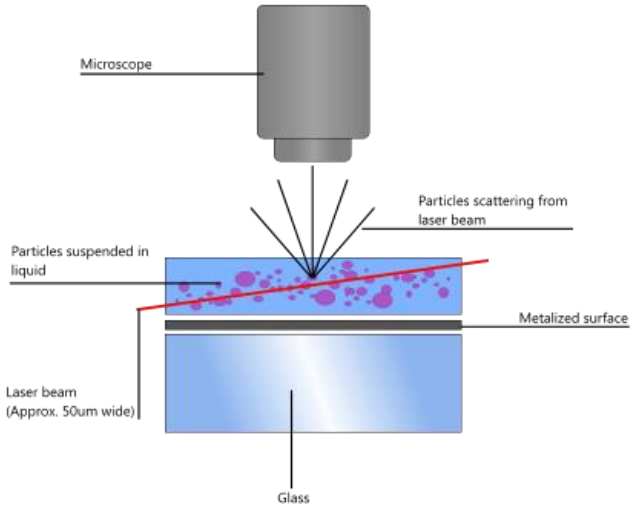

Figure 2.9: Schematic of the NTA system

Utilising Nanosights' NTA instrument the Brownian motion of nanoparticles in HEPES was measured on a particle-by-particle basis. The sample chamber was flushed with the eluent, in this case HEPES, followed by addition of a diluted

sample of 100 μL of nanocapsules. This sample was further diluted by altering the ratios of sample to eluent composition as required.

2.5.3. Methods for stability tests and solution preparation

General stability of vesicles was achieved by simple fluorescence measurements following addition of Triton X100 or HEPES buffer. A large increase in fluorescence upon addition of Triton X100 compared to HEPES buffer indicated stable vesicles. This test was performed immediately following formation, purification and in some cases crosslinking steps.

Upon successful formation and completion of the immediate stability test, their longer-term stabilities were examined. Long-term stability studies were performed in various different conditions. These include, pH and temperature.

2.5.4. pH stability assay and osmotic pressure measurement.

HEPES buffer was adjusted to achieve different pH ranging from 4 to 8. This was followed by vesicle incubation in the pre-prepared pH adjusted HEPES buffer solutions in 96 well plates, at various temperatures.

2.5.5. Temperature stability assay

Changes to the temperature were achieved by storing in temperature-controlled incubators. Test solutions were pipetted onto 96 well plates with water in the out wells of the plate. The plates were sealed with masking tape, wrapped in foil and placed in zip-lock bags before incubating at set temperature for a period of 14 days, for long-term stability assays.

2.6. Preparation of bacterial cultures

2.6.1. Materials and equipment

LB Broth (#L3022) and Tryptic Soy Broth (#22092) - obtained from Sigma-Aldrich (UK).

Different strains of pathogenic bacteria: *P. aeruginosa* and Methicillin sensitive *S. aureus.* (MSSA, RN4282, RN6390B, RN6911); and one strain of non-pathogenic bacteria: *Escherichia coli* DH5α, were cultured for the purpose of sensitivity studies.

2.6.2. Sterilisation

Maintaining sterile conditions is essential when working with biological samples. All work involving the use of biological samples was conducted in Class II safety cabinets, in addition to the use of 70% alcohol solutions or bleach to disinfect the surfaces and any containers entering or leaving the cabinet.

Sterilisation of media and any equipment used in cabinets was conducted by autoclave, which uses heat sterilisation. The autoclave system decontaminates solutions and equipment at 121°C and 15psi for 15mins[9]

2.6.3. Principals of bacterial growth

Bacteria follow the process of binary fission to grow and reproduce in fixed proportions. This is a form of asexual reproduction. During the stage of reproduction and growth, the temperature and the nutrient available play an important role. The temperature for optimal bacterial growth is dependent on the strain, with 37°C being the typically used temperature. The type of nutrient required is also dependent on the strain, thus different media are used for growth of different bacteria. In this study, Tryptic Soy Broth (TSB) was used for all strains of *S. aureus* and Luria Broh (LB) was used for *P. aeruginosa* and *E. coli.*

In research laboratories, bacterial growth take place on solid agar plates, in 37°C incubators to isolate single colonies followed by culture in liquid medium in 37°C shaking incubators. Given that mutation does not occur, all cells in the resulting culture should be identical to the mother cells of the original colony.

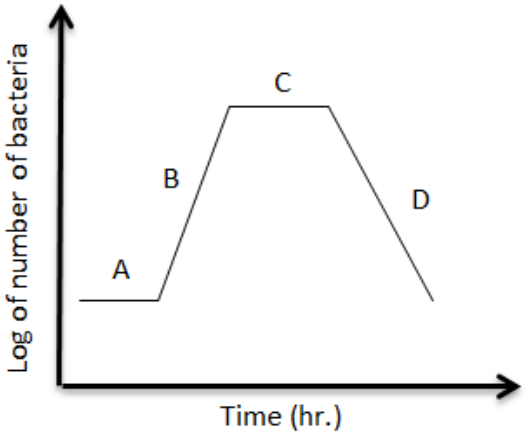

Figure 2.10: The stages of bacterial growth. A: initial lag phase, B: exponential growth phase, C: stationary phase, D: logarithmic decline phase.

The population growth of bacteria occurs in several stages. The initial phase is termed the lag phase, followed by the exponential log phase in which the increase in population density follows a logarithmic pattern. This is then followed by a stationary phase in which population increase equals population death, resulting in no general increase in population. Finally there is a logarithmic decrease in population, where lack of nutrients and space (steric hindrance) results in death[10] (Figure 2.10).

2.6.4. Bacterial culture preparation

Culturing of *P. aeruginosa* and *E. coli* DH5α was carried out in Luria broth (LB). For *S. aureus* it was carried out in Tryptic Soy Broth (TSB). Bacteria obtained from stocks were cultured at 37 °C in broth over 18 h (overnight). The 18 h culture was diluted to a concentration of $1x10^6$ CFU mL^{-1}. This re-diluted culture was added to vesicle solutions, in a 1:1 ratio, after which fluorescence and control absorbance measurements were taken over a minimum of 17h.

2.6.5. Bacterial supernatant preparation

500µL of overnight (18h) bacterial cultures were grown in conical flasks containing 50mL of corresponding media. These were cultured for a further period of 18h. The 2nd overnight cultures were centrifuged twice (5000 rev min^{-1}, 15 min), to remove whole bacterial cells and debris. The supernatants were collected, filter-sterilised through 0.22 µm filters and stored at -20 °C. These supernatants were tested against each vesicle type in a 1:1 ratio and fluorescence was monitored over 100 mins.

2.7. Hydrogel and prototype preparation

2.7.1. Materials and equipment

Gelatin (#48723), agarose(#A9529), hypromellose (#H3785), agar (#A1296) were obtained from Sigma-Aldrich (UK). FmocFF was obtained from BACHEM (UK). Components for the polyacrylamide gels were obtained from First Water Ltd. (UK).

2.7.2. Hydrogel preparation

Preparation of natural hydrogels involved heating and stirring of the buffer solution containing gelling agents. Once the gelling agents had dissolved into the buffer solution, the formation of these gels occurred during the cooling stages of the buffer solutions.

2.7.3. Preparation of natural hydrogel

A. **Gelatin:** the HEPES buffer solution containing required amounts of gelatin was heated to 60 °C with stirring for 10 mins. The solution containing vesicles was added to the warm solution of gel and further stirred to ensure uniform distribution of vesicles throughout the gel mixture. The mixture was immediately used for further analysis.

B. **Agarose**: Agarose gels were prepared in HEPES buffer by microwaving the solutions for 3 mins at 850ca. As for the gelatin mixture, vesicles were mixed into the warm (around 37°C) gel mixture and used immediately for further analysis.

C. **Agar**: agar gels were formed by dissolving the appropriate amount of agar into HEPES buffer and heating with stirring until a clear solution was formed. Vesicles were mixed into the warm gel (around 37°C) and used immediately for further analysis.

D. **Xanthan and guar gum**: Different amounts of the gelling agents were added to HEPES buffer and heated with stirring until the entire gelling agent had dissolved.

E. **Hypromellose**: Hypromellose gels were prepared by heating half of the required HEPES buffer to 80°C. Followed by addition of hypromellose powder with continuous heating and stirring. Finally, once all of the powder had dissolved, the solution was continuously stirred but at room temperature and the remaining half of the HEPES buffer was added and stirred further for at least 30 mins. The gel was then allowed to form overnight before vesicles were added and used for further analysis.

F. **Polyacrylamide hydrogels:** the original formulation contained 2.86 mL of deionized H_2O, 3.57g of glycerol, 3.57g of acrylamide monomer as well a mixture of the photo-initiator and crosslinker. Variation of the gel was carried out by replacing the water content with HEPES buffer or vesicle solution. Preparation of the pre-crosslinked gel mixture involved initial stirring of aqueous solutions with glycerol for 5 mins before addition of the other components. The solution was stirred for at least 30 mins in the dark, before vesicle solutions were added.

G. **FmocFF gel**: FmocFF stock solutions were prepared in DMSO and stored at -20°C. The 'solvent-switch' method was followed with FmocFF stock: water ratio of 1µL: 49µL. The gel was allowed to set for 45 mins before any addition of further reagents.

2.8. Toxicity assays

2.8.1. Materials and equipment

DMEM and DPBS media were purchased from Fischer scientific (UK). Trypsin EDTA cell resazurin were obtained from Sigma-Aldrich (UK).

2.8.2. Eukaryotic keratinocyte and fibroblast Cell culture

HaCaT Cells were grown in Dulbecco's Modified Eagle Medium (DMEM) with 10% fetal bovine serum (FBS) and Penicillin, Streptomycin and Glutamine (PSG) in a tissue culture incubator at 37°C and 5% CO_2. Cells were revived and grown to achieve 70% confluent monolayers of cells in T25 cm^3 or T75 cm^3 flasks. Once 70% confluence was achieved, the cells were washed in PBS and fresh growth media was added with vesicles at different concentrations, lysed vesicles at different concentrations and controls. 10% Triton X-100 was used as a positive control (cytotoxic to cells). The cells were incubated with the different testing solutions for 24, 48 and 72 h.

2.8.3. Resazurin assay

Following incubation of cells with testing solutions, media was removed from the well, washed with PBS and 500µL of 10% resazurin solution in cell growth media was added to each well. The plate was further incubated for 2 h at 37°C and 5% CO_2

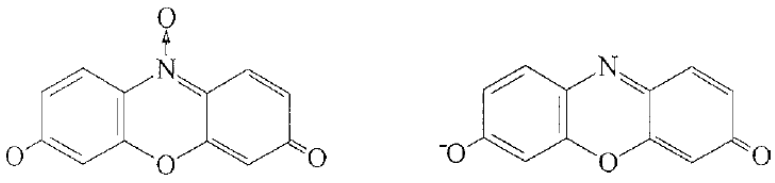

A **B**

Figure 2.11: Structure of **A** resazurin and **B** resorufin[11].

Resazurin (A) can be reduced to form resorufin (B), with a change of colour from deep blue to pink. The mechanism of the transfer from resazurin to resorufin by eukaryotic cells is thought to involve the reduction of NADH[12]. NADH is an important biochemical vector used to indicate the viability of cells[13].

$$NADH + A + H^{+} \longrightarrow NAD^{+} + B + H_2O \qquad (1)$$

Equation (1) shows the proposed reaction scheme of reduction of resazurin by NADH to yield resorufin and NAD^{+}

The fluorescence of resazurin was measured using a BMG LAB tech micro plate reader. Excitation and emission filters of 544 nm and 590 nm were used for fluorescence intensity measurements of resazurin [14,15].

2.9. Prototype preparation methods

2.9.1. Materials and equipment

Non-woven polypropylene fabric was obtained from Boots Pharmacy, Collagen I was obtained from Invitrogen, and plastic backing sheets were obtained from Mölnlycke Health Care (Sweden).

2.9.2. Gel-block system

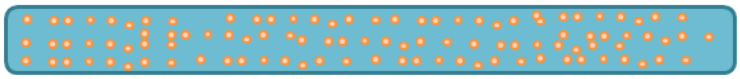

Figure 2.12: Representation of gel block system

Gel-block systems were prepared by loading 500µL of 1:2 ratio of vesicle to gel mixtures into each well of 12 well plates. The gels were then allowed to set at 4°C for a minimum of 30 mins. The prototypes were stored at 4°C and discarded following 2 days of storage without use.

2.9.3. Gel coated fabric

Non-woven polypropelene fabric was cut to 2cm in diameter circular fragments, washed in ethanol, dried and further washed in HEPES buffer (x2). The wet-in-HEPES pieces of fabric were dip coated, twice, in a 1:2 ratio of vesicle to gel mixture before storing at 4°C. The gel coated fabric prototypes were also discarded when exceeding 2 days of storage without use. For experimental analysis, two layers of the coated fabric were used per well of a 12 well plate (Figure 2.13).

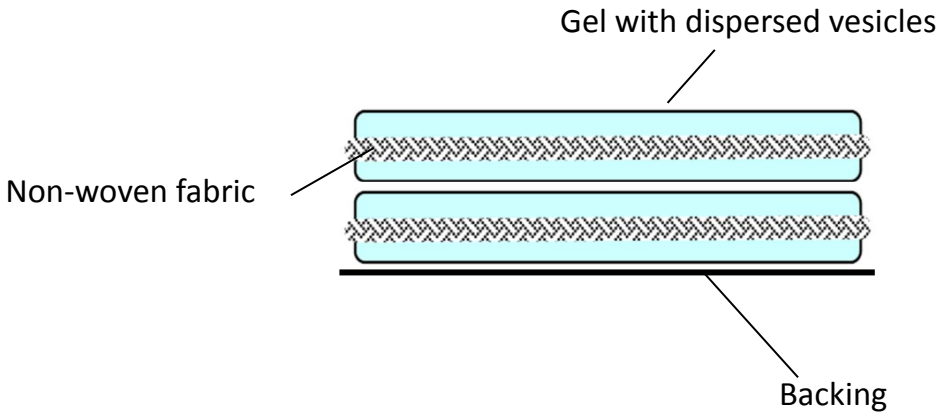

Figure 2.13: Diagrammatic representation of prototype layout in each well of a 12 well plate, with two layers of coated fabric

2.9.4. Collagen coated prototype

The collagen coated prototypes followed the same preparation method as for the gel-coated prototype, with an additional coating in 1% collagen solution following two dips in the vesicle/gel mixture.

2.9.5. Stability and sensitivity assay

Overnight stability assays were carried out by overnight incubation of gel-blocks with HEPES buffer and Triton as a control. Fluorescence measurements were carried out by well scan analysis using the fluorometer described in section 2.1.6.

Sensitivity assays were carried out using overnight bacterial culture as well as bacterial supernatant. However, as previous results demonstrated that bacterial supernatants showed sufficient response for the purpose of this study, supernatant studies were the preferred option for sensitivity analysis.

For assays using overnight bacterial culture, 1mL of overnight culture with cell density of $1x10^6$ CFU/mL was used. For assays using supernatant, 500µL of bacterial supernatant was used.

2.9.6. Fluorescence reading

The stability and sensitivity analysis of prototype dressings were carried out by measuring fluorescence intensity. Prototypes were made in 12 or 24 well plates and 10x10 well scan measurements were taken rather than single point scans taken when using 96well plates. This was done in order to obtain accurate fluorescence readings of vesicles that may be unevenly distributed.

2.9.7. Analysis of fluorescence results

An average of the well scan was calculated using the values obtain from the middle of the well (figure 2.14). The values selected in the red box on Figure 2.14 were used to calculate the average well scan values.

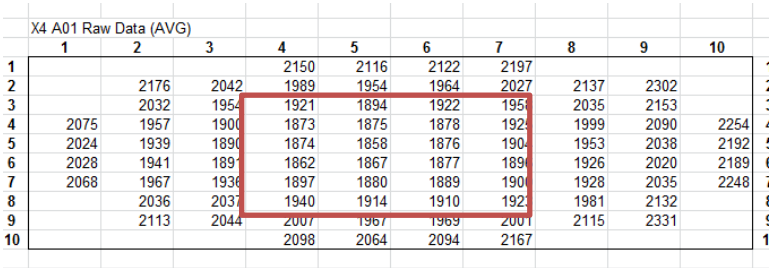

X4 A01 Raw Data (AVG)

	1	2	3	4	5	6	7	8	9	10
1				2150	2116	2122	2197			
2		2176	2042	1989	1954	1964	2027	2137	2302	
3		2032	1954	1921	1894	1922	1953	2035	2153	
4	2075	1957	1900	1873	1875	1878	1929	1999	2090	2254
5	2024	1939	1890	1874	1858	1876	1904	1953	2038	2192
6	2028	1941	1891	1862	1867	1877	1896	1926	2020	2189
7	2068	1967	1936	1897	1880	1889	1906	1928	2035	2248
8		2036	2037	1940	1914	1910	1923	1981	2132	
9		2113	2044	2007	1967	1969	2001	2115	2331	
10				2098	2064	2094	2167			

Figure 2.14: Representation of well scan. The values indicated by the red box were taken for calculation of average of well scan

2.9.8. Cell attachment assays

1mL of media containing cell density of $2x10^5$ cells mL^{-1} was loaded onto each well. The wells were pre-loaded with a gel to stop migration of cells onto the surface of the tissue culture well plate (apart from the positive control where the cells were grown on the surface of the tissue culture well plate) as well as the collagen coated dressings and the agarose dressings placed into each well. The cells were allowed to proliferate onto the surfaces for 30 mins. The solution was then removed, wells were carefully washed with PBS and 1mL of tissue culture media was replenished. The cells were then incubated at 37°C and 5% CO_2 for 48h.

Following 48h incubation, the media was removed and the wells were washed with PBS. Rezasurin assay was carried out to assess cell viability. 500µL of resazurin assay solution (10% resazurin in tissue culture media) was added into each well and the cells were further incubated for 2h before the fluorescence was measured.

2.10. References

1. Lakowicz, J., *Principles of Fluorescence Spectroscopy*. Springer: 2006; Vol. 1,

2. Grignon, N.; Touraine, B.; Durand, M., 6(5)Carboxyfluorescein as a Tracer of Phloem Sap Translocation. *American Journal of Botany* **1989,** *76* (6), 871-877.

3. Fluorescence Spectrophotometry. In *Encyclopedia of Life Sciences*, Macmillan Publisher Ltd: 2002.

4. Graeme-Cook, K,; Kikington, R. A., *Instant notes in microbiology*. 2nd ed.; Bios Scientific Publisher, 1999**,** Vol. 2,

5. Blanchard, C.; Blanchard, Atomic Force Microscopy. *Chemical educator* **1996,** *1* (5), 1-8.

6. Magonov, S. N.; Elings, V.; Whangbo, M. H., Phase imaging and stiffness in tapping-mode atomic force microscopy. *Surface Science* **1997,** *375* (2–3), L385-L391.

7. Ji, E. K., The fluorescent polydiacetylene liposome. *Bulletin of the Korean Chemical Society* **2003,** *24* (5), 667.

8. Nayar, R.; Hope, M. J.; Cullis, P. R., Generation of large unilamellar vesicles from long-chain saturated phosphatidylcholines by extrusion technique. *Biochimica et Biophysica Acta (BBA) - Biomembranes* **1989,** *986* (2), 200-206.

9. Verran, J.; Whitehead, K., Factors affecting microbial adhesion to stainless steel and other materials used in medical devices. *International journal of artificial organs* **2005,** *28* (11), 1138-1145.

10. Koch, A. L., Control of the bacterial cell cycle by cytoplasmic growth. *Critical Reviews in Microbiology* **2002,** *28* (1), 61-77.

11. Candeias, L.; MacFarlane, D. S.; McWhinnie, S. W.; Maidwell, N.; Roeschlaub, C.; Sammes, P., The catalysed NADH reduction of resazurin to resorufin. *Journal of the Chemical Society, Perkin Transactions 2* **1998,** (11), 2333-2334.

12. Cook, D. B.; Self, C. H., Determination of one thousandth of an attomole (1 zeptomole) of alkaline phosphatase: application in an immunoassay of proinsulin. *Clinical Chemistry* **1993,** *39* (6), 965-971.

13. Haugland, R. P.; Spence, M. T.; Johnson, I. D., *Handbook of fluorescent probes and 1research chemicals*. Molecular Probes Eugene, OR: 1996, Vol. 6.

14. Shiloh, M. U.; Ruan, J.; Nathan, C., Evaluation of bacterial survival and phagocyte function with a fluorescence-based microplate assay. *Infection andlimmunity* **1997,** *65* (8), 3193-3198.

15. Magnani, E.; Bettini, E., Resazurin detection of energy metabolism changes in serum-starved PC12 cells and of neuroprotective agent effect. *Brain Research Protocols* **2000,** *5* (3), 266-272.

Chapter Three: Vesicle optimisation

3.1. Introduction to vesicle optimisation

In this chapter, the different types of vesicles designed for optimal stability and sensitivity to bacterial toxins will be addressed. Numerous types of vesicles were designed and tested for their stability in different pH buffers, biological media, as well as across a range of temperatures. Along with their stability, their sensitivity

to bacterial supernatant was screened, and the vesicle with the optimum stability as well as sensitivity was chosen as the candidate for further development.

3.1.1. Vesicle naming convention

Vesicles were named according to the stabilising agents utilised along with their percentage by volume, followed by the bulk lipid found within the vesicle. For example, vesicles using a 10% volume of 10,12-Tricosadiynoic acid (TCDA) with a mixture of 20% cholesterol, 2% DPPE and 68% DPPC were named 10% TCDA-DP.

3.1.2. Defining vesicle stability

Vesicle stability can be categorized into three classes: initial stability, short -term stability and long-term stability. The initial stability is the stable formation of vesicles, following the stages of purification with NAP- 25 column and crosslinking of the relevant stabilising agents. The short term stability is the stability of vesicles during an overnight study run at 37°C. The long term stability indicates stability of vesicles over a period of 14 days at given temperature or pH.

3.1.3. The Stability-response parameter

The stability response parameter was used to convert the arbitrary fluorescence values to values which can be used to compare different vesicles types. The stability-response parameter of the vesicles was calculated using the following parameter:

$$\text{Stability} - \text{response parameter:} \quad SR = \frac{F_f}{F_i} \qquad (1)$$

Where F_i is the initial vesicle fluorescence value and F_f is the final vesicle fluorescence value following completion of a given study. For stability assays, F_f is the final vesicle fluorescence after addition of lytic agent following a full stability study. The addition of the surfactant Triton X-100™, giving rise to total vesicle

disruption, was considered to deliver the maximum fluorescence obtainable. For short-term stability assays, F_i is the initial fluorescence value prior to conducting any studies. For long-term stability assays, F_i is the fluorescence value obtained following incubation for 14 days. For overnight assays, F_i is the fluorescence before addition of test solution for overnight incubation and F_f is the fluorescence following overnight incubation.

3.1.4. Stability issues

In order for these vesicles to be used as bacterial sensors immobilised in dressings, certain stability criteria have to be met. So as to prevent false positives, vesicles had to demonstrate stability with respect to factors such as temperature, pH, dehydration as well as biological components such as inflammatory responses of the human body, eukaryotic cells, exudate and wound fluid.

As discussed previously, the most common form of uniformLy distributed vesicles is a large unilamellar vesicle. These are relatively stable in solution; however stability is largely dependent on the type as well as the combination of lipids used. The majority of research on utilising vesicles as vehicles of active ingredients has been focused on producing vesicles that are stable in solution until the target site is reached. Numerous methods were investigated in order to achieve the desired stability, including coating vesicles with protective nanoparticles, coating vesicles in gels and using stabilizing agents.

Controlling lysis such that it only occurs upon a specified environmental trigger is central to achieving targeted delivery. In order to accomplish this goal, maintaining the vesicle stability in a wide range of temperatures and pHs is essential. Accomplishing and maintaining vesicle stability at 37°C (human normal body temperature), was one of the major requirements within this study, thus the majority of the studies were carried out at 37°C.

3.1.5. Thermal stability

The thermal stability of vesicles in this study is closely related to the lamellar phase transition temperature of the core lipids. As mentioned in Chapter 1, transition temperature refers to the temperature required for transition of the lipid bilayer between gel and liquid-crystalline states. This transition involves van der Waals forces between adjacent fatty acid chains. As a result, the longer the chain, the higher the temperature required to disrupt the interaction between the chains.

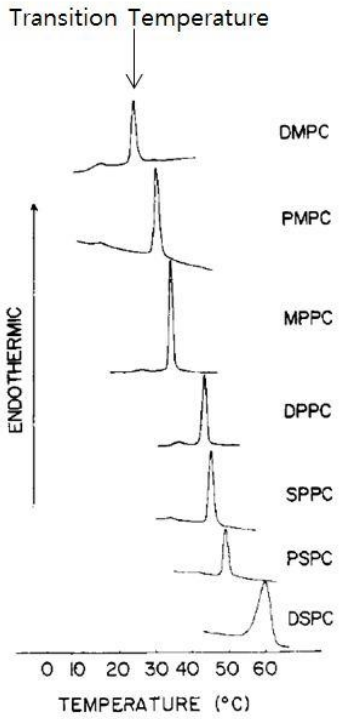

Figure 0.1: Representation of the transition temperatures of various lipids. The peak of each curve indicates the 'melting temperature' of the lipids from gel to liquid- crystalline states. The plot indicates that as the lipid chain length increases, the transition temperature increases[1].

The temperature stability at each phase varies, subject to the hydrocarbon chain length of the lipid.. This is due to the increase in interactions between the hydrocarbon chains as the chain length increases, indicating an increase in van der Waals forces between the chains. Figure 3.1 shows the relationship between the transition temperature and the chain length of the lipid.

3.1.6. Stabilising agents

Various methods of vesicle stabilization for targeted drug delivery and triggered release of vesicles have been explored in the literature. An example of this would be incorporation of polyethylene glycol (PEG) lipids.

Furthermore, previous research conducted by the group showed that stabilisation was achieved by incorporation of photo-polymerisable components, introducing localized cross-linked areas within the vesicle system, inducing stability.

There is evidence in the literature that various different methods have been explored to ensure stability of vesicles. Modification of lipid bilayer using mixed lipid mixtures is one of the most looked at areas of stabilization. Formation of 'stealth liposomes' can be achieved by addition of PEGylated lipid is a large area of showing prolonged blood circulation time.

Previous research conducted by the group involved the use of photo-polymerisable fatty acids, such as polydiacetylenes. Polydiacetylenes such as 10,12-Tricosadynoic acids have a hydrophilic head group and a hydrophobic tail group, thus can be easily incorporated into lipid membrane bilayers. The stabilizing mechanism is not fully understood, however upon photo-polymerisation at 254nm, stability of DMPC vesicles was shown to improve.

3.1.6.1. Polydiacetylenes stabilized vesicles

The use polydiacetylenes (PDA) such as 10,12-Tricosadiynoic acid (TCDA), in lipid membranes was first shown by Kolusheva *et al.* in 2000[2]. TCDA is a polydiacetylenes molecule (see figure 3.2 below), which can self- assemble due to its amphiphilic nature, consisting of polar head group and a hydrophilic tail containing a diacetylene moiety. These monomers can be polymerised by UV irradiation at 254nm[3,4].

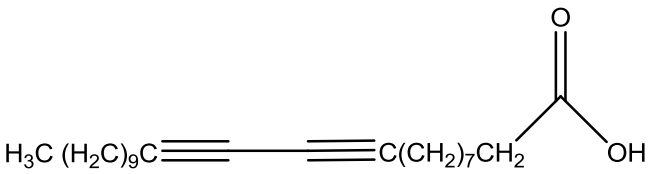

Figure 0.2: Structure of 10,12-Tricosadiynoic acid (TCDA)

TCDA goes through a colour transition from blue to red, following incorporation into lipid bilayers or the colour change can also be induced by an external stimuli such as heat, association with organic solvent, UV light as well as mechanical stress. The colour profiles associated with incorporation of difference concentrations of TCDA is shown by diagram **A** of Figure 3.3.

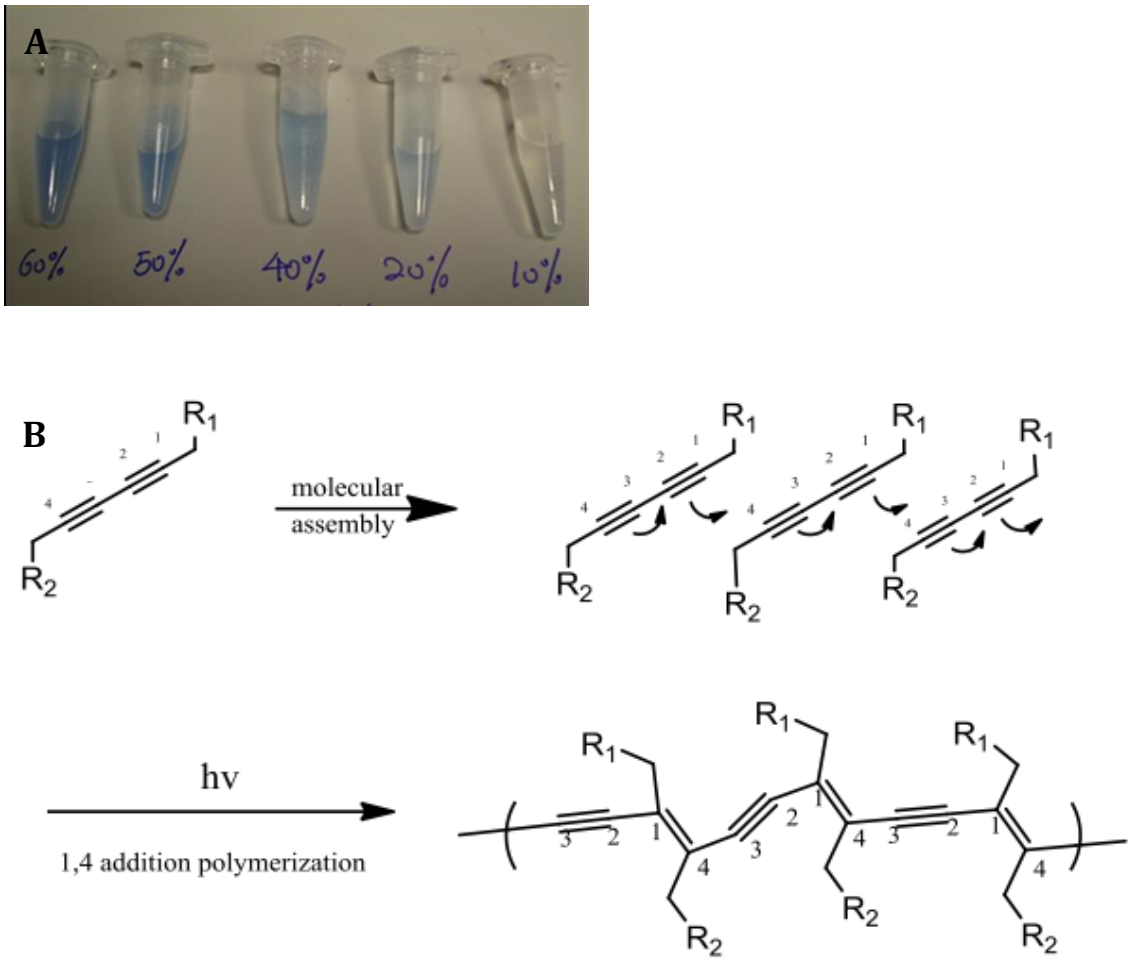

Figure 0.3. A Representing the colour profiles associated with different dilutions of TCDA. As well as representation of TCDA crosslinking, initiated by formation of radicals of **B** irradiated TCDA to from the polymerised product. Acknowledgment to Jin Zhou Ph.D. thesus 2011.

The highly ordered TCDA can be potopholimersed by irradiation with 254 nm UV. A free radical initiated chain reaction initiates the polymerisation. When these diacetylene moiety-containing monomers are incorporated into lipid vesicles and polymerised, this gives rise to polydiacetylene vesicles, vesicles with rigid regions, forming stable/destabilized vesicles[5].

The incorporation of TCDA into lipid mixtures and formation of stabilised vesicles for development of bacterial toxin sensitive vesicles was researched and reported by *Zhou et al*[6]. Within this project, the concept introduced by *Zhou et al*. was further elaborated to develop further stabilised and sensitive vesicle systems.

3.1.6.1. DC8,9PC stabilized vesicles

1,2-bis(tricosa-10,12-diynoil)-sn-glycero-3-phosphocholine (DC8,9PC) is a photo-polymerisable lipid with highly reactive diacetylene groups, which can be photo-polymerised to create polymerised regions[7,8]. The miscibility of DC8,9PC with other lipids were shown by previous studies, demonstrating the potential of DC8,9PCs in stabilisation of lipid vesicles in a similar manner to TCDA.

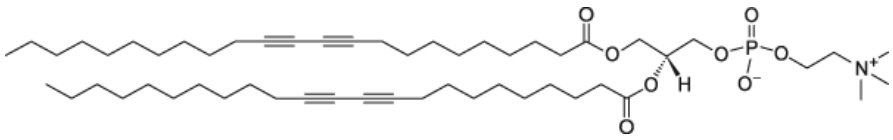

Figure 0.4: Chemical structure of 1,2-bis(10,12-tricosadiynoyl)-*sn*-glycero-3-phosphocholine, (DC8,9PC)

3.1.6.2. PEG stabilization

Stealth liposomes are the term used to describe the group of vesicles stabilised using PEG. PEG–lipids have a polyethylene glycol chain on the headgroup of a phospholipid, which can be incorporated into lipid mixtures and subsequently giving rise to liposomes. An example of a developed pegylated liposomal carrier

would be Dox-NP, in which the peg-stabilised liposome acts as a drug carrier for cancer therapy[9].

3.1.7. Sensitivity of vesicles

As well as exhibiting appropriate stability, the vesicles need to be sensitive to their trigger, which in this case are bacterial membrane damaging proteins. One of the ways of ensuring sensitivity is by creating a system which resembles eukaryotic cells. Membrane damaging toxins often require cholesterol to bind to the surface of the membrane. In addition to cholesterol, membrane fluidity is thought to be important in tuning the sensitivity of vesicles to bacterial proteins[10].

3.1.7.1. Membrane fluidity

Membrane fluidity is closely related to the packing efficiency of lipid fatty acid chains. In a liquid-crystalline state, the hydrocarbon chains of the phospholipids are in constant motion and fully disordered, this occurs at higher temperature. As the temperature is decreased, hydrocarbon chains extend and the fatty acid chains become highly ordered, and van der Waals interactions hold the chains closely packed. This is called the gel-crystalline state (Figure 3.5). The temperature at which this change in state occurs is the phase transition temperature, T_m, previously referred to in Chapter 1.

Liquid-Crystalline **Gel-Crystalline**

Figure 0.5: the transitions between liquid-crystalline and gel-crystalline phase of a lipid bilayer

For a lipid bilayer to demonstrate sensitivity to bacterial toxins, a liquid-crystalline phase of the lipid bilayer is preferred over the gel-crystalline phase, due to the rigidity of the gel-crystalline phase interfering with the action of bacterial toxins.

3.1.7.2. Addition of Cholesterol

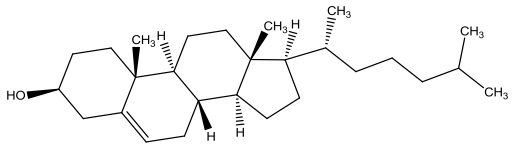

Figure 0.6: Structure of cholesterol

Cholesterol is an important and vital constituent of cell membranes. It is mostly hydrophobic but has a polar hydroxyl group, which allows the molecule to be amphipathic and can thus be inserted into a lipid bilayer (Figure 3.6). Cholesterol causes the phospholipid molecule to be in an 'intermediate state', and interferes with the close packing of the fatty acid chains. It increases the fluidity of the hydrocarbon chain below the gel-to-liquid crystalline phase and decreases the fluidity above the gel-liquid crystalline phase[11]. This has a 'destabilising 'effect on lipid bilayers, causing it to be close to a gel-crystalline phase, enabling the lipid bilayer to be more sensitive to bacterial toxins. Cholesterol makes up approximately 20% of the cell membrane. As a result, a 20% cholesterol proportion by volume was incorporated into the lipid bilayer[12].

3.2. Vesicle formation and characterisation

Vesicle preparation methods and list of vesicle compositions can be found in Chapter two of this document. Vesicle formation and characterisation was achieved using various visual and analytical techniques, during and after formation and purification of vesicles.

During the stages of vesicle preparation, vesicle formation was visually observed by the change in transparency of the lipid-containing solution mixture. This is illustrated in figure 3.7 where there is a clearly visible change in appearance of the solution before (A) and after extrusion (B).

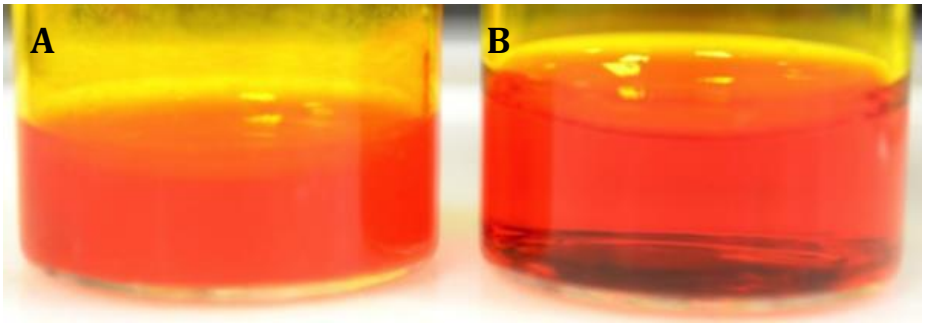

Figure 0.7: A. Aqueous solution containing lipid mixture: opaque before extrusion **B.** The opaque solution becomes transparent following extrusion (x3 at 60°C).

3.2.6. Vesicle characterisation during purification

Vesicles were characterised at the purification stage. In Figure 3.7 a plot of the fluorescence intensity vs. eluent volume shows two peaks, of which the peak with the lower maximum intensity represents self-quenched fluorescence of dye encapsulated in vesicles, and the peak with the higher maximum intensity represents un-quenched fluorescence of free-flowing dye.

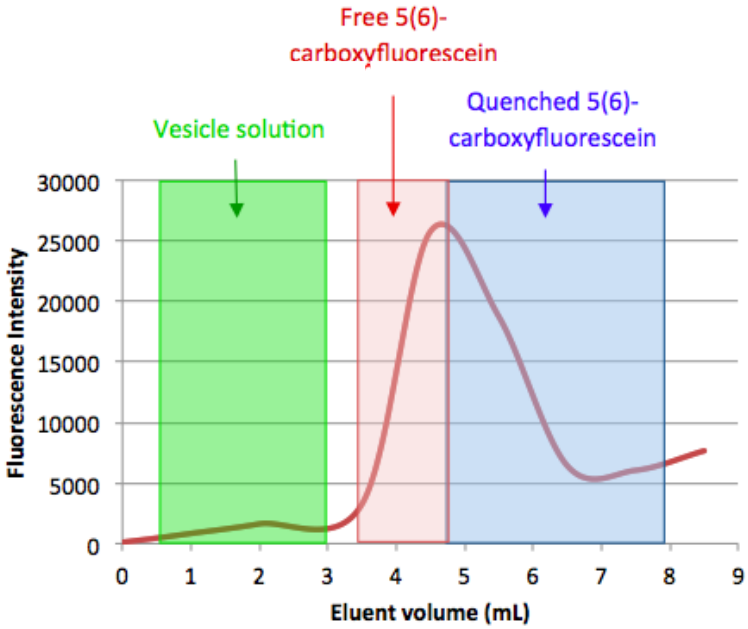

Figure 0.8: Fluorescence intensity of eluent using NAP-25 column. Acknowledgment: Jessica Bean Ph.D. candidate, Department of Chemistry, University of Bath.

The portion of the eluent solution containing vesicles, highlighted in green in figure 3.8, was isolated from any non-encapsulated dye and collected for further analysis.

3.2.7. Vesicle size characterisation

The Nanoparticle Tracking Analysis (NTA) was used to determine the size of the 25% TCDA- DP vesicle system, as well as determining the number of particles in a given volume of solution (Figure 3.9).

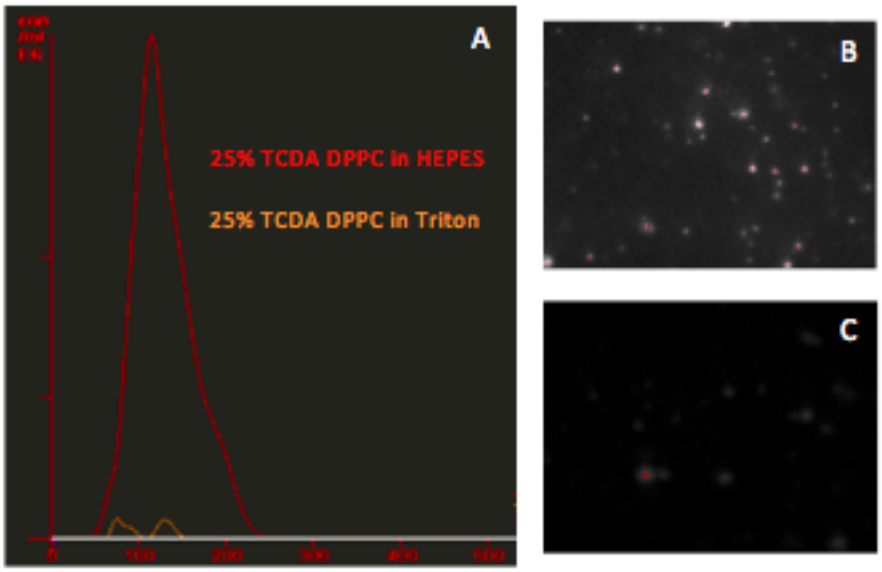

Figure 0.9: A. Plot of the size and population of DPPC vesicles in HEPES (red) and in Triton solution (orange). The decrease in population of 100nm vesicles is clearly visible, as the detergent is introduced. **B**. Showing the capture of the video taken for analysis of vesicles in HEPES. **C**. Showing the capture of the video taken for analysis of vesicles on addition of Triton.

The NTA shows a peak at 100nm, indicating the presence of 100nm vesicles when diluted in HEPES and on addition of Triton X-100, this peak disappears, and indicating absence of 100nm vesicles. This suggests that Triton X-100 successfully lyses vesicles. The NTA also showed that vesicle concentration could be approximated to approximately $1x10^{12}$ particles mL^{-1}.

3.2.8. Vesicle characterisation by microscopy

Further vesicle characterisation was carried out with the use of Atomic Force Microscopy (AFM). Vesicles were immobilised, by covalent bonding, onto maleic anhydride coated glass slides. Maleic anhydride coating of glass slides was achieved by means of plasma polymerisation. The AFM images below (Figure3.10) show vesicle attachment on the modified glass slides. A uniform distribution of vesicles can be observed with approximately 100nm in size. This is consistent with the size of vesicles expected to form through extrusion, confirming that the extruded size is the size of the end product.

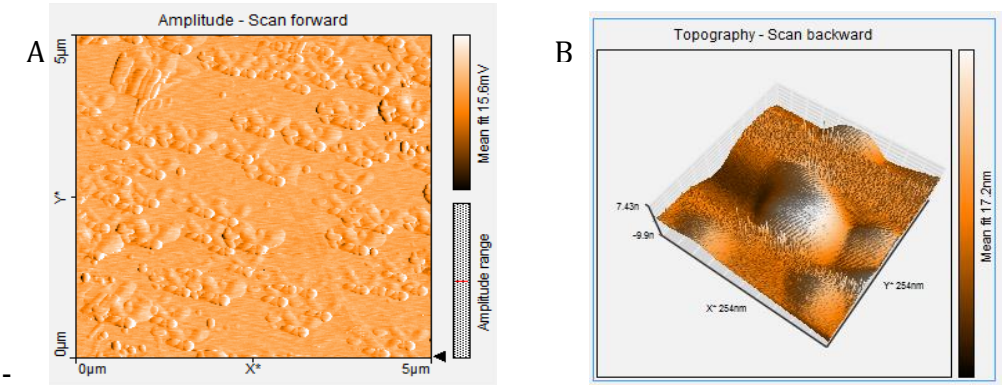

Figure 0.10: AFM of vesicles on Maleic anhydride coated glass slides. **A.** shows a forward amplitude scan zoomed in at frame size of 5µm. **B.** shows a backwards Topography scan zoomed at frame size of 254nm.

3.2.9. Summary of vesicle characterisation

Formation of uniform sized vesicles was achieved by means of a solvent evaporation method followed by extrusion through membranes with a pore size of 100 nm. Various characterisation methods were used to successfully detect the presence of vesicles with encapsulated self-quenched carboxyfluorescein. On further analysis, the size of the vesicles was confidently identified by means of numerous methods, to be 100 nm.

3.3. Vesicle stabilisation using 'stabilising agents'

Vesicles incorporating different types of stabilising agents were prepared and tested to discover the 'ideal' vesicle composition that exhibited appropriate stability as well as sensitivity to bacterial supernatant.

3.3.6. Incorporation of stabilizing agents in DMPC vesicles

As referred to in Section 3.1, previous research conducted by the group demonstrated that adding TCDA into the vesicle membrane improved the stability of DMPC vesicles. Following on from these results, various different methods were used to attempt to further improve the general stability of DMPC vesicles, using stabilizing agents such as DC8,9PC, PEG lipids and TCDA.

3.3.7. TCDA stabilised vesicles

Varying concentrations of TCDA were incorporated into DMPC vesicles containing cholesterol and DMPE. The short-term stability of the vesicles in HEPES was studied overnight, as well as sensitivity to a lytic agent with Triton X-100 as a positive control; the results are shown in figure 3.11.

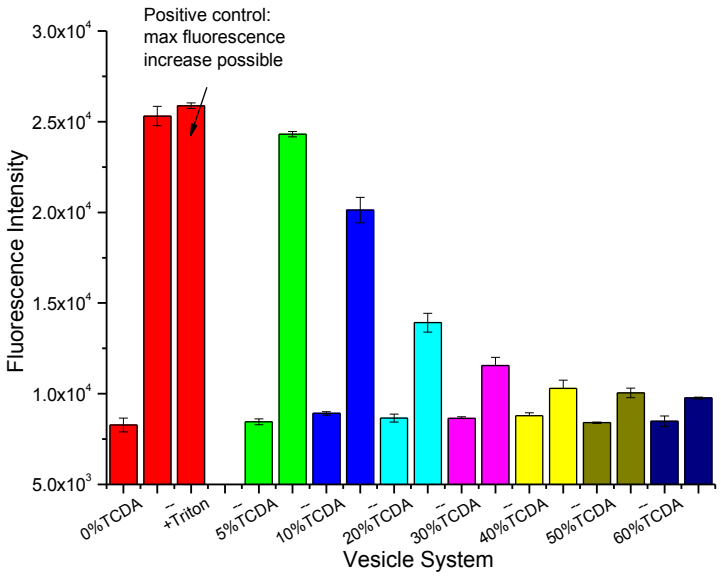

Figure 0.11: Stability measurements of TCDA-DM systems with varying concentrations of TCDA. Study performed by J.Zhou, University of Bath[13].

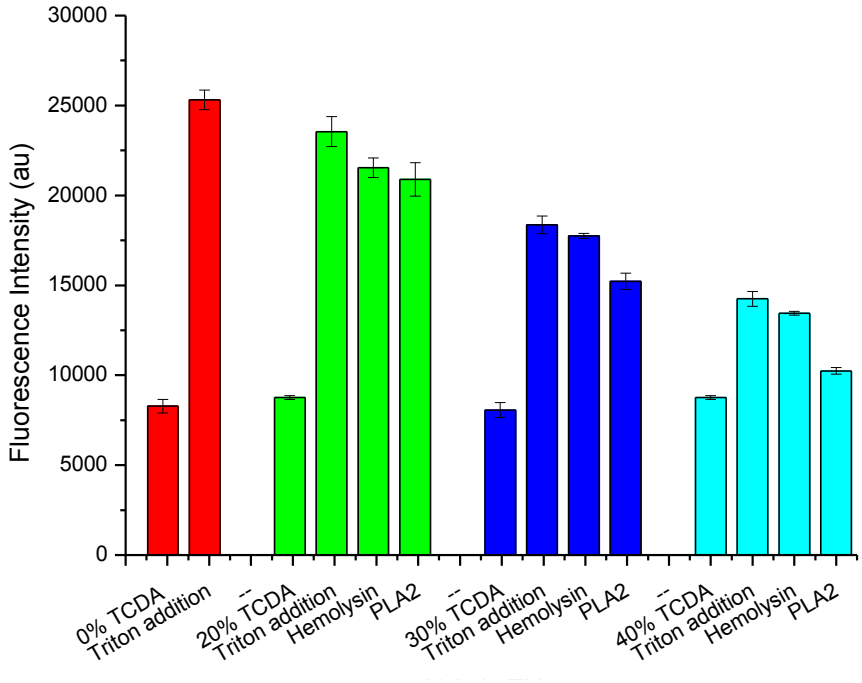

Figure 0.12: Toxin tests on vesicles with TCDA concentrations varying from 0% to 40%.; illustrating the optimum TCDA concentration (high sensitivity and stability) may be between 20% and 30%. Study performed by J. Zhou, University of Bath.

The two plots above (figures 3.11 and 3.12) indicate that the optimum balance between stability and sensitivity lies between TCDA concentrations of 20 and 30%. An in-depth study, summarised in figure 3.12, shows the response of 20, 25 and 30% TCDA-DM systems. The results were translated to show SR-parameter values in order to ease comparison between vesicle types.

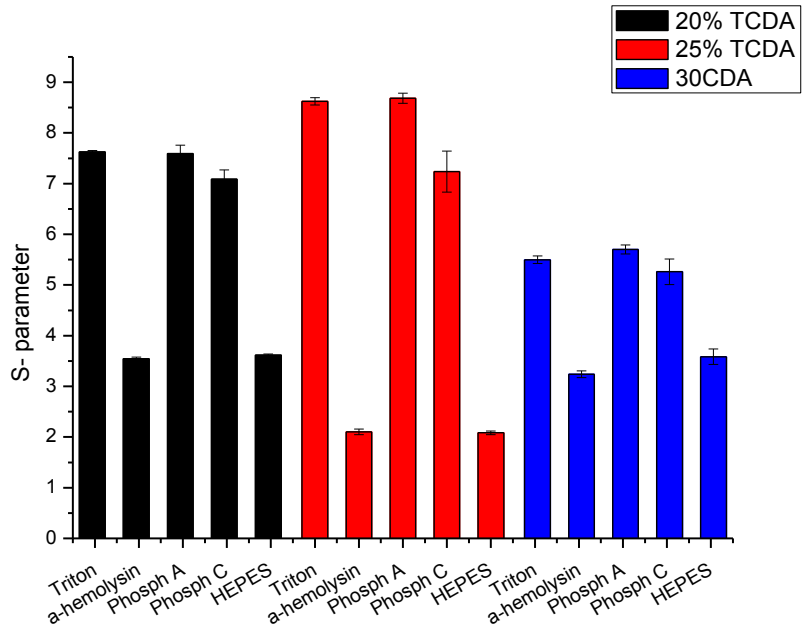

Figure 0.13: Effect of TCDA concentration on sensitivity of DMPC vesicles to purified toxins. Fluorescence intensity values were converted to SR-parameter values to aid analysis of results

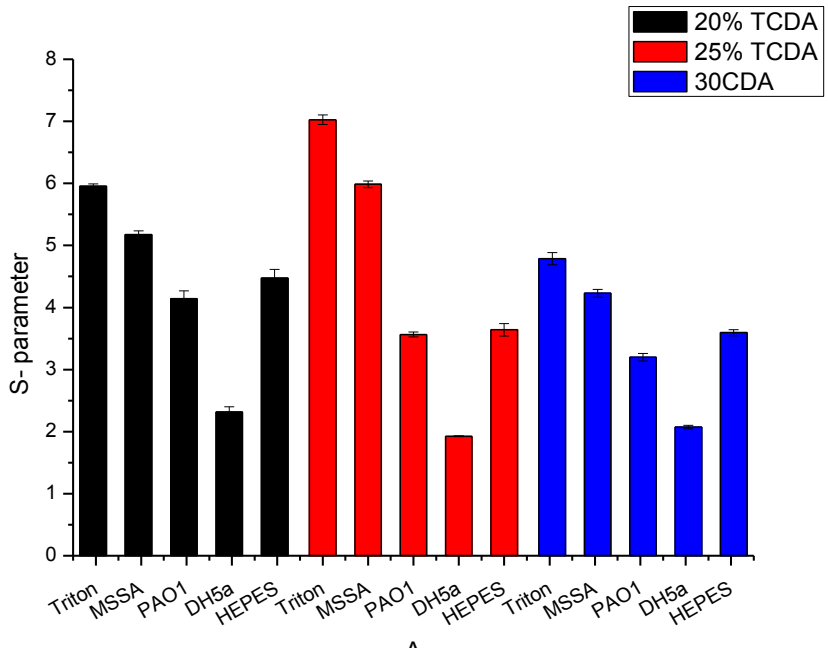

Figure 0.14: Effect of TCDA concentration on sensitivity of DMPC to bacterial supernatant. Fluorescence intensity values were converted to SR-parameter values to aid analysis of results.

Using the data summarised in figures 3.13 and 3.14, the optimum concentration of TCDA in a DMPC system was concluded to be 25% TCDA. A vesicle containing 25% TCDA-DM was shown to have improved stability overnight at 37°C in HEPES, compared to the 20% TCDA-DM system. When comparing the 25 and 30% TCDA-DM systems, the 25% TCDA-DM system was shown to be more stable and sensitive. This result was rather contradictory to the trend observed by J. Zhou, of increasing stability with an increase in TCDA. The result was confirmed by numerous repeats, indicating an optimum stability and sensitivity was achieved at 25% TCDA of the DMPC lipid mixture.

3.3.8. Studying the stabilizing effects of DC8,9PC in DMPC vesicles

DMPC vesicles containing various percentages (ranging from 0 to 100%) of DC8,9PC, were formulated. In contrast to reported results, DC8,9PC incorporated vesicles showed limited stability, and no improvement in stability was observed compared to TCDA incorporated vesicles. Upon overnight storage an increase in fluorescence intensity was observed, probably due to passive leakage.

3.3.9. Studies of the stabilizing effects of PEG lipids in DMPC vesicles

Varying concentrations of PEG 550- and PEG1000-containing DMPC-based lipid vesicles were formulated. Vesicles incorporating PEG 550 failed to form; there was an absence of the first fluorescence peak observed during the purification process.

Vesicles incorporating PEG1000 exhibited increased fluorescence following storage. This maybe have been due to formation of unstable vesicles, increased passive leakage of encapsulated dye due to increased fluidity of membrane, as well as delayed release of un-encapsulated dye entrapped within the highly entangled long PEG head group.

As a result PEG stabilised vesicles exhibited no improvement in stability when compared to the TCDA-DM system. These results have been tabulated along with other vesicle types in Section 3.5 of this Chapter.

3.4. Vesicle stabilisation by increasing lipid chain length

Further vesicle stabilisation studies were carried out with respect to increasing the lipid chain length of the bulk lipid, with the intention of improving stability with increasing transition temperature. These were carried out using DPPC (C16) and DSPC (C18) in the place of DMPC (C14) as the bulk lipid.

3.4.6. Studying the effect on stability of changing the phospholipid chain length of TCDA containing vesicles

Two samples of 25% TCDA vesicles were prepared using DMPC as the bulk lipid and DPPC as the bulk lipid, respectively. Vesicle stability was compared by incubation at 37°C in a 96 well plate overnight, and their SR-parameters were calculated following addition of Triton X-100 as the lytic agent (figure 3.15).

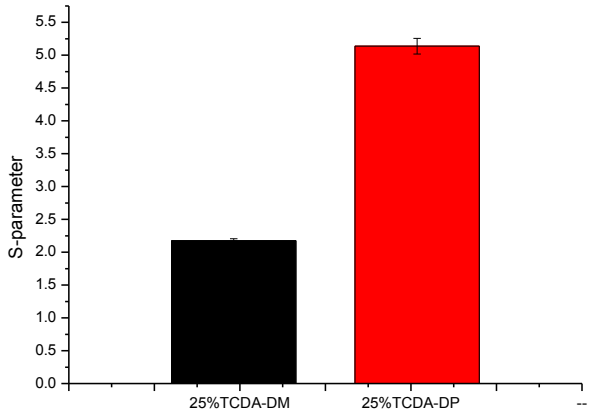

Figure 0.15: SR-parameters calculated following overnight incubation at 37°C. The SR-parameter of the 25% TCDA-DP system is more than double that of the 25% TCDA-DM system, indicating improved stability by incorporation of TCDA in place of the DMPC in the DPPC system.

The SR-parameter of the 25% TCDA-DP system was shown to be more than double that of the 25% TCDA-DM system. This indicates that increasing the bulk lipid chain length from C14 to C16, improved the stability of vesicles incorporating 25% TCDA.

3.4.7. Studying the effect of changing phospholipid chain length of TCDA-containing vesicles, on their sensitivity to bacterial supernatant

Vesicle stability was improved by usage of a longer chain lipid, DSPC (C18). To assess sensitivity, systems were tested with bacterial supernatant by overnight incubation at 37°C. The fluorescence intensities were used to calculate the SR-parameter. Results show that 25% TCDA-DS system is less sensitive to *S. aureus* MSSA 476 supernatant, however similar sensitivities are observed on incubation with and *P. aeruginosa* PAO1 supernatants compare to the 25% TCDA-DP system (Figure 3.16). Overnight stabilities in HEPES and *E. coli* DH5a supernatant have been shown to be similar.

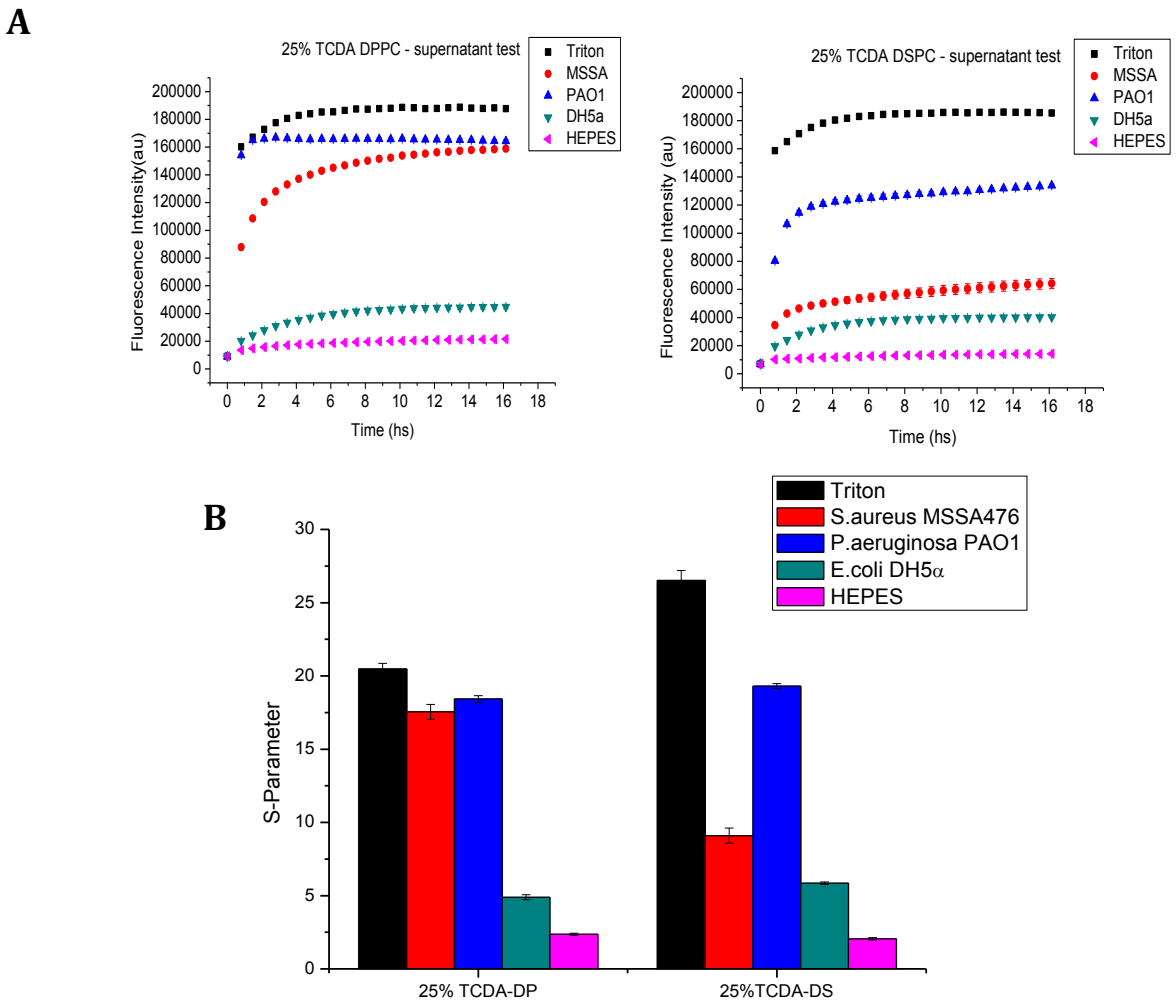

Figure 0.16: A: Overnight response curves of the 25% TCDA-DP and the 25% TCDA-DS systems tested against bacterial supernatants. **B:** SR-parameters of the fluorescence intensities.

The 25% TCDA-DS vesicles show overall decreased sensitivity compared to the 25% TCDA-DP system. This effect in sensitivity may be due to decreased fluidity of the bulk DSPC lipids within the membrane, as the DSPC lipids have longer chain lipids compared to DPPC, thus the interactions between the chain groups will increase, decreasing the fluidity of lipids.

An abnormality was found during the preparation stage of the 25% TCDA-DS system. Following crosslinking of the TCDA vesicles, the solution turned green rather than yellow, and gave rise to a green precipitate (Figure 3.17). In order to determine whether the precipitation occurring was due to the use of TCDA in longer chain lipids, DSPC vesicles were prepared using varying concentrations of TCDA.

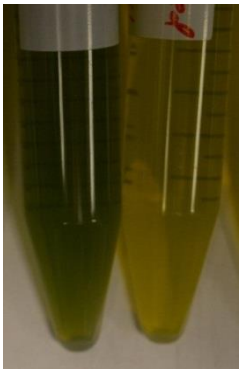

Figure 0.17: Crosslinked 25% TCDA-DS vesicles. Upon crosslinking, some solutions turned green and a precipitate was observed, whilst other solutions showed no difference.- suggesting that incorporation of TCDA into the vesicle system makes the system more difficult to standardise.

3.4.8. Studying the effect of changing concentration of TCDA in DSPC vesicles

DSPC based vesicles with TCDA concentrations of 0, 5, 15 and 25% were prepared. The 25% TCDA-DS system exhibited formation of green precipitate following crosslinking, whereas the other systems showed no precipitate formation. The sensitivity to bacterial supernatant and the stability in HEPES was studied by an overnight assay (figure 3.18).

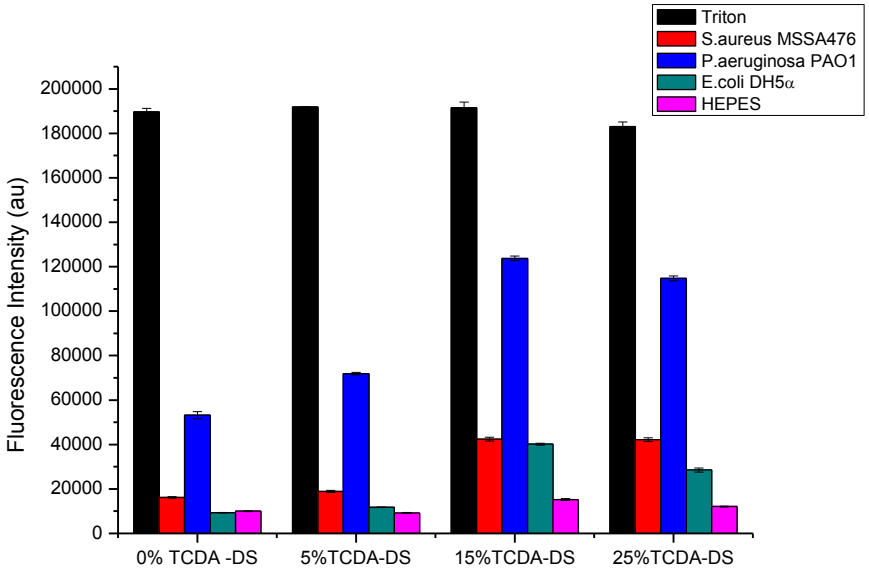

Figure 0.18: Overnight stability and sensitivity at 37°C of TCDA-DS vesicles with varying concentrations of TCDA. General trend observed: sensitivity increases with increasing concentration of TCDA, while stability decreases.

The results of the bacterial supernatant assay suggest that as the concentration of TCDA increases, the stability decreases and the sensitivity increases, suggesting that TCDA has a de-stabilising effect on vesicles with longer chain bulk lipids, rather than a stabilising effect. This can also suggest that instead of creating stabilised regions, as in DMPC systems, in systems using longer chain lipids, destabilised regions may be forming. The 15% TCDA shows higher sensitivity and lower stability compared to 25% TCDA, suggesting that 25% TCDA was to be a more favourable candidate to continue with throughout the project.

3.5. Summary of Vesicle optimisation

Table 0.1: Summary of stability of vesicles of various compositions with stability – response parameter values, following long-term stability studies. *No increase in fluorescence on addition of Triton.[14]

Vesicle Name	*Main lipid constituent*	*Secondary component*	*Stabilizing agent*	*Initial stability (formation of vesicles following purification and polymerization if needed)*	*Stability – response parameter, S pH 7 / 37 °C / 14 days*
DMPC	DMPC (14:0) 78 %	Cholesterol 20% DMPE 2%	None	Yes	1*
30% DC8,9PC-DM	DMPC (14:0) 40 %	Cholesterol 30 %	DC8,9PC (23:2) 30%	No	N/A
40% DC8,9PC-DM	DMPC (14:0) 40 %	Cholesterol 20 %	DC8,9PC (23:2) 40%	No	N/A
10% PEG550-DM	DMPC (14:0) 68 %	Cholesterol 20% DMPE 2%	PEG 550 (14:0) 10%	No	N/A
10% PEG1000-DM	DMPC (14:0) 68 %	Cholesterol 20% DMPE 2%	PEG 1000 (14:0) 10%	Yes	1*
25% TCDA-DM	DMPC (14:0) 53 %	Cholesterol 20% DMPE 2%	TCDA 25%	Yes	1*
DPPC	DPPC (16:0) 78 %	Cholesterol 20% DPPE 2%	None	Yes	2.01
15% TCDA-DP	DPPC (16:0) 63 %	Cholesterol 20% DPPE 2%	TCDA 15%	Yes	1.52
10% DPPG-DP	DPPC (16:0) 53 %	Cholesterol 20% DSPC 15% DPPE 2%	DPPG 10%	Yes	3.84
10% DSPG-DP	DPPC (16:0) 53 %	Cholesterol 20% DSPC 15% DPPE 2%	DSPG 10%	Yes	5.12
DSPC	DSPC (18:0) 78 %	Cholesterol 20% DSPE 2%	None	Yes	1.69
15% TCDA-DS	DSPC (18:0) 63 %	Cholesterol 20% DSPE 2%	TCDA 15%	Yes	3.70
2% DOPC-DS	DSPC (18:0) 76 %	Cholesterol 20% DSPE 2%	DOPC 2%	Yes	2.28

More than 70 different types of vesicle formulations were studied within the research group, a selection of these vesicles and their SR-parameters are listed in Table 3.1. A recent publication in Langmuir details the studies conducted comparing the different types of vesicles formulated by other members of the group. Three leading vesicle formulations were chosen and their stabilities and sensitivities were carefully studied. The leading vesicles were 10% DSPG PD, 15% TCDA DS and 2% DOPC DS. The work involving these three vesicles have been carried out in conjunction with Serena Marshall, Ph.D. candidate in the Toby Jenkins' research group, University of Bath, UK. This work has recently been reported in Langmuir[14].

3.5.6. pH stability of leading vesicles

Table 0.2: The effect of pH changes on the stability of the three leading vesicles. The effect was monitored over a 14 day period. The SR-parameter values were calculated following 14 day storage at 37 °C and lysis using Triton X-100.

Vesicles	*pH stability at 37 °C (Stability Response Parameter, **SR**)*		
	5	6	7
15% TCDA-DS	3.21 (±0.2)	3.57 (±0.1)	3.70 (±0.2)
2% DOPC-DS	4.86 (±0.2)	6.41 (±0.4)	2.28 (±0.3)
10% DSPG-DP	3.84 (±0.8)	4.51 (±0.6)	5.12 (±0.4)

According to the data obtained from the long-term pH stability study, the 15% TCDA-DS system showed the most consistent SR-parameter values throughout the ranges of pH tests. The 2% DOPC-DS system showed excellent stability at pH 6, however a relatively low stability at pH 7. The 10% DSPG-DP vesicle system also showed good stability in all the range of pH tests.

3.5.7. Sensitivity to whole bacteria and bacterial supernatant

In these later assays, a different strain of *S. aureus* to previous studies was used. A more clinically relevant TSST-1 (Toxic shock syndrome toxin) producing strain of *S. aureus*, RN4282 was used instead of *S. aureus* MSSA476 to assess the sensitivities of the three leading vesicles.

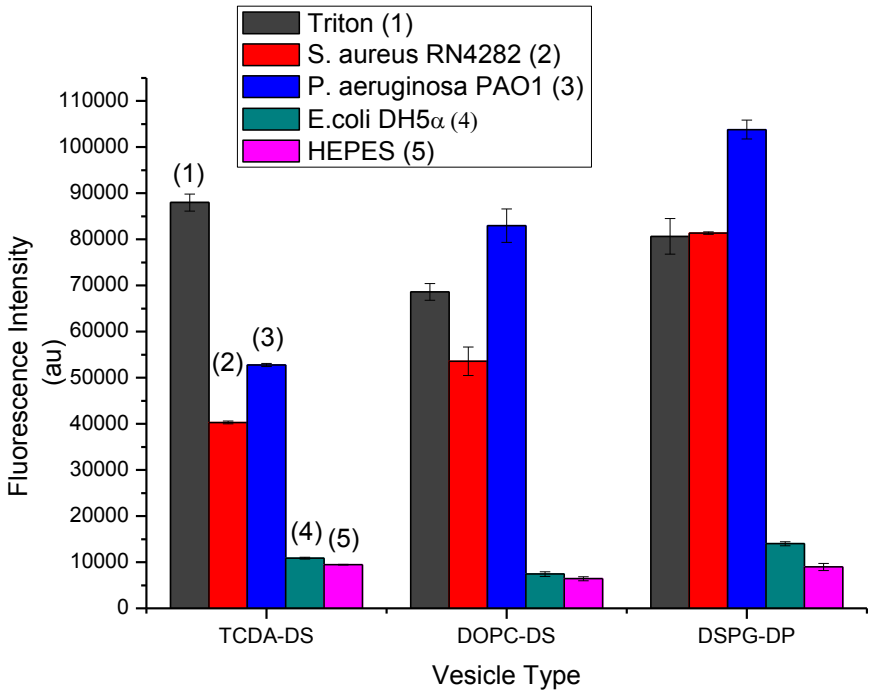

Figure 0.19: Vesicle response to bacterial supernatant after 100 mins of exposure: (1) Triton-X100,(2) *S. aureus* RN4282, (3) *P. aeruginosa* PAO1, (4) *E. coli* DH5α, (5) HEPES buffer.

The raw fluorescence intensity measurements have been displayed graphically in figure 3.19. Overall, all three vesicles systems show stability in *E. coli* DH5α supernatant and HEPES and sensitivity to *S. aureus* RN4282 and *P. aeruginosa* PAO1 supernatants as well as the control, Triton X-100. The relatively higher response of the 10% DSPG-DP system compared to the other two systems maybe due to use of DPPC as the bulk lipids unlike DSPC used by the other two systems. Overall weaker interaction of the tail group of the DPPC system can be responsible for an increased susceptibility to bacterial toxin interactions.

Table 0.3: SR-parameter values following overnight incubation with pathogenic bacteria cells (*S. aureus* RN4282 and *P. aeruginosa* PAO1 and relative non-response from HEPES buffer, *E. coli* DH5α, LB broth, TS Broth (TSB) and Triton X-100 was the positive control.

Vesicle type	*Triton*	*S. aureus (RN4282)*	*P. aeruginosa (PAO1)*	*E. coli (DH5α)*	*HEPES*	*LB broth*	*TS Broth*
15% TCDA-DS	31.9 (±0.33)	6.34 (±0.33)	12.0 (±0.09)	3.21 (±0.45)	1.24 (±0.03)	3.17 (±0.77)	1.60 (±0.03)
2% DOPC-DS	25.1 (±0.36)	6.38 (±0.06)	33.2 (±2.77)	1.93 (±0.05)	1.43 (±0.04)	1.69 (±0.13)	1.28 (±0.08)
10% DSPG-DP	43.4 (±0.15)	7.70 (±0.09)	36.9 (±2.17)	2.44 (±0.16)	1.20 (±0.18)	2.12 (±0.14)	2.82 (±1.78)

The results of sensitivity analysis using bacterial supernatant and whole bacteria show that the 15%TCDA-DS system was the least sensitive, and that the 10% DSPG-DP system was the most sensitive (figure 3.19 and table 3.3). The 2% DOPC-DS system showed relatively good stability and sensitivity results, however reproducibility of vesicle production was low. The relatively lower sensitivity observed systems could also be associated as relatively higher stability. As a result, although the 15% TCDA system showed the lowest sensitivity, it was used for further research towards the development of a responsive wound dressing.

3.6. Conclusion

This study concentrated on formulating vesicles with varying compositions and concentrations of stabilising lipids in a constant concentration of 20% cholesterol, 2% PE with varying concentration of bulk PC (depending on concentration of stabilising agent used). Incorporation of 25% TCDA in vesicles with bulk lipid of DMPC was found to show the most desirable stability and sensitivity out of the numerous stabilising agents tested.

Further optimisation of vesicles was achieved by varying the bulk lipid chain length; C14, C16 and C18. Replacing the DMPC in the 25% TCDA-DM system with the longer chain DPPC (C16) improved the stability of vesicles and subsequent analysis using DSPC (C18) showed further stability. The 25% TCDA-DS system was proven to have low reproducibility, due to formation of black residue in vesicle solutions, which was latter discovered to be TCDA which was not incorporated within the vesicle system. Upon analysis of lowing concentrations of TCDA in the DSPC system, 15%TCDA-DS vesicles were chosen as the final vesicle candidate for further development within the study.

Validation of the stability and sensitivity of the 15% TCDA-DS system was achieved by comparison with two other vesicles systems developed by other members of the group. A series of pH and temperature stability assays over a period of 14 days, as well as sensitivity assays against whole bacterial culture and bacterial supernatant, were carried out and fluorescence intensity values and SR-parameter values were compared. The 15% TCDA-DS system were shown to have comparable stability and sensitivity features to the other two vesicle systems, thus this system was chosen for further development of a wound dressing with pathogenic detection capabilities in conjunction with wound healing properties.

3.7. References

1. Keough, K. M. W., Gel to liquid-crystalline phase transitions in water dispersions of saturated mixed-acid phosphatidylcholines. *Biochemistry* **1979,** *18* (8), 1453.

2. Kolusheva, S.; Boyer, L.; Jelinek, R., A colorimetric assay for rapid screening of antimicrobial peptides. *Nature Biotechnology* **2000,** *18* (2), 225-227.

3. (a) Henriksen, I.; Våagen, S. R.; Sande, S. A.; Smistad, G.; Karlsen, J., Interactions between liposomes and chitosan II: Effect of selected parameters on aggregation and leakage. *International Journal of Pharmaceutics* **1997,** *146* (2), 193-203; (b) Sriwongsitanont, S., Physicochemical properties of PEG-grafted liposomes. *Chemical & Pharmaceutical Bulletin* **2002,** *50* (9), 1238.

4. Henriksen, I.; Smistad, G.; Karlsen, J., Interactions between liposomes and chitosan. *International Journal of Pharmaceutics* **1994,** *101* (3), 227-236.

5. Zhou, J.; Tun, T. N.; Hong, S.-h.; Mercer-Chalmers, J. D.; Laabei, M.; Young, A. E. R.; Jenkins, A. T. A., Development of a prototype wound dressing technology which can detect and report colonization by pathogenic bacteria. *Biosensors and Bioelectronics* **2011**, 30 (1), 67-72,

6. Zhou, J.; Loftus, A. L.; Mulley, G.; Jenkins, A. T. A., A Thin Film Detection/Response System for Pathogenic Bacteria. *Journal of the American Chemical Society* **2010,** *132* (18), 6566-6570.

7. Singh, A.; Markowitz Michael, A.; Tsao Li, I.; Deschamps, J., Enzyme Immobilization on Polymerizable Phospholipid Assemblies. In *Diagnostic Biosensor Polymers*, American Chemical Society: 1994; Vol. 556

8. Yavlovich, A.; Singh, A.; Tarasov, S.; Capala, J.; Blumenthal, R.; Puri, A., Design of liposomes containing photopolymerizable phospholipids for triggered release of contents. *Journal of Thermal Analysis and Calorimetry* **2009,** *98* (1), 97-104.

9. Lasic, D.; Needham, The "Stealth" Liposome: A Prototypical Biomaterial. *Chemical Reviews* **1995,** *95* (8), 2601-2628.

10. Thet, N. T.; Hong, S. H.; Marshall, S.; Laabei, M.; Toby, A.; Jenkins, A., Visible, colorimetric dissemination between pathogenic strains of *Staphylococcus aureus* and *Pseudomonas aeruginosa* using fluorescent dye containing lipid vesicles. *Biosensors and Bioelectronics* **2012,** *41* (0), 538-543.

11. Yeagle, P. L., *The Structure of Biological Membranes*. CRC press 2011.

12. Alberts B.; Jonhnson, A.; Lewis, J.; Raff, M.;Roberts, K.; Walter, P., *Molecular Biology of the Cell*. Garland Science, 2007

13. Zhou, J. *Study and development of a 'smart' wound dressing technology which can detect and inhibit/kill the colonisation of pathogenic bacteria*. PhD diss., University of Bath, Bath, 2011.

14. Marshall, S.; Hong, N. T.; Thet, A. T. A.; Jenkins, Effect of Lipid and Fatty Acid Composition of Phospholipid Vesicles on Long-Term Stability and Their Response to *Staphylococcus aureus* and *Pseudomonas aeruginosa* Supernatants. *Langmuir* **2013,** *29* (23), 6989-6995.

Chapter Four: Hydrogel and prototype dressing development

4.1. Introduction

This chapter presents the results obtained from the screening process of different hydrogels for vesicle immobilisation with respect to their properties to achieve optimal vesicle stability and sensitivity. Vesicles were dispersed into simple hydrogel formulations; their long-term stabilities at a range of different temperatures were assessed, and their sensitivities to whole bacteria as well as bacterial supernatant were investigated.

4.2. Hydrogels

Due to the amphiphilic nature of lipids and the bilayer of lipid vesicles, the lipid-based nanocapsules being studied require a moist environment for optimum stability. In order to maximise the stability of vesicles, the proposed method is to immobilise these vesicles in a hydrogel matrix, easpecially as most commercially available wound dressings are hydrogel-based. Furthermore, the proposed use of the sensor is for burn wound management along with the development of a dressing for burn wound care, which mostly use hydrogel based treatment system.

4.2.1. Polysaccharide gelling agents

As discussed in Chapter 1, one of the most important factors of a wound dressing is its biocompatibility, in order to minimise side effects arising from the composition of the dressing. As a result, the use of natural ingredients for development of wound care products and pharmaceutical devices is on the increase[1].

In this study, different types of polysaccharides, such as gelatin, guar gum, agar and agar derivatives, have been exploited as gelling agents for immobilisation of vesicles. Polysaccharide-based gelling agents and gums are widely used by the food and cosmetic industries as stabilising and thickening agents and emulsifiers. Polysaccharides such as agar and agar derivatives, namely agarose, have been utilised in microbiology to provide a solid surface for bacterial growth and as a medium for analytical scale electrophoresis for the separation of proteins[2].

4.2.1.1. Gelatin

Gelatin is an irreversibly hydrolysed form of collagen, often obtained from animals, the latter being mostly porcine derived. It is largely used as a gelling agent in the food industry, as well as in some pharmaceuticals. Recent developments have introduced gelatin as a matrix for tissue engineering[3] and as injectable drug delivery[4].

Both porcine and synthetic gelatins were studied in this investigation. Gelatin gels were formed in HEPES buffer.

4.2.1.2. Agar and Agarose

Agar is a gelling agent obtained from the cell walls of certain species of the Rhodophyceae class of seaweed [5]. It is a polymer consisting of agarose and agaropectin which consists of subunits of galactose[6]. Agar has a relatively low gelling temperature and high melting temperature[7]. This property is highly desirable for scientific use, especially in microbiological applications where high incubation temperatures are required (37°C).

Agarose consists of repeating monomeric units of agarobiose, which is a disaccharide of D-galactose and 3,6-anhydro-L-galactopyranose. Agarose is the purified form of agar (without agaropectin), and thus exhibits similar properties. The low degree of chemical complexity and the broad range of chemical, thermal and physical stability of agarose makes it less likely to interact with biomolecules, thus, it is often the preferred matrix for use with biological substances such as proteins and nucleic acids[8].

4.2.1.3. Polysaccharide gums

Xanthan and guar gum are both polysaccharides, used extensively in the food industry as stabilisers and thickening agents[7]. Xanthan gum is derived from glucose, sucrose or lactose. It was the first polymer produced by fermentation of carbohydrates[9]. The production of xanthan uses the bacterial stain *Xanthomonas campestris* [10]. Guar gum is derived from guar beans. It mainly consists of galactose and mannose[11].

4.2.2. Other hydrogels utilised in this study

4.2.2.1. Hypromellose

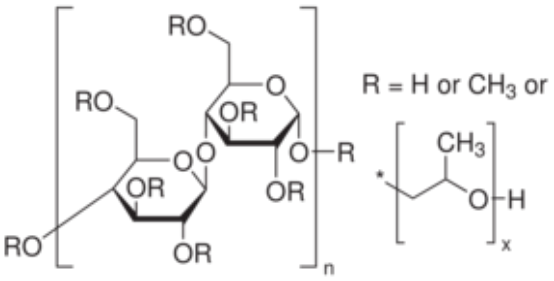

Figure 0.1: Chemical structure of Hypromellose

Hydroxypropyl methylcellulose (HPMC), also known as Hypromellose, is a synthetic polymer typically used in the pharmaceutical industry to coat active ingredients, or in the food industry to use as a vegetarian alternative to gelatin[12]. Hypromellose forms a sticky, viscose and clear gel. The chemical structure of the gel is given in figure 4.1.

4.2.2.2. Polyacrylamide hydrogel foam

Polyacrylamide hydrogel can be used to produce absorbent foam such as in a hydrogel dressing, which could potentially act as a matrix for immobilisation of lipid vesicles, as well as act as an absorbent and adhesive hydrogel dressing for wound management.

4.2.2.3. Fmoc protected dipeptides

The formation of three dimensional hydrogels using dipeptides have been investigated for a wide range of applications in the field of biomaterials and healthcare development[13]. These gels have been investigated for use as scaffolds for growth of cells for tissue culture, as well as tissue engineering and regeneration purposes[14].

Small amphiphilic dipeptide molecules (figure 4.2) have been shown to form fibrous structures that entangle and allow the formation of gel through hydrogen bonding and π- π stacking between the peptides[15]. The gelation of these peptides

can be induced in a number of ways, including pH change[15b], enzyme action[16] and solvent polarity changes[14b].

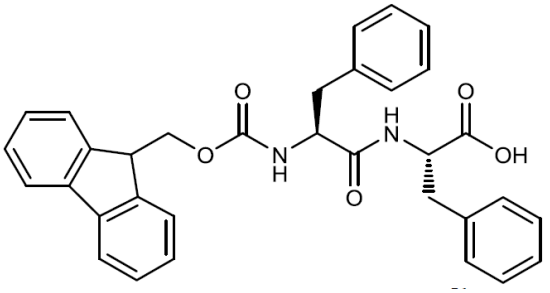

Figure 0.2: Structure of Fmoc-diphenylalanine (FmocFF)

4.2.3. Properties of gel required for use as a vesicle immobilisation matrix

The primary role of the gel is to act as an immobilisation matrix for the vesicles. The gel must not interfere with the activity of vesicles. Therefore, one of the most important requirements for the gel matrix is the ability to stabilise the vesicles without interfering the lysing mechanism by bacterial supernatant. Upon lysis of vesicles, the dye released by the lysis of the vesicle has to be visible; as a result a transparent and translucent gel would be beneficial.

Table 0.1: Gels prepared using HEPES Buffer

Hydrogel	*Appearance of gel*	*Physical property of gel*
Agar	Colourless, transparent at low concentrations of gelling agent. However, becomes opaque as the concentration of gelling agent increases.	Gels set as block at gelling agent concentration above 0.6wt%.
Agarose	Colourless, transparent at low concentrations of gelling agent. However, becomes opaque as the concentration of gelling agent increases.	Gels set as block at gelling agent concentration above 0.6wt%.
Gelatin	Slight yellowy coloured gel formed. Transparent gel formed.	Gels set as block at high gelling agent concentration. Can be crosslinked using glutamic acid to from gels at lower gelling agent concentration.
Hypromellose	Clear and transparent gel formed.	Runny with high viscosity gel formed.
Agar/Hypromellose	Clear and transparent gel formed	Gel set as block.
Agarose/Hypromellose	Clear and transparent gel formed	Gel set as block
Xanthan gum	Opaque gel formed	Runny gel formed

Pectin	Opaque gel with slight yellowy colour gel formed	Runny with relatively low viscosity gel formed
Guar gum	Opaque, colourless gel formed	
Polyacrylamide hydrogel foams	Clear and transparent gel formed.	Gel set as block when Uv crosslinked.
Chitosan	Clear and transparent gel formed.	Runny gel formed

The table above (table 4.1) shows observed results of the colour, transparency and rheological properties of the gels formed. This process allowed for optimised choice of gels to be further studied in depth at later stages in the project. The colourlessness and transparency of the gels were two of the main desired properties. As well as the colour, formations of a block gel without the addition of further crosslinker were desirable, in order to retain a low degree of chemical complexity. The gelling agents that produced gels with potential as vesicle immobilisation matrixes were tested further for vesicle stability.

4.3. Hydrogel fabrication and initial vesicle stability in gels

4.3.1. Defining stability

Stability of vesicles in gels can be defined in a similar way to the stability of vesicles described in the previous chapter, Chapter 3. Initial stability was determined by the colour of the solution on addition of vesicles to the gel solution; immediate colour change (yellow to green) indicated unstable vesicles. SR-parameter values on addition of Triton X-100 and HEPES were calculated. A high value was desired on addition of Triton X-100, indicating a high response and a low value was required on addition of HEPES (close to 1) indicating stability. Long term temperature stability was measured in a similar manner to vesicles in solution. The studies were carried out in 96 well plates, a large increase in fluorescence upon lysis with Triton X-100 or bacterial supernatant following incubation at 37°C over a period of 14days, indicated stable vesicles.

4.3.2. Stability of vesicles when embedded in hydrogels

Hydrogels, especially biopolymer gels have been of particular interest recently, due to their unique physical, thermal and mechanical properties. Biomimetic polymer gels are used in cosmetics, personal care products, and pharmaceutical and as encapsulation media of active ingredients. Their ability to hold aqueous solutions allows for a constantly hydrated environment, and an ideal environment in which to embed lipid vesicles. Various different hydrogels, ranging from simple water-soluble polysaccharides to more complex polymer hydrogels have been studied in order to obtain the optimum medium for vesicle immobilization and prototype development.

4.3.3. Studying the initial stability of vesicles

Various naturally derived hydrogels were screened with respect to vesicle stability. The tabulated results, given in table 4.2, of the initial screening process list a number of promising candidates showing good initial vesicle stability.

Table 0.2: Vesicle stability was assessed by observing for immediate appearance of the fluorescence on addition of vesicle solution to gel. 'Stable' in this case indicates that fluorescence increase upon addition of vesicle solution to gel was not immediate. Unstable indicates that the solution appeared fluorescent immediately after addition of vesicle solution to gel.

Hydrogel	*Vesicle Type*		
	TCDA-DM	TCDA-DP	TCDA-DS
Agar	Unstable	Stable	Stable
Agarose	Unstable	Stable	Stable
Gelatin	Unstable	Stable	Stable
Hypromellose	Stable	Stable	Stable
Agar/Hypromellose	-	Stable	Stable
Agarose/Hypromellose	-	Stable	Stable
Polyacrylamide hydrogel foams	Unstable	Unstable	Unstable
FmocFF	Unstable	Unstable	Unstable

From the results tabulated above, four of the gelling agents listed were taken on for further analysis. Long-term stability analyses were carried out over extended periods of time at elevated temperatures. Short-term stability was determined by overnight response analysis at 37°C. The studies were carried out in 96well plates.

4.4. Vesicle sensitivity in gel matrixes

The initial stability and sensitivity of vesicles dispersed in gel matrices were assessed. Their sensitivity to Triton X- 100 was observed before analysis with bacterial supernatant. Fluorescence measurements were obtained before and after addition of lysing agent, and the SR-parameter was calculated. A large difference in SR-parameter values was desired between the value obtained on addition of Triton X-100 and that of HEPES.

4.4.1. Fmoc FF

For a 15% TCDA-DS system, vesicles were added to 2mg mL^{-1} FmocFF gel in a 2:1 gel to vesicle ratio. Immediate fluorescence increase could be observed on addition of the vesicles (figure 4.3).

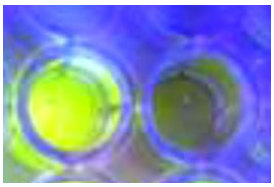

Figure 0.3: Instability of vesicles when added to 2mg mL^{-1} FmoFF gel compared to HEPES buffer.

The osmolality of the vesicle solution as well as the gel, before formation of a set gel, and following formation of a set gel, were tested using an Osmometer. The osmometer measures the concentration of solute per kilogram of solvent and an osmotic pressure in moles.kg^{-1} can be obtained in this manner (table 4.3).

Table 0.3: The osmolality and pH of the FmocFF gel as well as the vesicle solution. This work was carried out by Charlotte Spencer, MChem student at the University of Bath, UK[17]

Test solution	*Osmolality mOsm/kg*	*pH*
FmoFF gel (before gelation)	570	5
FmocFF (after gelation)	404	-
Vesicles	212	7.4

In addition to the difference in osmolality, the difference in pH (table 4.3) and large fibre formation due to the low pH of the gel could also be the cause of vesicle instability[18].

4.4.2. Polyacrylamide

Polyacrylamide gels were fabricated using the materials and formulation supplied by First Water Ltd. The gels were formed by the combination of the acrylamide monomer, glycerol, water and a photo-polymerising mixture. Vesicle solutions were added to the pre-crosslinked gel mixture, and various formulations were assembled using different concentrations of water. Vesicle response was measured following addition of Triton X-100. Figure 4.4 shows images of vesicles fluorescing upon addition of the pre-gel mixture.

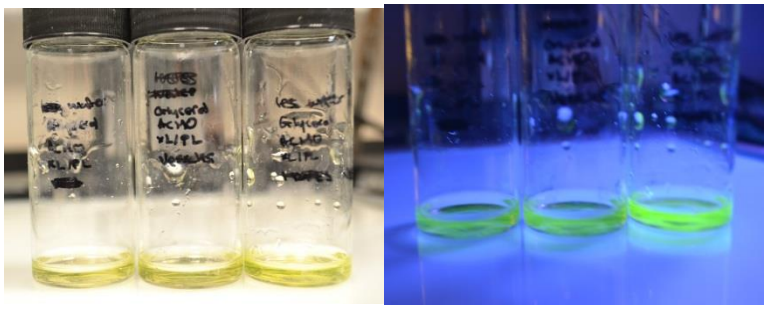

Figure 0.4: images taken under day-light and under UV-lamp at 254nm, indicating lysed, fluorescent vesicles.

A

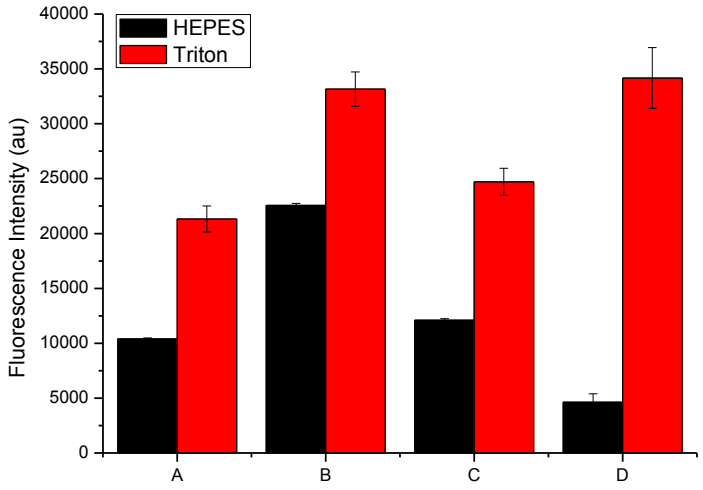

B

Gel Type	*SR- parameter value on addition of Triton*
A	2.05 (± 0.116)
B	1.47 (± 0.071)
C	2.04 (± 0.103)
D	7.39 (± 1.36)

Figure 0.5: Response of vesicles to addition of Triton X-100 and HEPES buffer. **A**: original ingredient of gel **B**: 1mL of water replaced with vesicle solution from the original recipe **C:** total water content of the original recipe replaced with HEPES with additional vesicle solution **D**: vesicle diluted with HEPES to yield the same dilution as in gel mixtures.

Vesicles did not show stability in the polyacrylamide gel, as observed in the data and figures given above. The SR- parameter values on addition of Triton X-100 are much lower when added to the mixture of vesicles in gel compared to the control; the same dilution of vesicles in HEPES.

4.4.3. Gelatin

15% TCDA-DS vesicles were added to a pre-prepared solution of 4% gelatin, in a 2:1 gel to vesicle solution ratio. The immediate response of vesicles in the gel matrix was measured by the addition of Triton X-100 and HEPES as a control. The desired response being an at least 2-fold increase in fluorescence upon addition of the lysing agent and as low increase as possible on addition of HEPES.

The gelatin mixture showed a large SR-parameter of 7.67 (±0.213) on addition of Triton and 1.05 (±0.016), a value close to one, on addition of HEPES. Following on from these results, measurements were made on the response of the vesicles in the matrix to bacterial supernatant.

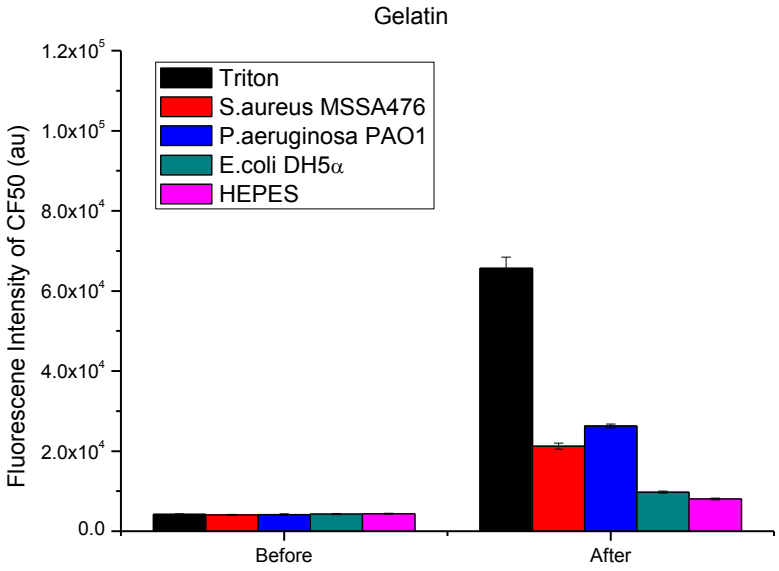

Figure 0.6: The overnight response of vesicles dispersed in gelatin gel to bacterial supernatant at 37°C. Vesicles were dispersed into the gel and incubated overnight with supernatant of *P. aeruginosa* PAO1, *S. aureus* MSSA476 and *E. coli* DH5α, as well as Triton X-100 as a positive control and HEPES as a negative control.

4.4.4. Hypromellose

The 2% hypromellose system utilised contained a hypromellose/gel mixture in a 2:1 ratio. The mixture was tested against Triton X-100. The SR-parameter values were 10.1 (±0.398) on addition of Triton X-100 and 0.937 (±0.018) on addition of HEPES. The gel/vesicle mixture was then tested with bacterial supernatant; Figure 4.7.

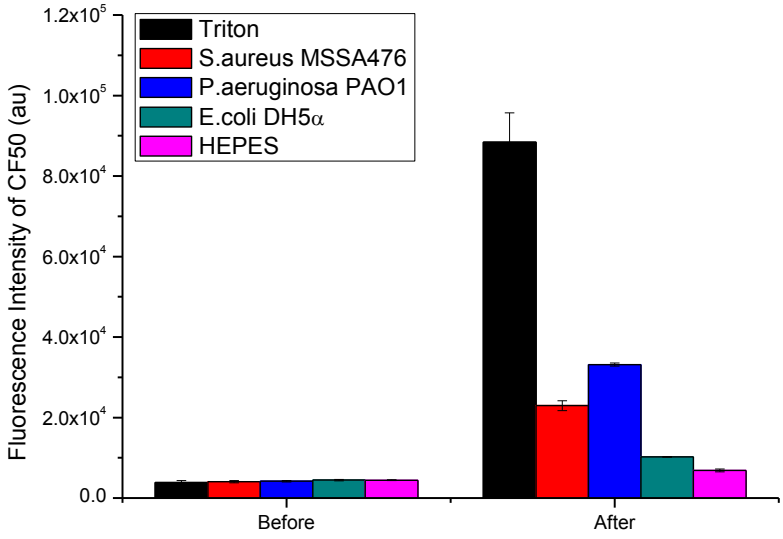

Figure 0.7: Response of vesicles immobilised in hypromellose. Upon incubation with supernatant of *P. aeruginosa* PAO1 and *S. aureus* MSSA476, a fluorescence increase can be observed, along with a slight increase in fluoresce when incubated with *E. coli* DH5α due to passive leakage. Triton X-100 and HEPES were used as controls.

4.4.5. Agar and agarose

The 1% agar and 0.7% agarose systems were used to prepare a 2:1 ratio of gel: vesicle mixture.

As with previous gel systems, the vesicles dispersed in agar and agarose were tested with Triton X-100 to obtain SR-parameter values. The SR-parameter values obtained for the agar system were 10.8 (±0.418) on addition of Triton X-100 and 0.991 (±0.061) on addition of HEPES.

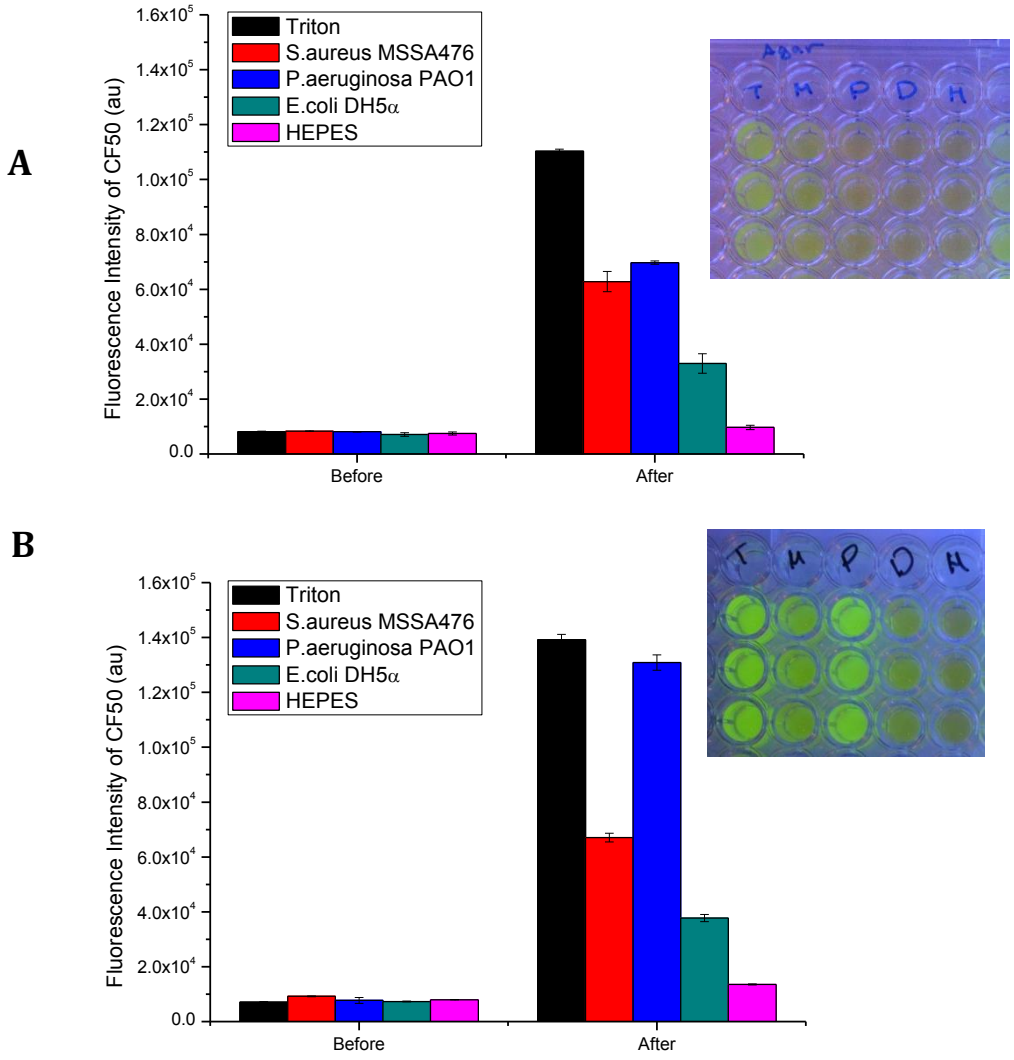

Figure 0.8: The overnight response of vesicles in **(A)** agar gel matrix and (B) in agarose gel matrix, upon incubation at 37°C with bacterial supernatant; lysis of vesicles shown by *P. aeruginosa* PAO1, *S. aureus* MSSA476 and the positive control, Triton X-100. Vesicles show stability in negative control, HEPES, however slight instability is indicated by incubation with *E. coli* DH5α. Images on the right of each graph show the visual response on incubation with Triton X-100 (T), *S. aureus* MSSA476 (M), *P. aeruginosa* PAO1 (P), *E. coli* DH5α(D) and HEPES (H).

The plots and the images in figure 4.8 show the response of vesicles in both the agar and the agarose systems. Both systems show sensitivity to supernatant of *P. aeruginosa* PAO1 and *S. aureus* MSSA476. The agarose system yielded a larger increase in fluorescence intensity on addition of Triton X-100 and *P. aeruginosa* PAO1 compared to the agar system. The response of both systems was similar to *S. aureus* MSSA476. A slight increase in fluorescence intensity was detected on incubation with supernatant of *E. coli* DH5α; however the systems were stable in HEPES buffer. The properties of agar and agarose are similar; however, due to the overall higher responses of the agarose system compared to the agar, the agarose system was selected for further analysis over the agar.

4.5. Systematic study of vesicle stability in gels

Following the short-term stability and sensitivity analysis, the following gels were selected for further analysis; gelatin, hypromellose and agarose. The long-term stability of vesicles in the gel matrix was studied over a period of 14 days at 37°C. This section includes the results of the study involving C981, a carbopol gel system that was being examined in parallel by a member of the research group (Serena Marshall, University of Bath). The C981 gel was used as a comparative gel system.

In order to test the gels in a systematic manner, an additional three promising vesicle systems were utilised.

4.5.1. Osmolality in relation to vesicle stability

The C981 gel was used as a comparative model. From the osmotic pressure ratio values obtained, see table 4.4 below, the C981 system was predicted to be the least stable hydrogel for dispersion of vesicles.

Table 0.4: The osmolality ratio values were calculated based on the ratio of the osmotic pressure (mOsm/kg H_2O) of each vesicle type against each solution. A value close to 1 is optimal. This table has been modified from the original obtained from Marshall et. al. *Langmuir* 2013.

	TCDA-DS	*DOPC-DS*	*DSPG-DP*
HEPES	1.02 (± 0.004)	1.05 (± 0.002)	1.04 (± 0.010)
Gelatin	0.960 (± 0.005)	0.984 (± 0.002)	0.977 (± 0.01)
C981	0.638 (± 0.003)	0.654 (± 0.001)	0.649 (± 0.006)
HM	0.960 (± 0.004)	0.984 (± 0.002)	0.976 (± 0.009)
Agarose	0.938 (± 0.004)	0.961 (± 0.002)	0.954(± 0.009)
LB	1.80 ($\pm 3 \times 10^{-5}$)	1.751 ($\pm 4 \times 10^{-6}$)	1.767 (±0.002)
TSB	1.446 (±0.001)	1.474 (±0.002)	1.420 (±0.002)

The stability of successfully stabilized vesicles, when dispersed in different hydrogel based delivery matrices, was investigated using a long term stability

assay, where the vesicles dispersed in the gel matrix are incubated at 37°C over a period of 14 days. Upon completion of the 14 day incubation period, vesicles were lysed with bacterial supernatant to measure any increase in fluorescence (figure 4.10).

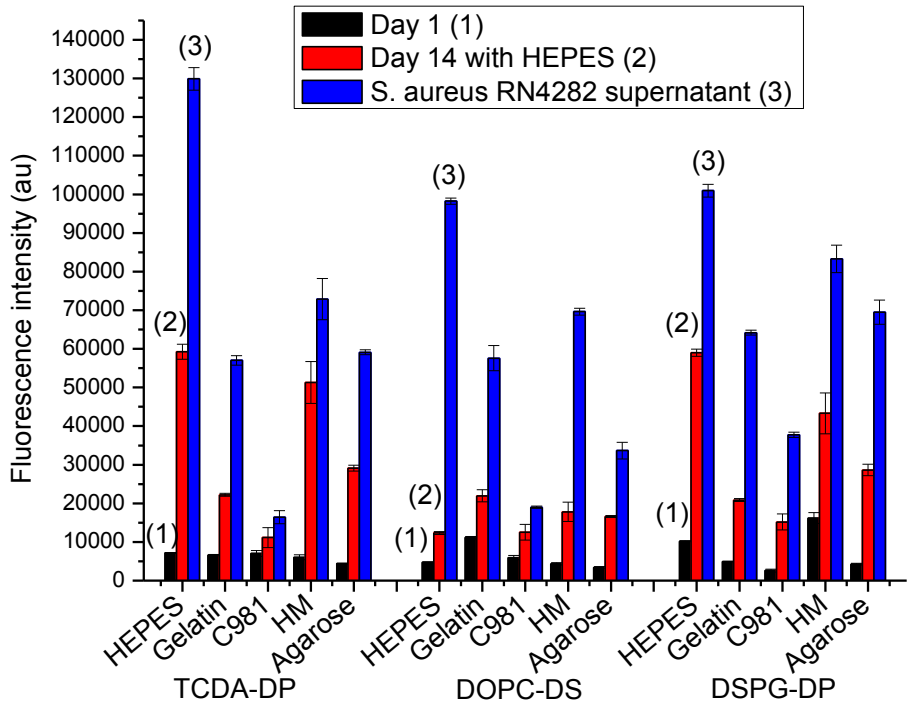

Figure 0.9: The effect of hydrogel matrices containing the three leading vesicle. Vesicles dispersed in each gel formulations were stored at 37 °C for 14 days, followed by addition of *S. aureus* RN4282 supernatant to obtain a value of F_f, or HEPES as a negative control.

From the results obtained (figure 4.9), gelatin and agarose systems showed desirable stability and sensitivity for all three vesicles types tested. This is indicated by the large difference between 'Day 14 with HEPES' and '*S. aureus* RN4282 supernatant'. The hypromellose gel showed sensitivity on addition of lysing agent, but a relatively poor stability can be observed by the high fluorescence intensity of addition of HEPES on day 14.

4.5.2. Detailed vesicle stability in Agarose gel

The stability of the three vesicle systems in agarose gel was studied over 14 days at 37 °C in order to better understand whether the leakage of dye was a slow process throughout the 14 day period or a sudden burst at a specific point in time. The plot in figure 4.10 indicates a slow release in dye throughout the measured time period. This suggests that the release of dye is due to a passive leakage from the vesicles rather than a release due to lysis of vesicles.

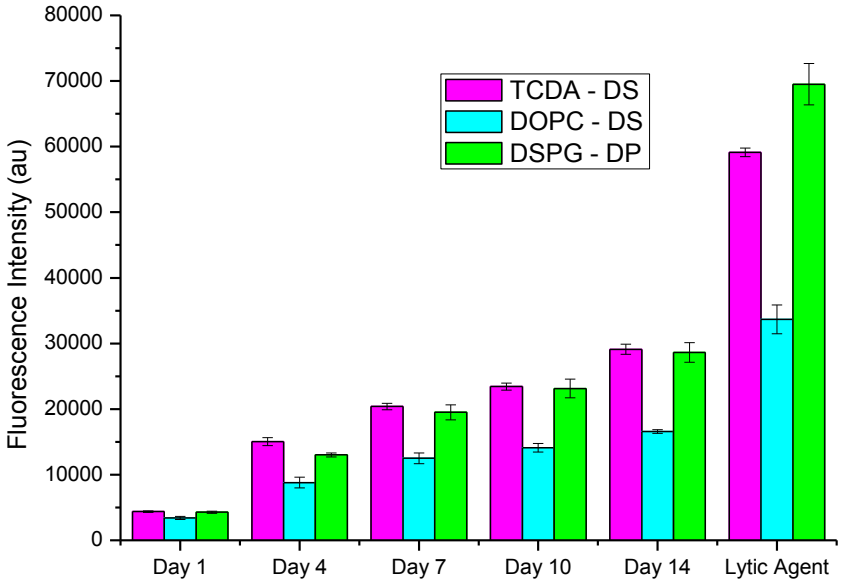

Figure 0.10: Change in fluorescence of three lead vesicle types in agarose gel at 37 °C over 14 days, and response to lytic supernatant from an overnight culture of *S. aureus* RN 4282 at 14 days.

4.5.3. Summary of vesicle stability in gel matrixes

Vesicles were dispersed in solutions of gel prior to the gelation process. The stability was primarily judged by observational analysis. Immediate colour changes (from yellow to green) on addition of vesicles to the pre-gelation mixture indicated instability of vesicles. On observation of an immediate colour change, a low SR-parameter value on addition of lytic agent was seen (close to 1), which was not desirable for development as a stability-inducing immobilisation matrix for vesicles. For gels which displayed high SR-parameter values on addition of lytic agent and a SR-parameter value on addition of HEPES, further gel response studies were carried out.

Following individual response studies on gels, a selection of hydrogels were compared to each other along with gels developed by other members of the research group. Their long-term stabilities and response to bacterial supernatant were studied and compared. The agarose system was identified as an ideal candidate for development as a vesicle carrier system.

In addition to comparing the gel systems, vesicles developed by other members of the group were analysed in the different gel matrices. The plot in figure 4.10 indicates that the DOPC-DS vesicles have the potential to be the 'ideal' candidate for development of the wound dressing. They show good stability and sensitivity throughout most of the gels tested; however, consistent reproducibility vesicle production was a hurdle to overcome. Thus, further studies were carried out using the 15% TCDA-DS system.

4.6. Fmoc FF –Agarose gel multi-layer assembly

Stabilisation of vesicles in FmocFF gel was unsuccessful. However, the interesting property of this gel was used to develop a bacterial 'logic gate system' (see section 4.5.8 for a detailed description).

As previously discussed, FmocFF can form hydrogel-like structures when appropriate gelation techniques are employed. Fibrous structures form and are held in place by hydrogen bonding and π- π interactions. Although these structures are not held in place by covalent bonding, the effect of addition of protease to breakdown the gel was studied. Low concentrations of protease from Streptomyces *griseu*s were found to induce breakdown of the FmocFF gel.

This property of the FmocFF gel was combined with the agarose gel system to develop a bacterial logic gate system which responds to the presence of both protease and bacterial toxin. The use of lipid vesicles for detection of bacterial toxin production has been reported in previous studies, and the incorporation of these vesicles into agarose hydrogels were shown to produce a stable detection system for toxin production by pathogenic bacteria[19].

In this investigation, a thin-film bacterial logic gate was engineered using the combination of Fmoc-Phe-Phe-OH gels and the agarose vesicle system.

4.6.1. Preparation of FmocFF/agarose gel multi-layer assembly

A 0.7% agarose gel was prepared in HEPES buffer. The gel was kept at a constant temperature of 38°C and vesicles were added in a 2:1 ratio of gel to the vesicle solution. 200μL of this mixture was loaded into each well of a 48 well plate and allowed to set at 4°C. To protect the vesicles from the FmocFF, 100μL of 0.7% agarose gel was added to the top of the agarose gel-containing vesicles. This gel was again allowed to set at 4°C. Finally, 2mg mL^{-1} FmocFF gel was prepared and allowed to gellate on the surface of the two agarose layers, to obtain the final FmocFF/agarose gel s multi-layer assembly. Figure 4.11 shows a cartoon representation of the gel multi-layer assembly system.

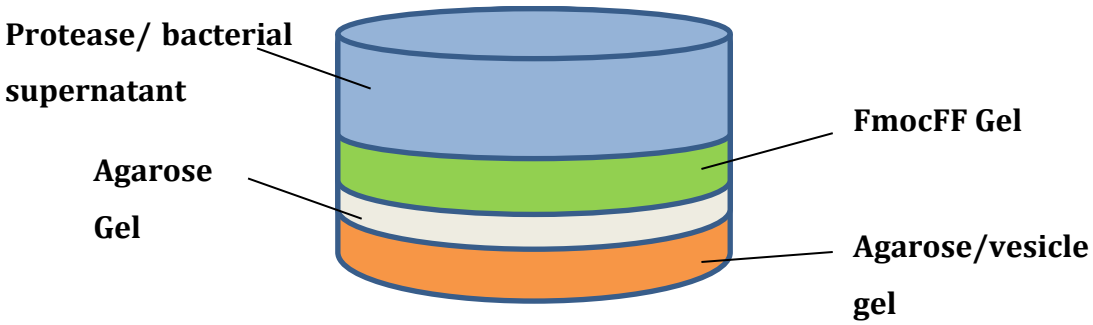

Figure 0.11: Diagram of gel multi-layer assembly

4.6.2. Testing the response of gels

Protease was added to the multi-layer assembly of gels and the agarose gel systems in 24 well plates. The plate was incubated at 37°C for 1hr to allow the breakdown of FmocFF gels. Following on from this, 100µL of bacterial supernatant and the corresponding controls were loaded on top of the gels and incubated overnight. Well scans were taken (using a BMG Labtech Fluostar Omega microplate reader, with excitation and emission filters of 485 and 520 nm, respectively) to measure lysis of vesicles in the agarose/vesicle layer: prior to the addition of protease; following 2hr incubation; and following overnight incubation at 37°C.

4.6.3. Protease assay

An agar petri dish compromising of 10% milk in brain heart infusion agar was prepared by mixing the milk solution to the agar, post autoclaving. Six 1cm diameter perforations were made on the agar plate and the holes were filled with 50µL of bacterial supernatant and corresponding control solutions. The plate was incubated overnight (18h) at 37°C.

4.6.4. Breakdown of FmocFF gel on addition of protease

Protease-induced breakdown of FmocFF gel was examined by means of comparative studies of protease added to a pre-formed gel and water added to an identical gel. The vials containing the FmocFF gel and each of the test solutions were inverted. Figure 4.12 shows the image of the vials illustrating intact gels when water was added, and collapsed gels when exposed to protease. This suggests that protease can include breakdown of FmocFF gels.

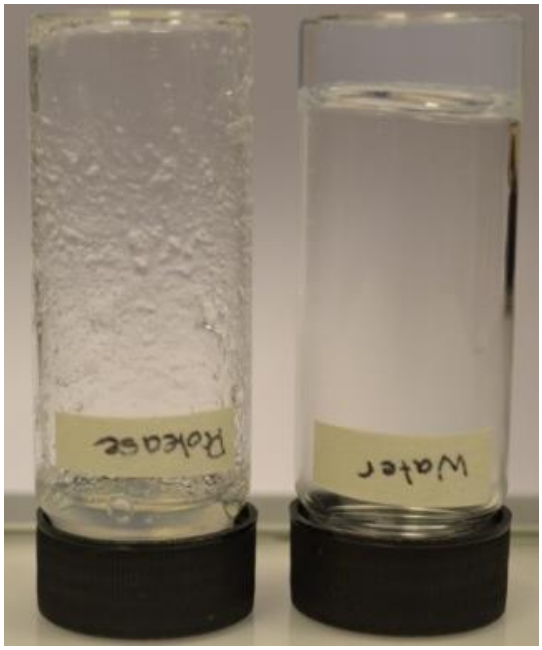

Figure 0.12: Image showing breakdown of FmocFF gel on addition of Protease using water as a control.

4.6.5. Stability and sensitivity of the FmocFF multi-layer assembly system

The gel systems were prepared in wells of 24 well plates. 100µL of Protease from *Streptomyces griseu*s was carefully pipetted on top of the FmocFF gel, water was pipetted as a control to an identical plate, both plates were incubated for at least an hour to allow initial breakdown of the peptide gel layer. Following the initial incubation stage, 100µL of bacterial supernatant and the corresponding controls were pipetted onto the FmocFF layer and incubated overnight at 37°C.

4.6.6. Response of vesicles in agarose with the additional pure-agarose layer to bacterial supernatant

The initial response of vesicles to bacterial supernatant in the presence and absence of protease was confirmed. The gel multi-layer assembly was prepared, without the FmocFF layer and protease was loaded into each well, and incubated for at least an hour before addition of bacterial supernatant. The fluorescence intensity of vesicles incorporated in the bottom agarose layer was measured after a 2 h incubation followed by an 18 h incubation (figure 4.13).

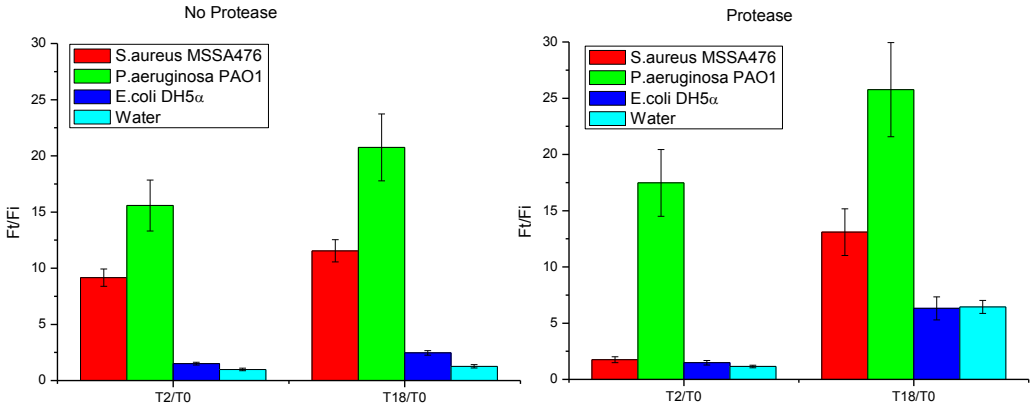

Figure 0.13: Stability response Parameter, SR, calculated and graphed for time points; T=2 h and T=18 h, following initial incubation of agarose/vesicle layer with the additional pure agarose layer (without the FmocFF gel layer) with water (a) and protease (b) for 1 h followed by 18 h incubation with bacterial supernatant at 37°C.

Vesicles were responsive to supernatant of *P. aeruginosa* PAO1 following 2 h incubation in the absence and presence of protease. However, vesicles showed response to *S. aureus* MSSA 476 after 18 h incubation in the presence of protease and a response at 2h in the absence of protease. The data indicates a slight destabilisation on addition of supernatant of *E. coli* DH5α and water in the presence of protease. In the presence of protease, a delay in the response of vesicles to *S. aureus* MSSA 476 can be observed, however following 18h incubations, the responses to the presence and absence of protease are comparable.

4.6.7. Response of the gel multi-layer assembly to bacterial supernatant in the presence of protease

The complete gel multi-layer assembly complex with the additional FmocFF layer on top of the pure agarose layer was incubated with protease, followed by incubation with bacterial supernatant. The fluorescence of vesicles in the bottom agarose layer was measured after 2h incubation and on completion of the 18h incubation period at 37°C. The FmocFF gel layer was broken-down by the initial incubation with protease. As a result, the subsequently added bacterial supernatant was able to diffuse into the agarose gel layer, and to lyse vesicles immobilised within the bottom agarose layer. The large SR-parameter upon addition of *S. aureus* MSSA476 and *P. aeruginosa* PAO1 indicates lysis of vesicles (figure 4.14).

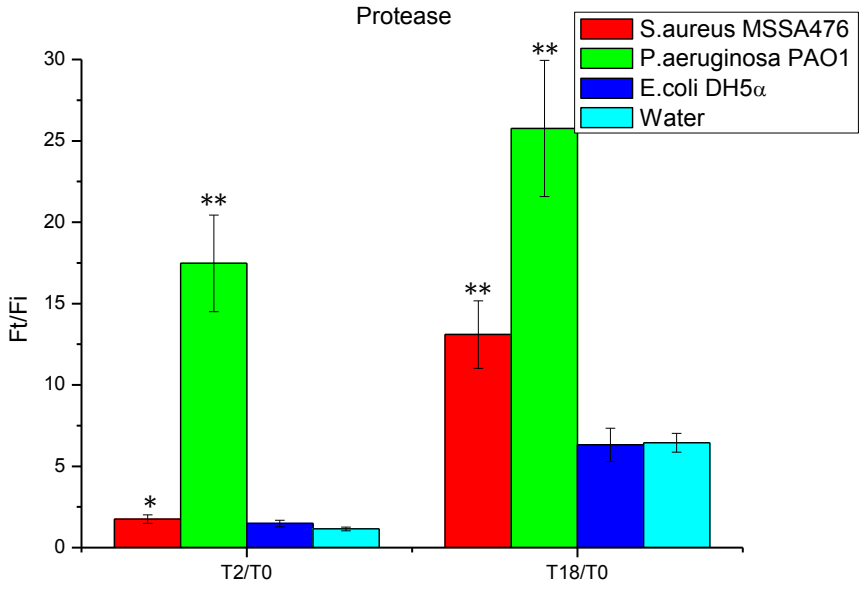

Figure 0.14: Stability response Parameter, SR, calculated and graphed at T=2h and T=18h following initial incubation of complete gel multi-layer assembly system with protease for 1 h, followed by 18h incubation with bacterial supernatant at 37°C. Statistical analysis were carried out by a Student's t-test, * P- value > 0.05, **P value < 0.05

From the results (figure 4.14), as well as the previous results obtained on the breakdown of FmocFF gels following incubation with protease and stability of gels upon incubation with water, it can be expected that without the addition of

protease, the FmocFF gels should be stable and thus the vesicles dispersed in the bottom layer of agarose should not lyse, regardless of the additional incubation with toxin-producing bacterial supernatant.

The above assay was repeated with addition of water instead of the initial addition of protease. As expected, without the addition of protease, the FmocFF gel layer inhibits the diffusion of toxins of *S. aureus* MSSA467, and stable vesicles can be observed by the low SR-parameter value obtained (figure 4.15). However, on incubation with *P. aeruginosa* PAO1, lysis of vesicles was observed following 2 h incubation. These results suggest the presence of protease in the *P. aeruginosa* PAO1 supernatant in sufficient enough concentrations to breakdown the FmocFF gel, and allow diffusion of lytic toxins for lysis of vesicles in the bottom agarose layer.

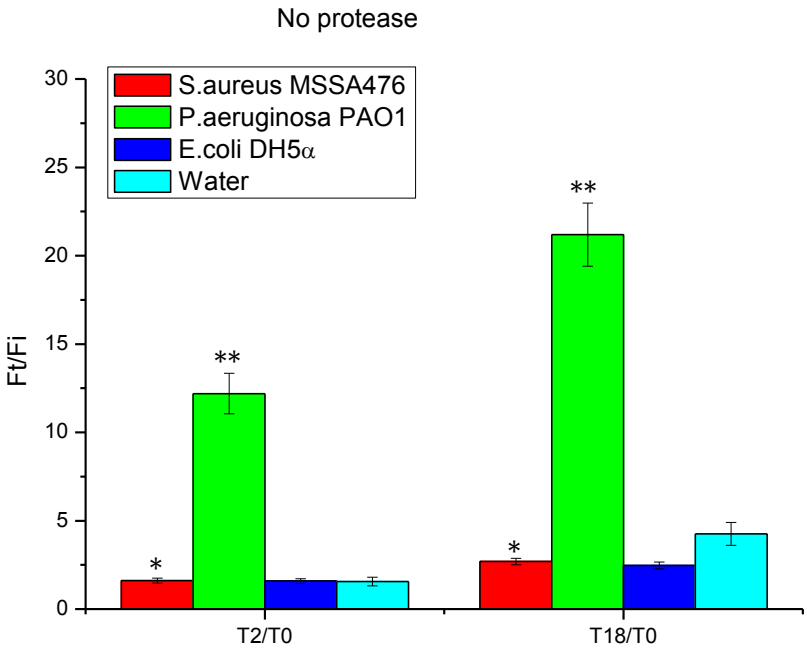

Figure 0.15: Stability response Parameter, SR, calculated and plotted at T=2h and T=18 h following initial incubation of the complete gel multi-layer assembly system with water for 1h, followed by 18h incubation with bacterial supernatant at 37°C. Statistical analysis were carried out by a Student's t-test, * P- value > 0.05, **P -value < 0.05

The results depicted in figure 4.15, indicate that *P. aeruginosa* PAO1 produces sufficiently high concentrations to cause breakdown of the FmocFF gel layer. This was tested using a simple proteolytic plate assay (figure 4.16).

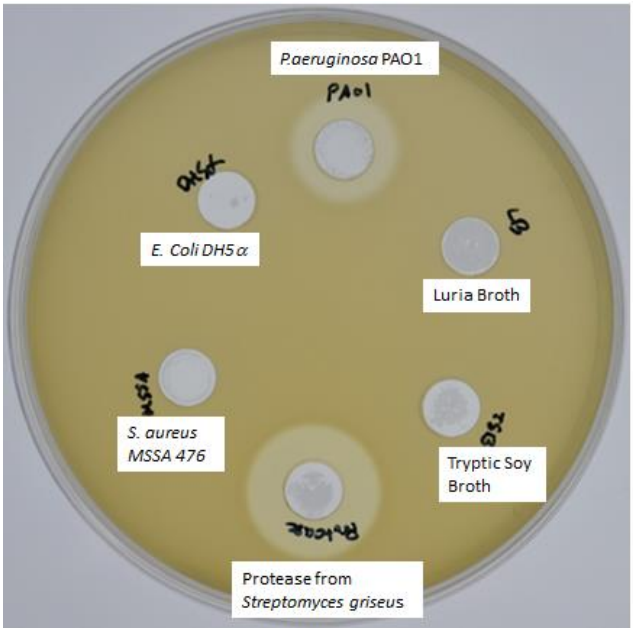

Figure 0.16: 10% milk BHI agar plate incubated with supernatant of *P. aeruginosa* PAO1, *S. aureus* MSSA476 and *E. coli* DH5α and protease as a positive control and broth solutions as negative controls, overnight at 37°C.

The formation of the halo-ring, displayed in figure 4.16, around the well which contained supernatant of *P. aeruginosa* PAO1 is also seen around the well which initially contained the control solution, protease. The halo-ring is absent around the wells which contained supernatant of *S. aureus* MSSA476 and *E. coli* DH5α as well as the two broth solutions used a controls. This suggests that the *P. aeruginosa* PAO1 produces protease in high enough concentrations to breakdown the proteins.

4.6.8. Microbial Logic gate

The gel multi-layer assembly system developed in this section is comprised of two responsive layers. The top layer consists of the protease responsive FmocFF gel and the bottom layer consists of vesicles dispersed in agarose gel, responsive to

bacterial toxins. From the results presented in this section (Section 4.5), the multi-layer assembly system can be described as a logic gate AND system. Table 4.5 demonstrates this in a tabulated form.

Table 0.5: Representation of logic gate

Protease	Toxin	Result
1	1	1
1	0	0
0	1	0
0	0	0

A logic gate describes a device that performs a logical operation by one or more inputs, which work in a logical way to produce a single logical output. A Boolean function is used by the device. In order for a logic gate system to be described as an AND system, the binary digits representing all the inputs have to display 1 in order to produce an output of 1. If one or more of the outputs display a 0, then the output binary digit will also be 0.

The gel system described in this section required the presence of protease and lytic toxin for a fluorescing gel. Consequently, if the protease and lytic toxin are described as the inputs and the resulting fluoresce of gel as the output, this system can be described as an AND gate.

4.7. Conclusions

In this chapter, the stability of vesicles was tested in a range of different hydrogels. A few of the leading systems were compared to systems developed by other members of the group. Through systematic analysis, the 15% TCDA- DS vesicles in agarose gel were revealed to show desirable stability and response of vesicles incorporated in the gel matrix.

Furthermore, a gel-multilayer system was developed, where an additional protease responsive FmocFF gel layer was added to the 15% TCDA-DS in agarose system. This allowed for further enhanced sensitivity to the already developed lytic toxin sensitive lipid based system, sensing for the presence high enough concentrations protease as well as the presence of membrane lytic toxins.

4.8. References

1. Wiltsey, C. T.; Christiani, T. R.; Williams, J.; Coulter, J. L.; Demiduke, D. N.; Toomer, K. A.; English, S. M.; Hess, B. A.; Branda, A. M.; Sheehan, J.; Kadlowec, J. A.; Tulenko, T.; Iftode, C.; Vernengo, A. J. In *Biomimetic hydrogels for tissue engineering of the intervertebral disc*, Bioengineering Conference (NEBEC), 2012 38th Annual Northeast; 394-395.

2. Renn, D.; Renn, Agar and agarose: indispensable partners in biotechnology. *Industrial & engineering chemistry product research and development* **1984,** *23* (1), 17-21.

3. (a) Young, S.; Wong, M.; Tabata, Y.; Mikos, A. G., Gelatin as a delivery vehicle for the controlled release of bioactive molecules. *Journal of Controlled Release* **2005,** *109* (1-3), 256-274; (b) Tabata, Y.; Hijikata, S.; Ikada, Y., Enhanced vascularization and tissue granulation by basic fibroblast growth factor impregnated in gelatin hydrogels. *Journal of Controlled Release* **1994,** *31* (2), 189-199.

4. Balakrishnan, B.; Jayakrishnan, A., Self-cross-linking biopolymers as injectable in situ forming biodegradable scaffolds. *Biomaterials* **2005,** *26* (18), 3941-3951.

5. Armisen, R., Agar. In *Thickening and Gelling Agents for Food*, Imeson, A., Ed. Springer US: 1997; pp 1-21.

6. Lahaye, M.; Rochas, C., Chemical structure and physico-chemical properties of agar. In *International Workshop on Gelidium*, Juanes, J. A.; Santelices, B.; McLachlan, J. L., Eds. Springer Netherlands: 1991; Vol. 68, pp 137-148.

7. Rinaudo, M., Main properties and current applications of some polysaccharides as biomaterials. *Polymer International* **2008,** *57* (3), 397-430.

8. Wang, N., Preparation and characterization of agarose hydrogel nanoparticles for protein and peptide drug delivery. *Pharmaceutical development and technology* **1997,** *2* (2), 135.

9. Margaritis, A.; Zajic, J. E., Mixing, mass transfer, and scale-up of polysaccharide fermentations. *Biotechnology and Bioengineering* **1978,** *20* (7), 939-1001.

10. Candia, J. L. F.; Deckwer, W. D., Xanthan Gum. In *Encyclopedia of Bioprocess Technology*, John Wiley & Sons, Inc.: 2002.

11. AM Goldstein, E. A., JK Seaman Guar gum. *Industrial gums* **1973**.

12. Burdock, G.; Burdock, Safety assessment of hydroxypropyl methylcellulose as a food ingredient. *Food and chemical toxicology* **2007,** *45* (12), 2341-2351.

13. Mohammed, J.; Murphy, W., Bioinspired Design of Dynamic Materials. *Advanced Materials* **2009,** *21* (23), 2361-2374.

14. (a) Jayawarna, V.; Richardson, S.; Hirst, A.; Hodson, N.; Saiani, A.; Gough, J.; Ulijn, R., Introducing chemical functionality in Fmoc-peptide gels for cell culture. *Acta Biomaterialia* **2009,** *5* (3), 934-943; (b) Jayawarna, V.; Smith, A.; Gough, J. E.; Ulijn, R. V., Three-dimensional cell culture of chondrocytes on modified di-phenylalanine scaffolds. *Biochemical Society transactions* **2007,** *35* (3), 535; (c) Jayawarna, V., Nanostructured Hydrogels for Three-Dimensional Cell Culture Through Self-Assembly of Fluorenylmethoxycarbonyl–Dipeptides. *Advanced Materials* **2006,** *18* (5), 611.

15. (a) Palui, G.; Banerjee, A., Pentapeptide based organogels: the role of adjacently located phenylalanine residues in gel formation. *Soft Matter* **2008,** *4* (7), 1430; (b) Mahler, A.; Reches, M.; Rechter, M.; Cohen, S.; Gazit, E., Rigid, Self-Assembled Hydrogel Composed of a Modified Aromatic Dipeptide. *Advanced Materials* **2006,** *18* (11), 1365-1370; (c) Smith, A. M.; Williams, R. J.; Tang, C.; Coppo, P.; Collins, R. F.; Turner, M. L.; Saiani, A.; Ulijn, R. V., Fmoc-Diphenylalanine Self Assembles to a Hydrogel via a Novel Architecture Based on π–π Interlocked β-Sheets. *Advanced Materials* **2008,** *20* (1), 37-41.

16. Wang, Q.; Bardelang, D.; Zaman, M.; Moudrakovski, I.; Pawsey, S.; Margeson, J.; Wang, D.; Wu, X.; Ripmeester, J.; Ratcliffe, C.; Yu, K., Interfacing Supramolecular Gels and Quantum Dots with Ultrasound: Smart Photoluminescent Dipeptide Gels. *Advanced Materials* **2008,** *20* (23), 4517-4520.

17. Spencer, C., Incorporation of phospholipid vesicles into a dipeptide hydrogel as part of a 'smart' wound dressing. University of Bath: Bath, 2013; p 60.

18. Raeburn, J.; Pont, G.; Chen, L.; Cesbron, Y.; Lévy, R.; Adams, D. J., Fmoc-diphenylalanine hydrogels: understanding the variability in reported mechanical properties. *Soft Matter* **2012,** *8* (4), 1168-1174.

19. Marshall, S.; Hong, N. T.; Thet, A. T. A.; Jenkins, Effect of Lipid and Fatty Acid Composition of Phospholipid Vesicles on Long-Term Stability and Their Response to *Staphylococcus aureus* and *Pseudomonas aeruginosa* Supernatants. *Langmuir* **2013,** *29* (23), 6989-6995.

Chapter Five: *In vitro* cytotoxicity

5.1. Introduction

The goal of the development carried out through this study is to produce a definitive dressing that indicates bacterial colonisation of the wound site. Most importantly, the dressing should not interfere with the wound healing process. In order to achieve this, the production of the dressing has to involve biocompatible material, with minimal cytotoxic effects and minimal disruption to cell differentiation.

In recent years, *in vitro* assays are being favoured over animal tests due to the cost, availability and rapid results of assays, as well as the ability to avoid negative publicity in the case of public discontent with animal testing. The development of hepatocyte cell lines with metabolic capabilities will allow testing of drug

metabolism and toxicity. Keratinocyte cell lines have been developed for assays involving toxicity testing of new topical drugs and treatments as well as conducting cell proliferation and growth assays.[1]

5.1.1. Eukaryotic Cells

Eukaryotic cells are complex multicellular cells which make up plants and humans. Cell structures are more complex compared to prokaryotic cells (figure 5.1). Eukaryotic cells consist of a cell membrane, which contains a cytoplasm in which the biochemical reactions of the cell occur and contains the nucleus, the mitochondrion and ribosomes (the detail of the structure is shown in figure 5.1)

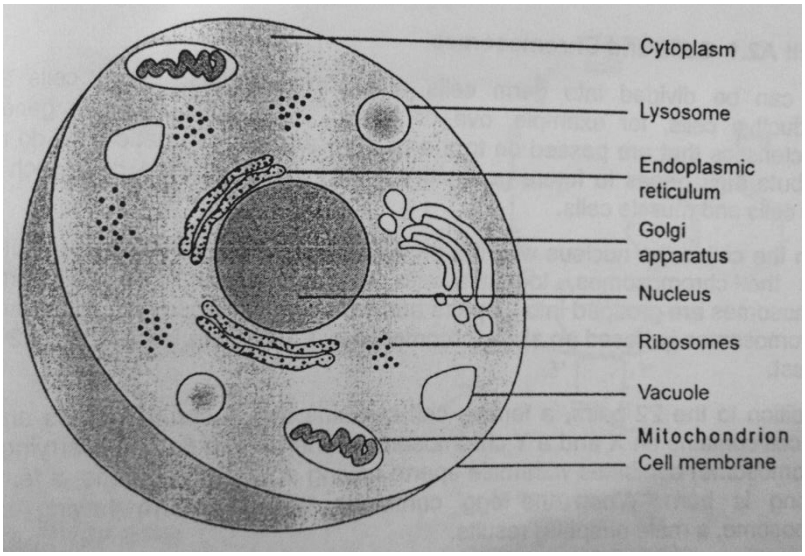

Table 5.1: Image showing the structure of a human Eukaryotic cell[1].

5.1.2. Use of Keratinocyte cell lines in *in vitro* assays

HaCaTs are immortalised keratinocytes obtained from the human skin. This cell line has been used by the research denomination for *in vitro* testing of various drugs and treatment methods developed involving the skin[2].

Although HaCaT cells have been immortalised, they retain the differentiation and morphologies of keratinocytes. They can be grown in normal growth medium[3], in contrast to the primary keratinocytes where cells obtained from a fresh skin sample require supplementary growth factors to survive in vitro. Furthermore,

they die quickly, making long-term studies hard to achieve[4]. As a result, HaCaTs are considered to have attractive aspects for use in an *in vitro* model for cytotoxicity assays. Moreover, *in vivo*, keratinocyte cell lines are the cells which are exposed to the topical products[5].

The compatibility of hydrogel dressings have been tested using HaCaT cell lines. HaCaT cell lines were used to test for the presence of cytotoxic components[6]. Previous studies used pre-incubated HaCaT cells to assess cytotoxicity by further incubation in media with suspended hydrogel components/extracts[6,7].

5.1.3. Use of Fibroblasts cell lines in *in vitro* assays

As well as keratinocyte cell lines, fibroblast cells lines are often used to perform cytotoxicity analysis of novel nanoparticles and dressing material[8, 6]. EA.hy926 is one of the most utilised human vascular endothelial cell line. The cell line was generated in 1983[9], and has been in use ever since for *in vivo* analysis, including cytotoxicity analysis[10].

5.1.4. Cell viability assessment

Cell viability was examined using assessment of mitochondrial activity, which correlates well with cell proliferation. The assays used for this are usually based on the use of a dye which reacts with a component of the mitochondria which can be detected due to a change in the colour of the dye. An example of a dye which reacts in this way is tetrazolium salt 3-[4,5-dimethylthiazolyl-2]-2,5-diphenyl tetrazolium bromide (MTT)[6]. An Alamar Blue assay involves the change of the colour of a dye, the assay comprises of resazurin which is reduced to resorufin by NADPH in the electron transport chain between the final reduction of oxygen and cytochrome oxidase enzyme[11].

5.2. Methods and materials used for cytotoxicity assays

The preliminary studies involved testing of cytotoxic effects of vesicles with respect to eukaryotic cells. Studies were carried out using two different cell lines; HaCaT, which are skin keratinocytes and Eahy926, which are blood vessel fibroblasts. Cell viability was measured using the Resazurin reagent obtained from Sigma Aldrich.

5.2.1. HaCaT and EA.hy926 Cell culture for cytotoxicity

Detailed descriptions of the techniques used for preparation of 70% confluent cells in T75-cm^2 flasks can be found in Chapter 2 of this document. Preparation of eukaryotic cells for analysis of cytotoxicity of vesicles and gels in solution were carried out in 24 well plates. Hepatocytometer was used to obtain cell density of $1x10^5$ cells mL^{-1}, 1mL was used to seed cells into each well. The cells were allowed to proliferate overnight under tissue culture conditions of 37°C and 5% CO_2. Following overnight incubation, the media was removed from the wells, washed with 1mL PBS (twice) and wells were replenished with fresh media containing testing solution. The cells were then further incubated for 24, 48 and 72 h under tissue culture conditions.

5.2.2. HaCaT and EA.hy926 Cell culture for supernatant assays

Cell seeding density of $1x10^4$ cell mL^{-1} was used to seed 100µL onto each well of tissue culture 96 well plates (final cell density of $1x10^3$ cells mL^{-1} in each well) and allowed to proliferate overnight. Following overnight incubation of cells, the media was removed, cells were washed in PBS and media was replenished with media containing vesicle solution. Following this procedure pre-diluted bacterial supernatant and the appropriate control solutions were added, before further incubation of 2 h under tissue culture conditions. After the 2 h incubation period, media was removed and transferred to a fresh 96 well plate for fluorescence measurements of vesicles. 10% resazurin in media was added to the remaining cells in the tissue culture plate and further incubated for 2h. The fluorescence of resazurin was then measured to assess cell viability.

5.2.3. Viability measurement

The viability of cells following exposure to vesicles was determined using the resazurin dye assay. Following exposure to vesicles, cells were incubated with 10% resazurin at 37°C for 2h. The fluorescence was measured using a BMG Lab Tech microplate reader with excitation and emission filters of 530nm and 580nm, respectively.

5.3. Results and discussion of cytotoxicity results

The cytotoxic effects of vesicles were tested on Eukaryotic cells. Keratinocyte, HaCaT cells as well as fibroblast, EA.hy926 cells were used for this analysis. As well as the cytotoxic effects of vesicles, the stability of vesicles in a eukaryotic environment was also studied by measuring their fluorescence increase upon addition of a lysing agent, following 24h incubation with eukaryotic cells.

5.3.1. Initial the calibration curve

The initial construction of calibration curves for each cell line in the different well plates was required for calculation of the number of cells per mL in a well plate for later studies.

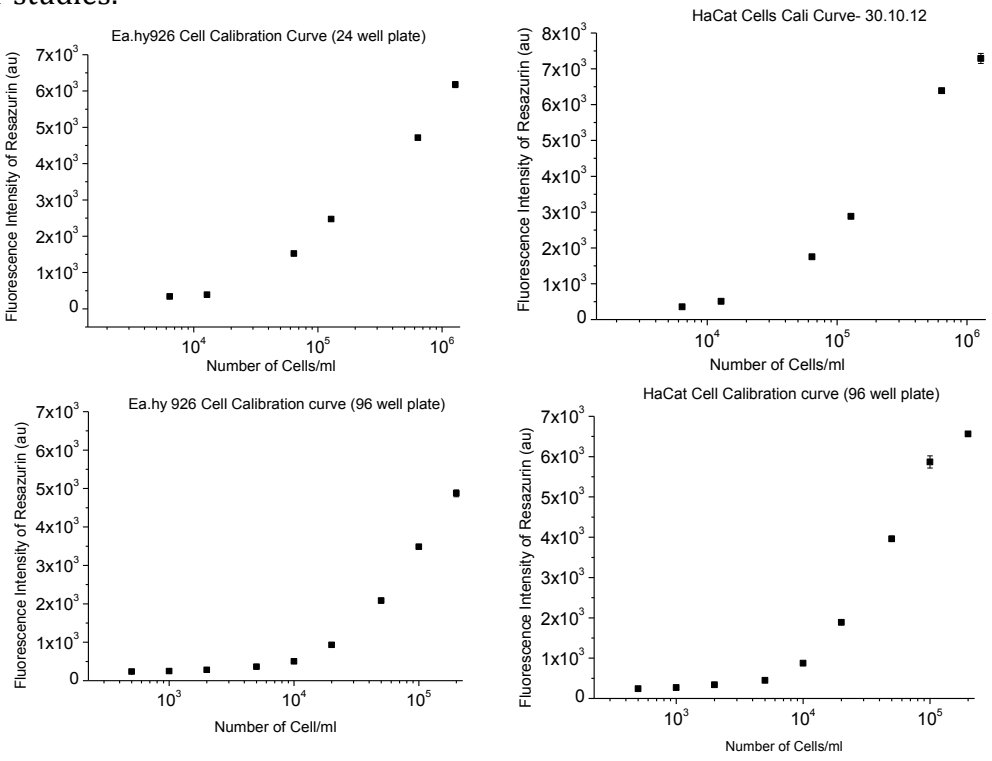

Figure 5.1: Calibration curves for HaCaT and EA.hy926 cell lines

The calibration curves were used to determine a rough estimate of the initial cell seeding density for each well plate type. An initial cell seeding density of

$1x10^4$ cells mL^{-1} was used for assays carried out in 96 well plates, and $2x10^5$ cells mL^{-1} was used for assays carried out in 24well plates.

5.3.2. Initial cytotoxicity analysis

An initial cytotoxicity assay was carried out over a period of 24 h for both types of cell lines. Cells were seeded onto 24 well plates and allowed to grow overnight, to obtain 70% confluent monolayer of cells on the surface of the tissue culture plate. Following on from this, the media was removed and replenished with fresh media containing each testing solutions; vesicles, lysed vesicles, Triton X-100 and HEPES. The lysed vesicle solution was prepared by a heat treatment process rather than the conventional method of addition of triton, as triton is also a solution used to obtain dead cells.

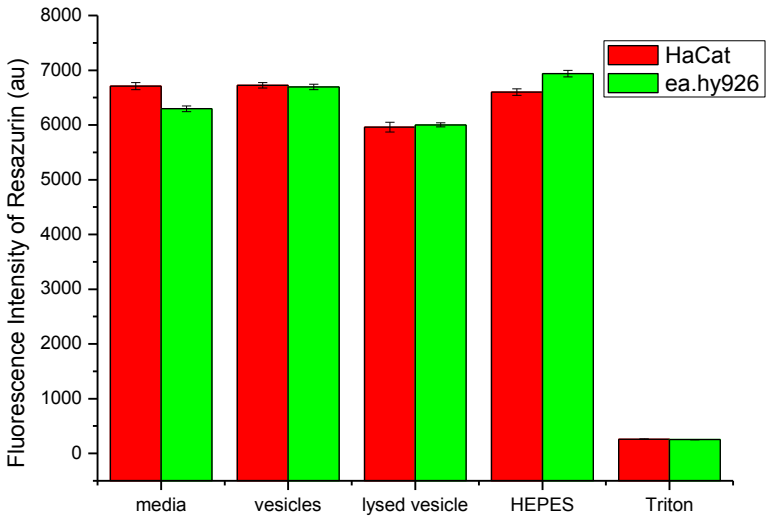

Figure 5.2: Results of cytotoxicity assay, showing non-cytotoxic effects of vesicles as well as lysed vesicles compared to the HEPES and pure media control to both types of cell lines.

Cell death can be observed by the low fluorescence value of resazurin. And cell viability was identified by fluorescence values of resazurin close to the values obtained from incubation in ordinary cell growth media. Both vesicles and lysed

vesicles were shown to have no significant initial cytotoxic effects when incubated over a period of 24h.

5.3.3. Stability of vesicles in the presence of eukaryotic cells

In addition to studying the cytotoxic effects of vesicles to eukaryotic cells, the stability of vesicles in the presence of eukaryotic cells was also studied. Following 24h incubation of cells with media containing each testing solution, i.e. vesicles and lysed vesicles, this media was removed and transferred to a 96 well plate. And the stability of vesicles was measured by addition of HEPES and Triton X-100 (Figure 5.3).

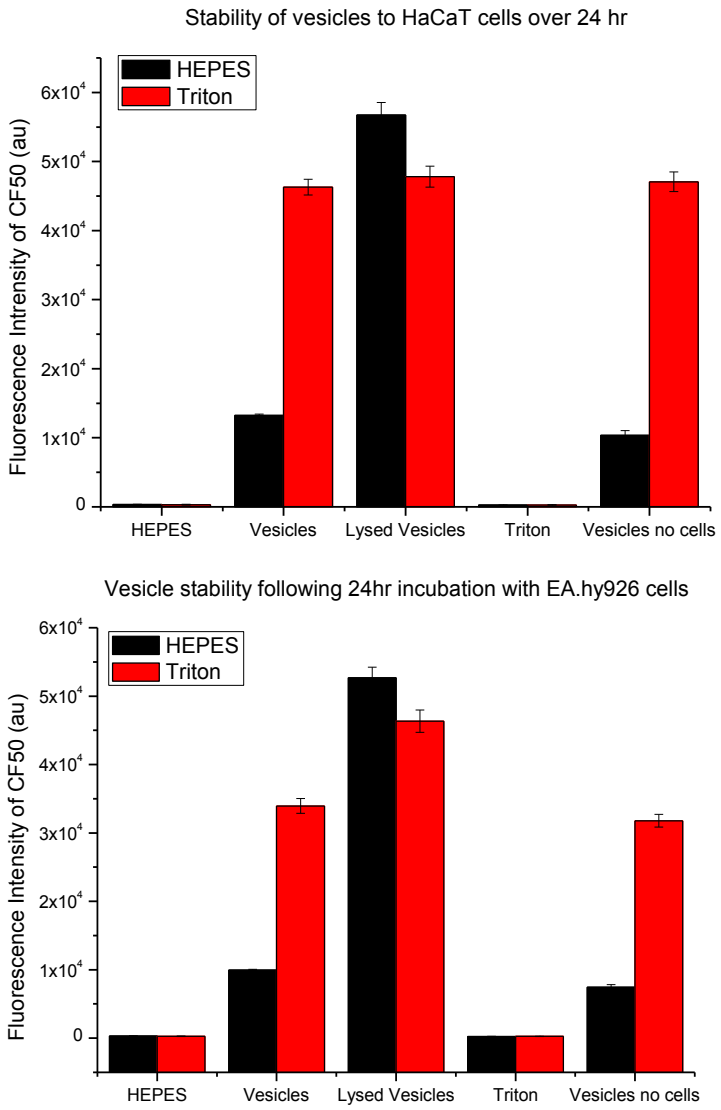

Figure 5.3: Stability of vesicles on incubation with HaCaT (top plot) and EA.hy926 cells (bottom plot). Following 24 h exposure to eukaryotic cells, stability was assessed by fluorescence intensity measurements on addition of Trion X-100 and HEPES.

5.3.4. Cytotoxicity of vesicles tested in well plates over 24, 48 and 72h

The 24h cytotoxicity assay presented promising results showing no significant cytotoxicity of vesicles to cells. The same assay was carried out for a longer incubation period; 24, 48 and 72h with results displayed by figure 5.4.

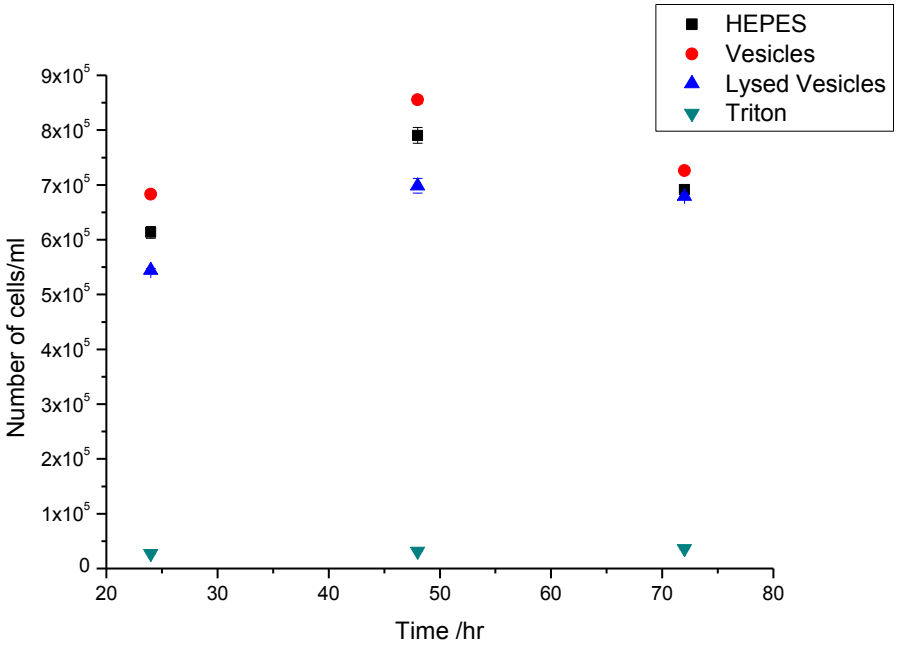

Figure 5.4: Shows the viability of HaCat cells when exposed to media containing vesicles over a period of 24, 48 and 72h. Resazurin assay was used to study the viability of cells.

The experimental resazurin fluorescence values were converted to cell density mL^{-1}. The graph plotted from these results indicates minimal cytotoxicity of vesicles as well as lysed vesicles compared to when cells were incubated with Triton X-100, where complete cell death can be observed.

5.3.5. Confocal images of cell incubated in media containing vesicles

Cell growth in tissue culture medium was compared to cell growth in tissue culture medium containing vesicle solution by observation using confocal imaging.

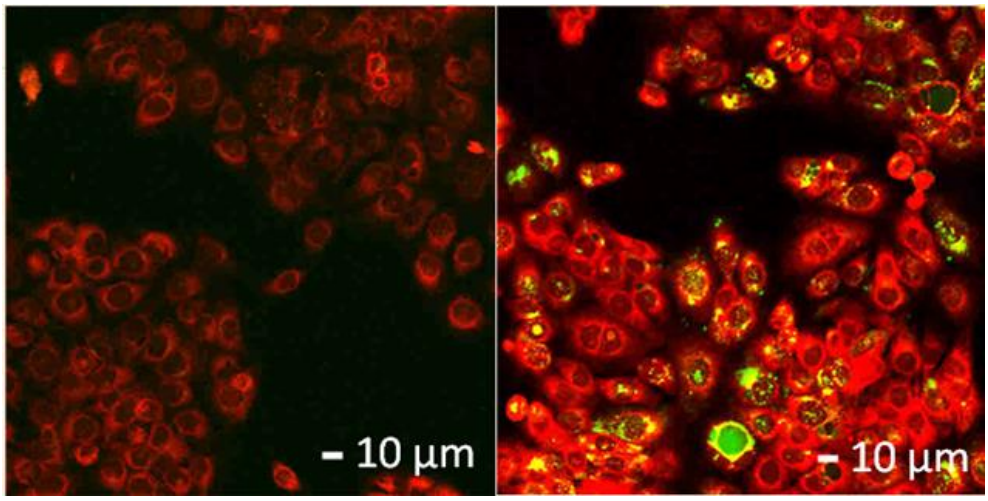

Figure 5.5: Confocal images of HaCat cells (A) vesicles incubated with HaCat cells (B) over a period of 24h. Stained with neutral red solution at X40 magnification.

Confocal images (figure 5.5) show similar cell growth patterns when cells were incubated in media containing vesicles and in media without vesicles. The image indicates the possible presence of both lysed and intact vesicles inside and outside the cell membrane. Thus there is the possibility that the cells uptake the vesicles. The uptake of vesicle by cells can be anticipated, as vesicles are only 100nm in size, and the compositions are similar to the compositions of the cell membrane. Furthermore, lysosome formation is a process which occurs within a cell as a mechanism of uptake of active ingredients.

5.3.6. Cellular response to vesicles in conjunction with bacterial supernatant

Vesicles were incubated with HaCaT cells along with bacterial supernatant at different concentrations. AGR positive (RN6390B) and negative (RN6911) strains were used to study the effect of eukaryotic cells on lysis of vesicles. As previously discussed, *S. aureus* strain AGR+ produces the toxins which lyse vesicles and lyse

eukaryotic cells, and *S. aureus* strain AGR- does not produce this toxin therefore should not lyse vesicles, neither should the eukaryotic cells. The AGR positive and negative systems show direct relevance to the system being developed since, as previously mentioned in Section 1.2.5.3. of Chapter 1, δ-toxin toxin is the major toxin responsible for lysis of membrane, and the production of this toxin is directly governed by the AGR system.

The response of vesicles in a eukaryotic environment was tested (figure 5.6)

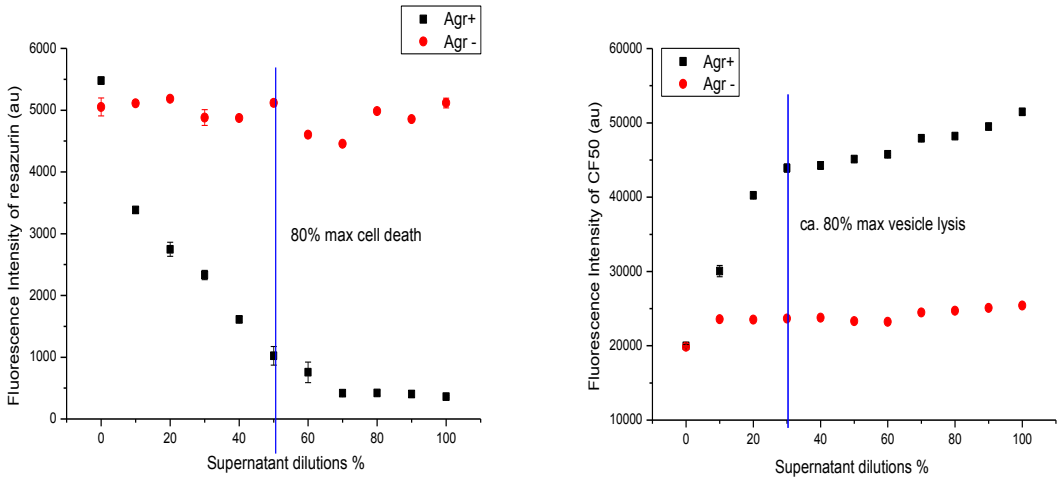

Figure 5.6: Showing response of vesicles to bacterial supernatant in a eukaryotic cell environment.

The plots above show that in order to achieve 80% cell death, a 50% supernatant dilution of AGR+ *S. aureus* RN6390B is required, whereas to achieve 80% vesicle lysis, a 30% supernatant dilution of AGR+ *S. aureus* RN6390B is required. In terms of the median lethal dose (LC50) of bacterial supernatant on cells, the value is at 20% supernatant dilution, whereas the corresponding value for vesicles (the median lethal dose of vesicles, V_{50}) is approximately 5% supernatant dilution. This is an indication that vesicles may be acting as an 'early warning system', providing evidence for the presence of pathogenic bacteria before cell damage occurs. Furthermore, the stability of vesicles as well as the lack of response by cells to AGR- *S. aureus* RN6911 suggests that vesicles will not lyse in the presence of non-toxin-producing bacteria.

As previously stated, the major toxin involved in lysis of cells and thus lysis of vesicles is δ-toxin. With the assumption that δ-toxin is the leading toxin involved in lysis of vesicles and cells, in order to determine the concentration of lytic proteins in the supernatant dilutions used, serial dilutions of δ-toxin were used to lyse vesicles and the fluorescence intensities were measured. According to the results in figure 5.7, assuming that V_{100} occurs with the addition of triton, V_{50} occurs at δ-toxin concentration between 2 and 2.5μM. As a result, one can estimate that approximately 5% supernatant dilution contains approximately 2μM concentration of δ-toxin. Thus approximately 2 μM concentration of δ-toxin is required for V_{50} and approximately 8 μM concentration of δ-toxin is required for LC_{50}.

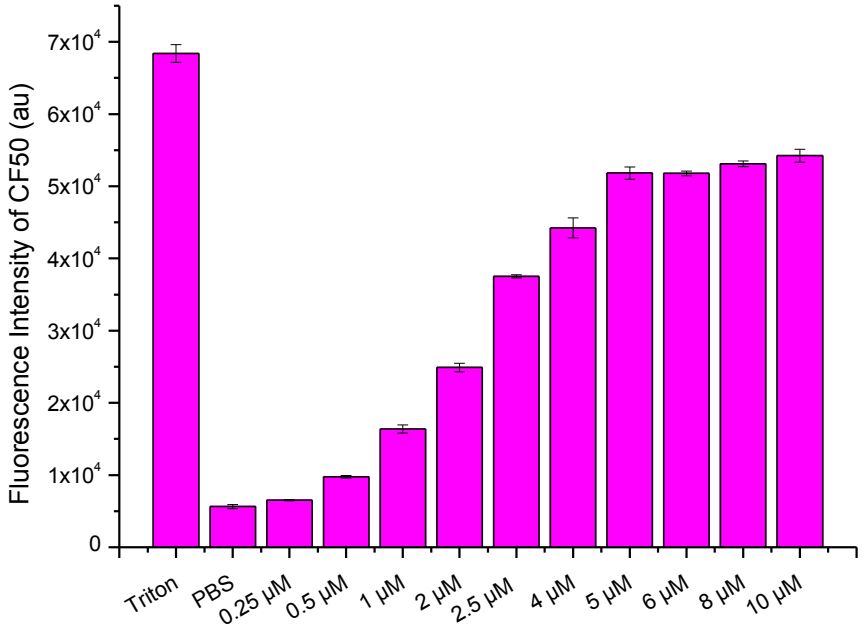

Figure 5.7: Vesicle lysis using serial dilution of pure δ-toxin

Furthermore, this study has shown that the activity of vesicles was not affected by presence of eukaryotic cells; vesicles were both stable to non-toxin-producing bacterial supernatant and responsive to toxin-producing bacterial supernatant in the presence of eukaryotic cells (HaCaT).

5.3.7. Cytotoxicity of gels in suspension

In addition to testing the cytotoxicity of vesicles, the cytotoxicity of the hydrogels intended to be utilised in prototype development were tested. Pure media was used as a positive control of stability and Triton X-100 as a negative control indicating cell death. The assay was carried out in a 24 well plate with initial seeding density of $2x10^5$ cells mL^{-1}. The cells were allowed to proliferate and grow to obtain 70% confluent cells in each well. The wells were washed in PBS and media containing test material were added. The cells were further incubated for 24h before conducting the cell viability assay using 10% resazurin solution in media.

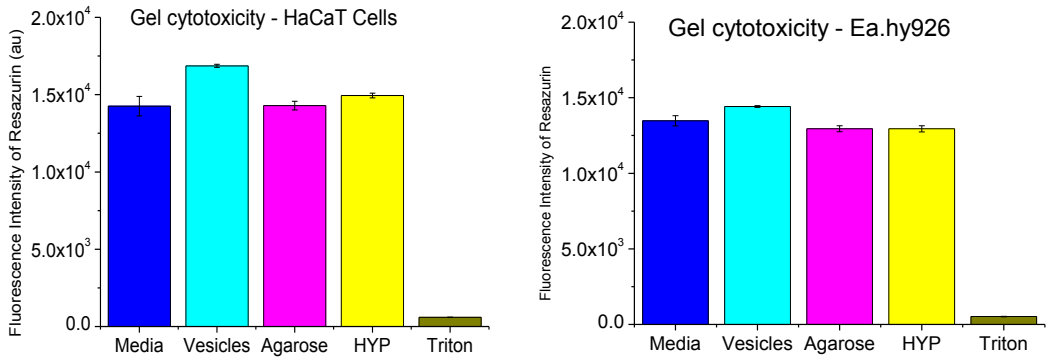

Figure 5.8: Response of eukaryotic cells to hydrogels dissolved in cell growth media over a period of 24h at 37°C and 5% CO_2. The viability of vesicles was measured using the resazurin assay.

Figure 5.8 displays the results obtained from the cytotoxicity assays indicate that the media containing hydrogels had minimal effect on the growth of established cells, compared to the cells incubated with Triton X-100, were complete cell death can be observed by the low fluorescence intensity.

5.4. Conclusions

Eukaryotic cells were used to assess the cytotoxicity of vesicles as well as any other materials planned for use in development of the prototype dressing. From the analysis carried out in this section, it can be proposed that vesicle lysis will occur before the toxins produced by the bacteria lyse the eukaryotic cells as the V_{50} of was lower than the $LC_{50.}$ Vesicles lysis following incubation with serial dilutions of pure δ-toxin allowed approximation of the concentration of δ-toxin required to obtain V_{50} and LC_{50}; respective values of 2μM and 8μM were obtained. Furthermore, no significant cytotoxic effects of hydrogels, intended to be utilised in prototype development, were found over a 24h period.

In conclusion, the vesicles and the gels being developed did not show significant evidence of cytotoxicity; hence, these components were used for further development. However, the *in vitro* assays carried out within this chapter utilized immortalised cell lines, which have been mutated to improve proliferation and prolonged growth. In order to obtain more representative results, the assays should be repeating using primary keratinocyte cell lines isolated from a fresh sample.

5.5. References

1. Ng, R., *Drugs: from discovery to approval*. Wiley. com: 2011.

2. Deyrieux, A.; Deyrieux, V. G.; Wilson, In vitro culture conditions to study keratinocyte differentiation using the HaCaT cell line. *Cytotechnology* **2007,** *54* (2), 77-83.

3. Deyrieux, A. F.; Wilson, V. G., In vitro culture conditions to study keratinocyte differentiation using the HaCaT cell line. *Cytotechnology* **2007,** *54* (2), 77-83.

4. Hennings, H.; Michael, D.; Cheng, C.; Steinert, P.; Holbrook, K.; Yuspa, S. H., Calcium regulation of growth and differentiation of mouse epidermal cells in culture. *Cell* **1980,** *19* (1), 245-254.

5. Vinardell, M. P.; Benavides, T.; Mitjans, M.; Infante, M. R.; Clapés, P.; Clothier, R., Comparative evaluation of cytotoxicity and phototoxicity of mono and diacylglycerol amino acid-based surfactants. *Food and Chemical Toxicology* **2008,** *46* (12), 3837-3841.

6. Roy, N.; Saha, N.; Humpolicek, P.; Saha, P., Permeability and Biocompatibility of Novel Medicated Hydrogel Wound Dressings. *Soft Materials* **2010,** *8* (4), 338-357.

7. Ziegler, K.; Görl, R.; Effing, J.; Ellermann, J.; Mappes, M.; Otten, S.; Kapp, H.; Zoellner, P.; Spaeth, D.; Smola, H., Reduced cellular toxicity of a new silver-containing antimicrobial dressing and clinical performance in non-healing wounds. *Skin Pharmacology and Physiology* **2006,** *19* (3), 140-146.

8. Napierska, D.; Thomassen, L. C.; Rabolli, V.; Lison, D.; Gonzalez, L.; Kirsch-Volders, M.; Martens, J. A.; Hoet, P. H., Size-Dependent Cytotoxicity of Monodisperse Silica Nanoparticles in Human Endothelial Cells. *Small* **2009,** *5* (7), 846-853.

9. Edgell, C.; McDonald, C. C.; Graham, J. B., Permanent cell line expressing human factor VIII-related antigen established by hybridization. *Proceedings of the National Academy of Sciences* **1983,** *80* (12), 3734-3737.

10. Bouïs, D.; Hospers, G. P.; Meijer, C.; Molema, G.; Mulder, N., Endothelium in vitro: A review of human vascular endothelial cell lines for blood vessel-related research. *Angiogenesis* **2001,** *4* (2), 91-102.

11. O'Brien, J.; Wilson, I.; Orton, T.; Pognan, F., Investigation of the Alamar Blue (resazurin) fluorescent dye for the assessment of mammalian cell cytotoxicity. *European Journal of Biochemistry* **2000,** *267* (17), 5421-5426.

Chapter 6: Prototype development

6.1. Introduction to prototype development

Commercially available hydrogel wound dressings are thin sheets of hydrogel on a semi-permeable plastic backing. Thus thin sheets of the gel with immobilised vesicles were fabricated and tested; these were referred to as gel-block systems. Throughout the study, limitations involving the gel-block system were identified, and gels were used to coat single sheets of fabric to overcome the limitations. As well as simple prototypes involving vesicles in a hydrogel system, an additional collagen coating allowed the formation of a prototype dressing with the capability of enhancing wound healing.

6.1.1. Wound Healing Process

Skin injury causes disruption to the tissue as well as to the surrounding blood vessels. An initial provisional extracellular matrix provides an environment for cell

migration. Macrophages and fibroblasts are activated by the platelets, which remove any debris and begin the process of wound closure. The wound healing process has been summarised by Schultz[1] into five stages which involve complex cellular and biochemical processes. The five stages are described as haemostasis, inflammation, migration, proliferation and maturation (remodelling) phases (figure 6.1).

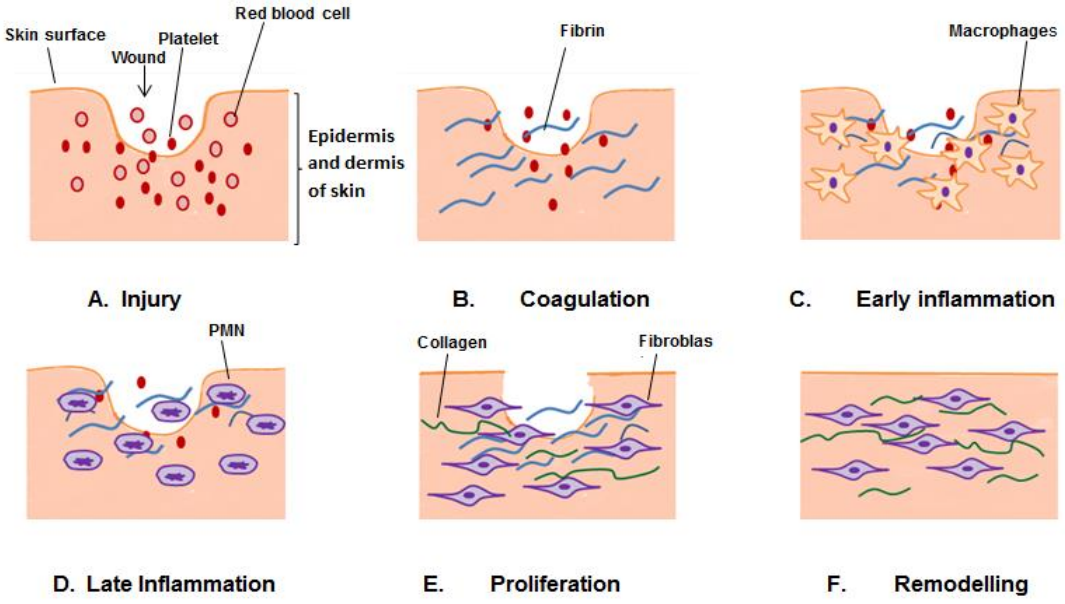

Figure 6.1: Diagram showing the different stages of wound healing process following an injury

6.1.1.1. Coagulation and inflammation

The preliminary response of the body upon occurrence of an injury is bleeding; this process removes bacteria and antigens from the wound site. This bleeding process causes the activation of haemostasis, in which the blood clots and platelets are engaged to form a temporary seal[2]. Simultaneous to the process of haemostasis, the inflammation phase occurs. This phase involves vascular as well as cellular responses. Vasodilation occurs due to the release of exudate, containing histamine and serotonin, allowing macrophages to enter the wound site to remove necrotic tissue. Neutrophils are also activated and begin to clean up the wound site of all foreign particles as well as any bacteria.

6.1.1.2. Migration and Proliferation

The migration phase follows the inflammation stages. This process involves the migration of epithelial cells and fibroblasts to the wound site. Along with the migration phase, the proliferation phase also involves the movement of cells. Extracellular matrix, such as collagen, is produced by fibroblasts allowing migration and cellular adhesion of keratinocytes[3], capillaries and lymphatic vessels. Collagen is an essential component giving the skin its strength and form[4].

6.1.1.3. Maturation and remodelling

The final stage of the wound healing process is the maturation and remodelling phase, involving the re-organisation of extracellular matrix, strengthening the epithelium and forming the connective tissue between cells. This is the stage which governs the final scar formation[4].

6.1.1.4. Abnormal wound healing

Chronic conditions such as diabetic foot ulcers have prolonged inflammation, impaired neovascularisation, a decreased synthesis of collagen, an increased level of protease, and a defective macrophage function, thus are prone to infection. Infection can delay the wound healing process.

6.1.2. Wound management

When managing skin injuries such as a burn, the aim is to achieve wound closure within the shortest period of time. The process of wound management involves several steps, including wound cleansing and debridement, followed by application of a dressing to keep the wound site moist and infection-proof, and promote healing. The wound healing process follows various complex steps, as described in section 6.1.1; disruption of any of these steps can result to delayed wound healing, scar formation and increase chances of infection.

6.1.3. Summary

The wound healing process involves various different stages, proteins and cell types. One of the most important factors in wound management is to minimize

disturbance of the self-healing process. Infection control is a major concern in wound management; faster wound closure and creating a barrier to prevent bacteria from entering the wound site can minimize the possibility of infections. Therefore design of a dressing that can protect the wound from external bacteria from entering as well as encourage faster wound closure, using hydrogels to retain a moist environment and biological material to provide an extracellular matrix for cell growth, would be advantageous.

From the results obtained in the previous section, the 15% TCDA-DS vesicles were chosen for further analysis. In this section, 15% TCDA-DS vesicles were incorporated into various gels selected from previous studies. Two types of prototype systems were examined; gel-block system where vesicles are dispersed in the matrix and a gel-coated fabric system where vesicles dispersed in a gel matrix are coated in fabric.

6.2. Gel-block type wound dressing

Current commercially available wound dressings such as Mepitel™ consist of a layer of hydrogel on a skin-coloured backing. As discussed in Chapter 3 and 4, the 15%TCDA –DS system showed the desired stability and sensitivity in various different conditions and gel matrixes. As a result, thin gel sheets with immobilised vesicles were fabricated and their stability and sensitivity was investigated.

A

B

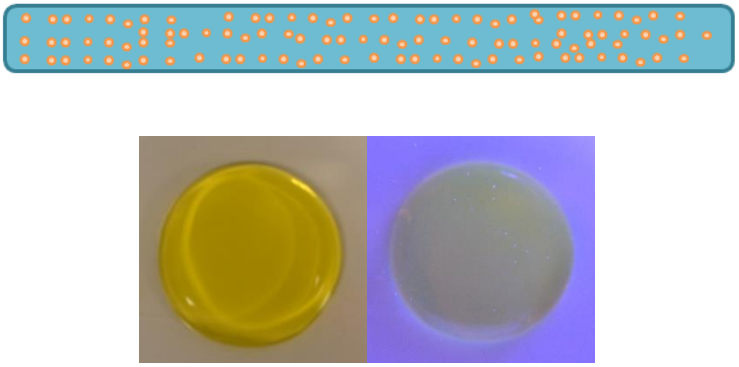

Figure 6.2: A: Cartoon representation of the structure of the gel-block type wound dressing. **B:** Photographic image of the gel-block system under day light (left) and under UV-light (right)

The block-gel forming agents gelatin, agar and agarose were used in this study, and sensitivity assays were carried out using the standard strains of bacteria, *S. aureus* MSSA476, *P. aeruginosa* PAO1 and E. coli DH5α.

6.2.1. Stability and sensitivity of Gelatin based gel-block type wound dressing

The overnight stability and sensitivity of gelatin based gel-block type wound dressing was tested at 37°C. The stability of the gel-block system was tested by incubation in HEPES and non-toxin producing bacterial supernatant, *E. coli* DH5α. The sensitivity of the gel-block system was tested by incubation in the supernatant of *S. aureus* MSSA476 and *P. aeruginosa* PAO1. The photographic image shows the visible change in fluorescence, correlating well with the fluorescence readings.

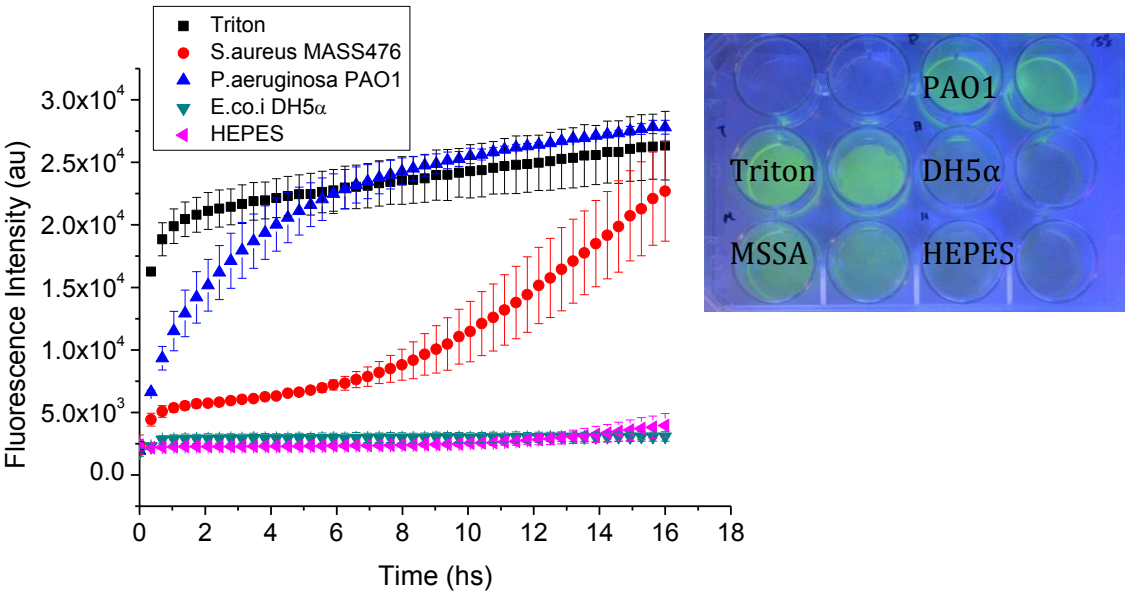

Figure 6.3: Overnight stability and sensitivity study of vesicles in gel-block system. The fluorescence of a 12 well plate was measure in an overnight study. Plot shows responsive vesicles in toxin producing bacterial supernatant, and stable vesicles in HEPES and *E. coli* DH5α.

The gelatin gel-block system displayed a visual colour change following incubation of the system in bacterial supernatant overnight at 37°C. Furthermore, this change was not observed for the negative controls nor for the wells incubated with *E. coli* DH5α (figures 6.3). These visual results were further confirmed by the overnight fluorescence measurements, which presented with an immediate response of vesicles to supernatant of *P. aeruginosa* PAO1 as well as the positive control (Triton X-100) and a gradual increase in fluorescence was shown by treatment with *S. aureus* MSSA 476. The delay response of vesicles in gel to MSSA 476

compared to PAO1 may be due the relatively slow diffusion of δ-toxin compared to rhanmolipid, which is the lysing agent responsible for lysis of membranes found in supernatant of PAO1.

6.2.2. Stability and sensitivity of Agar and Agarose based gel-block type wound dressing

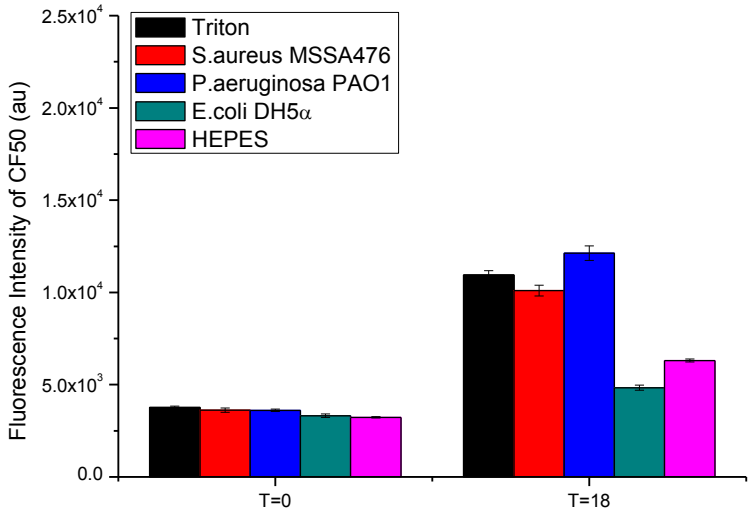

Figure 6.4: Average well scans of before addition of supernatant and after addition of supernatant and incubation at 37°C on agar gel-block systems.

The agar gel-block (figure 6.4) and the agarose gel- block (figure 6.5) type systems show responses to toxin producing bacterial supernatant. However, better stability was observed for the agarose system compared to the agar. Lower initial fluorescence (T=0) was observed for the agarose system in comparison to the agar. Furthermore, the high fluorescence intensity at T=18 of wells containing DH5α supernatant and HEPES for the agar system, can be evidence of leakage or instability of vesicles.

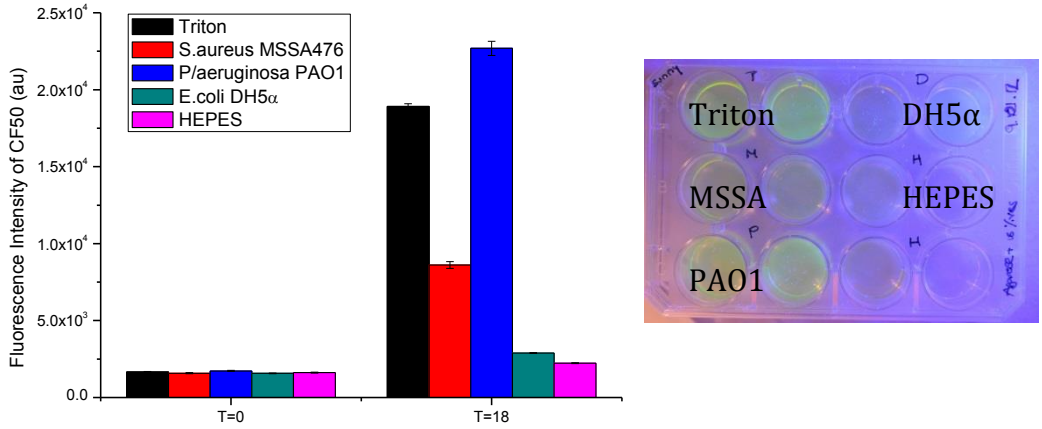

Figure 6.5: Average well scans of before addition of supernatant and after addition of supernatant and incubation at 37°C on agar gel-block systems.

6.2.3. Confocal imaging

A thin layer of the agarose gel-block system was prepared on a glass slide for image studies using confocal microscopy. The concentration of vesicles used was reduced to minimise background fluorescence during imaging, to approximately $1x10^8$ particles mL^{-1} instead of approximately $1x10^{12}$ particles mL^{-1}.

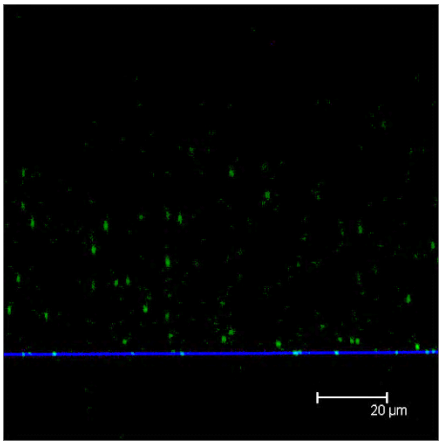

Figure 6.6: Cross section image of Z-stack of a thin layer of agarose gel-block system with vesicles of an approximate concentration of $1x10^8$ particles mL^{-1}.

The confocal cross section image of the gel shows a uniform distribution of single vesicles across the gel (figure 6.6).

With the success of imaging single vesicles in the agarose gel-block system, the lysis and stability of vesicles on addition of toxin-producing bacterial supernatant and non-toxin-producing bacterial supernatants were prepared for imaging The AGR+ *S. aureus* strain, RN6390B and the AGR- *S. aureus* strain RN6911 were used. As well as the AGR +/- strains, a methicillin-resistant *Staphylococcus aureus* (MRSA) strain USA300 (Lac) was also used to image the effect on vesicles.

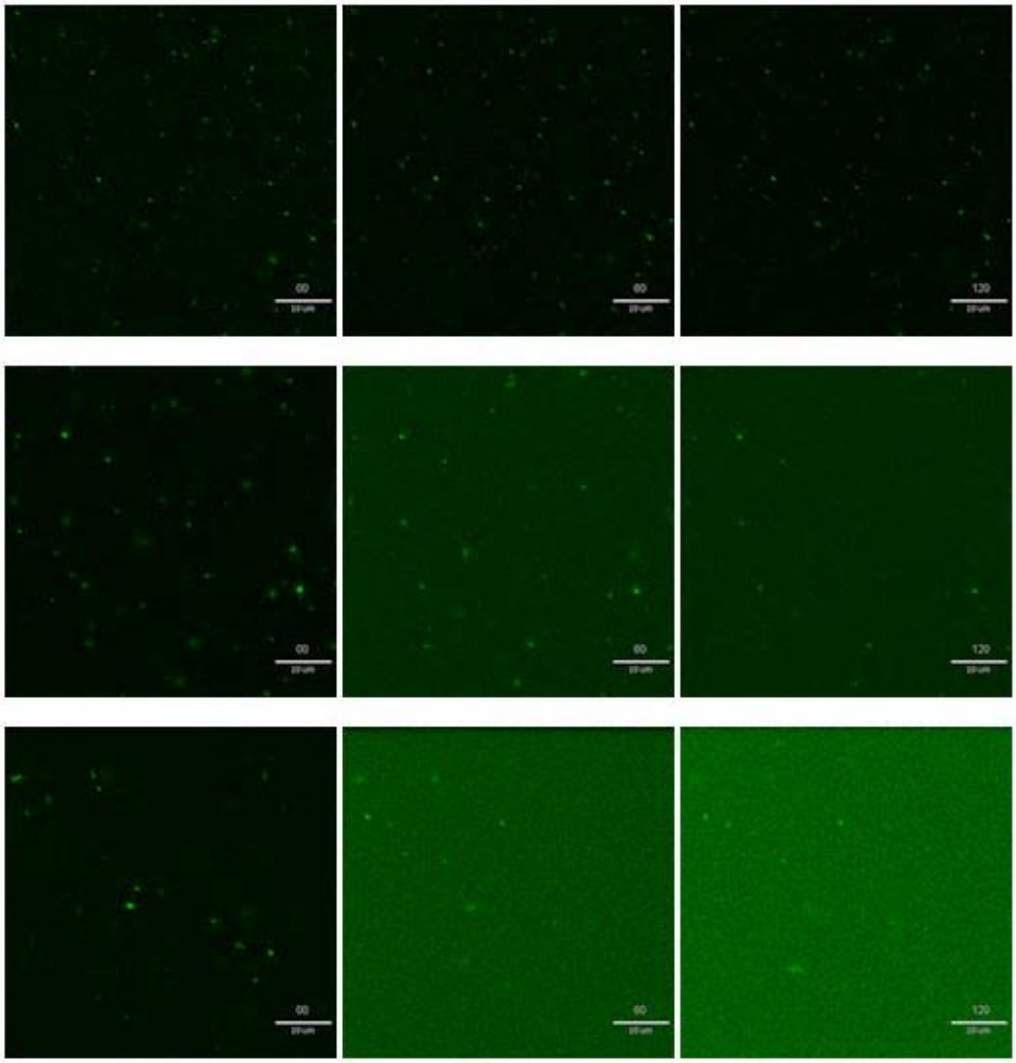

Figure 6.7: Thin layer of 15% TCDA-DS vesicles immobilised in agarose gel matrix confocal images of TCDA-DS vesicles immobilised in agarose gel on glass slide was imaged using confocal. **Top row:** effect of AGR- stain of *S. aureus* RN6911 supernatant on vesicles in gel matrix captured over time, showing no increase in background fluorescence over a 00, 60 and 120s time period. **Middle row:** effect of AGR+ stain of *S. aureus* RN6390B supernatant on vesicles in gel matrix over time, showing increase in background fluorescence within the first 60s. **Bottom row:** effect of *S. aureus* USA300 supernatant on vesicles in gel matrix over time, showing increase in background fluorescence within the first 60s. The scale bar represents 10μm.

The confocal microscopy images (figure 6.7) show that vesicles in the agarose gel system do not respond to supernatant of AGR- strain of *S. aureus* RN6911 within the time frame of 120s. Whereas an immediate increase in background fluorescence can be observed (at 60s), on addition of supernatant of AGR+ stain of *S. aureus* RN6390B. Furthermore, on addition of supernatant of lac USA300, an even larger increase in background fluoresce can be observed at 60s.

6.2.4. Limitations of the gel-block systems

The gel-block system has shown promising results in terms of sensitivity and stability of vesicles though overnight studies, measuring the change in fluorescence intensity. However, some limitations of the gel-block system have been identified.

6.2.4.1. Thickness of gel

The gel-block prototype presented so far have been fabricated by setting 500µL of gel/vesicle mixture into each well of a 12 well plate. Following complete gel formation, the thickness of the gel was measured to approximately 3mm. For the purpose of stability and sensitivity analysis, 500µL of control solution and bacterial supernatants were pipetted on top of the gel-blocks. Following overnight incubations at 37°C, only the vesicles on the top surface of the gel had lysed (figure 6.8). This was thought to be due to two main reasons; concentration of vesicle lysing agent in the bacterial supernatants and/or the slow diffusion rate of the lysing agents.

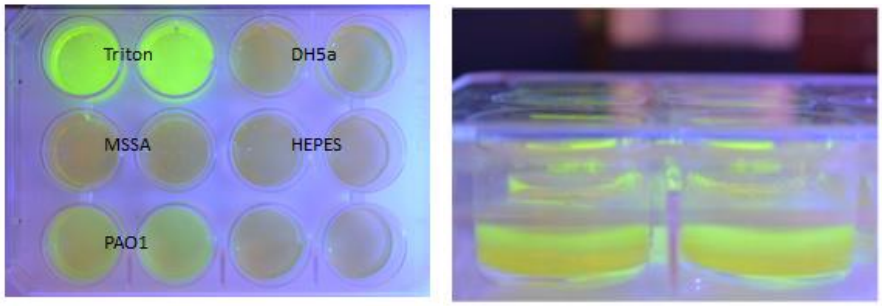

Figure 6.8. The effect of the thickness of gels on the diffusion of toxins from supernatant for lysis of vesicles. The thickness of the gel was measured to be approximately 3mm thick.

In order to overcome this barrier involving the thickness of the gel, a thinner gel block system was produced. However, the thinner gel-block systems were shown to be very fragile and more difficult to manage. Furthermore, dehydration of the gel matrix, causing vesicle lysis, was another major hurdle to overcome.

6.2.4.2. Dehydration effect

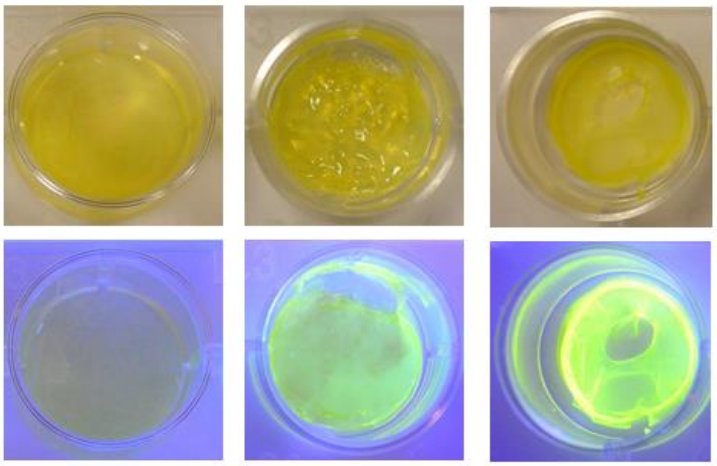

Figure 6.9: Image showing the effect of gel dehydration on stability of vesicles. Top three images were taken under day light and the bottom three images were taken under UV-light.

In addition to the thickness of the gel, dehydration of the gel-block system is a major issue for storage purposes. The image above shows agarose gel-block system stored in a sealed container over a period of 21 days. Images were taken on days 1, 10 and 21. Despite the low temperature and the sealed container, the gel-block system appears to have dried out by day 10, and the change in the colour of the system is visible under UV-light.

6.2.5. Summary of the gel-block system

A number of different gel block systems were developed using three gels that showed formation of block-gels from previous studies reported in Chapter 4. Out of the three gels, the system using agarose showed the most stable and sensitive system to bacterial supernatant. The confocal images show that vesicles responded

to Lac supernatant within 60 seconds of addition of supernatant and unresponsive to AGR- strain over a period of 120 seconds, when a very thin layer of gel was used. However, the block system exhibited slow diffusion of lysing agents when a thick gel system was utilised.

6.3. Gel coated fabric wound dressing

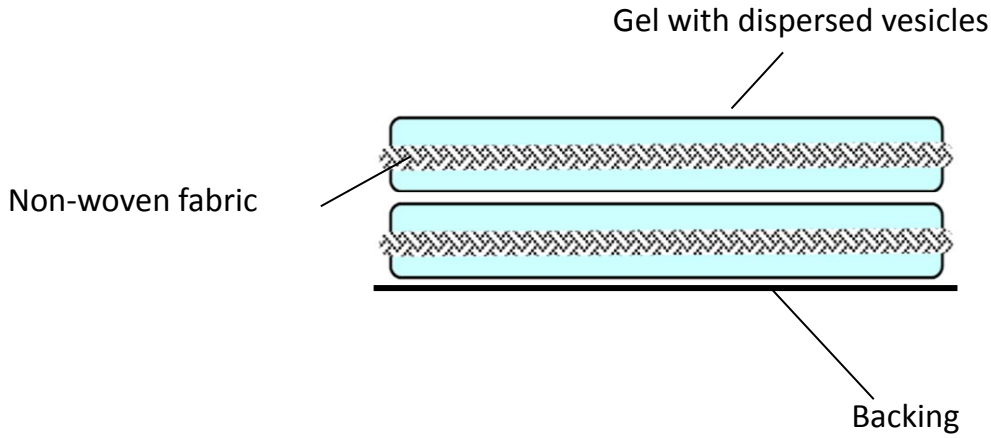

Figure 6.10: Diagram of the gel coated fabric system

The gel coated system was prepared by dip-coating a piece of fabric in the gel/vesicle mixture (2:1 ratio). The coated pieces of fabric were allowed to set at 4°C for at least 30 mins before use. Fresh samples were prepared for each study. Detailed description of the preparation method can be found in section 2.

6.3.1. Choice of Fabric

Non-woven polypropylene fabric was used, to give structural integrity to the gel (figure 6.11). Prior to coating the non-woven in solution of gel, the fabric was treated with isopropanol or ethanol to remove any residual oil from the fabrication process.

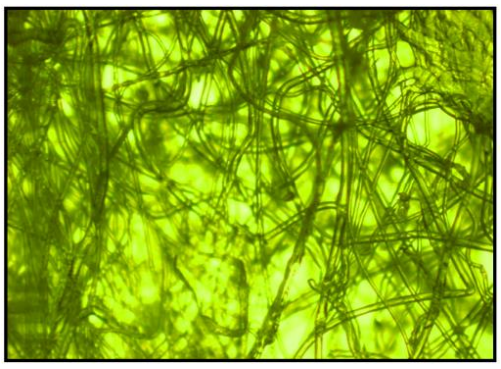

Figure 6.11: Light microscope image of untreated polypropylene fabric. Image acknowledgements: Neil Poulter, University of Bath Ph.D. Thesis, 2010.

6.3.2. Hypromellose coated fabric

Hypromellose is a viscos gel, which does not set to form a block (see Chapter 4 for details); as a result this gel could not be used for the gel-block system. However, it was considered for use in the gel coated fabric system.

The stability and sensitivity of the system was tested by incubation with bacterial supernatant and controls overnight at 37°C.

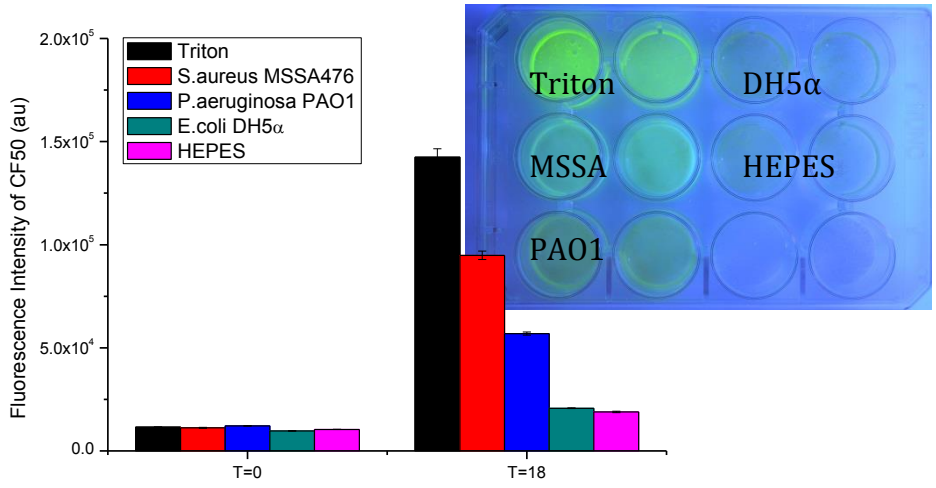

Figure 6.12: Showing average well scans of before addition of supernatant and after addition of supernatant and overnight incubation at 37°C on hypromellose coated systems.

15% TCDA-DS vesicles dispersed in hypromellose system showed stable vesicles in HEPES and *E. coli* DH5α and response to *S. aureus* MSSA476 and *P. aeruginosa* PAO1. These results were detected by fluorescence intensity measurements as well as visual colour difference (figure 6.12), where the wells with lysed vesicles are shown to fluoresce and this fluorescence is not visible where the majority of vesicles are intact.

6.3.3. Agarose/Hypromellose gel coated fabric

The hypromellose gel coated system showed a responsive and stable system, however, due to the viscosity of the gel, the gel did not remain on the fabric during the overnight study. As a result, in an attempt to aid the binding of the gel to the fabric, a gel mixture of agarose and hypromellose was used. The results showed a similar pattern to the pure hypromellose system. The agarose/hypromellose system was both stable and sensitive (figure 6.13). Despite obtaining desired results, due to the low miscibility of the two gels, results were difficult to reproduce.

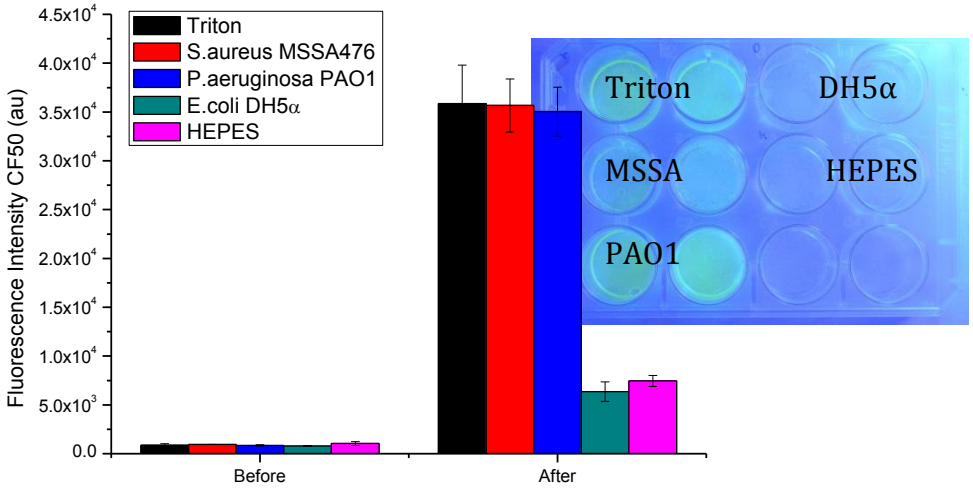

Figure 6.13: Showing average well scans of before addition of supernatant and after addition of supernatant and overnight incubation at 37°C on agarose/hypromellose gel coated systems.

6.3.4. Agarose coated fabric

The agarose/hypromellose mixture system was difficult to reproduce, therefore a pure agarose system was produced and the sensitivity and response was studied. The study using bacterial supernatant showed similar responses to the hypromellose and the agarose/hypromellose mixture systems, showing stability in *E. coli* DH5α , LB and TSB (negative controls), sensitivity to *S. aureus* MSSA476, *P. aeruginosa* PAO1 as well as the control, Triton X100.

Following on from a supernatant study, the agarose coated system was studied for its stability and sensitivity to whole bacteria, in an overnight study.

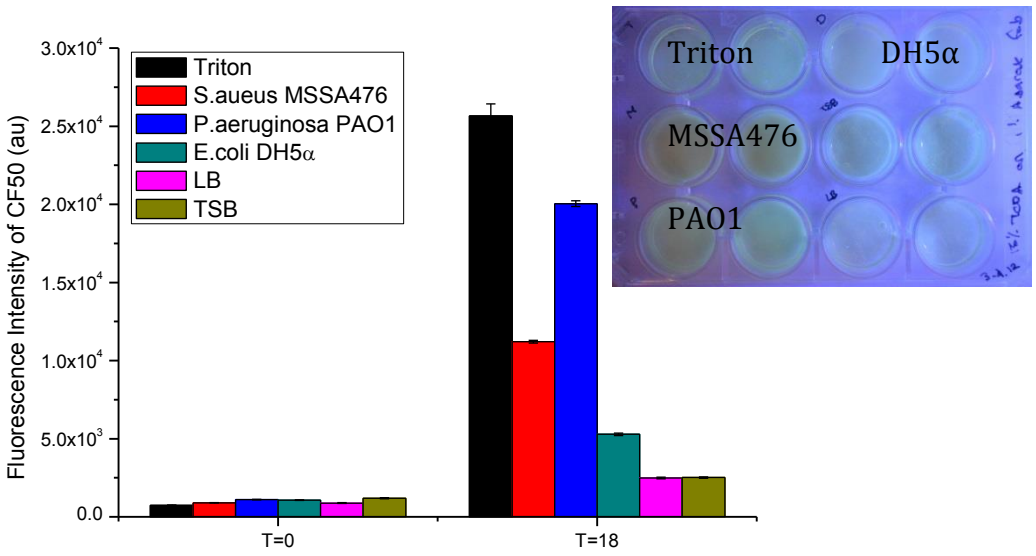

Figure 6.14: Showing average well scans of before addition of overnight bacterial culture and after overnight incubation at 37°C on agarose gel coated systems. Vesicles on the agarose system were shown to be responsive.

,

The results to the overnight study showed the desired response and stability. The subsequent studies involved different strains of bacteria used within the majority of this research. Notably the AGR positive and negative *S. aureus* stains.

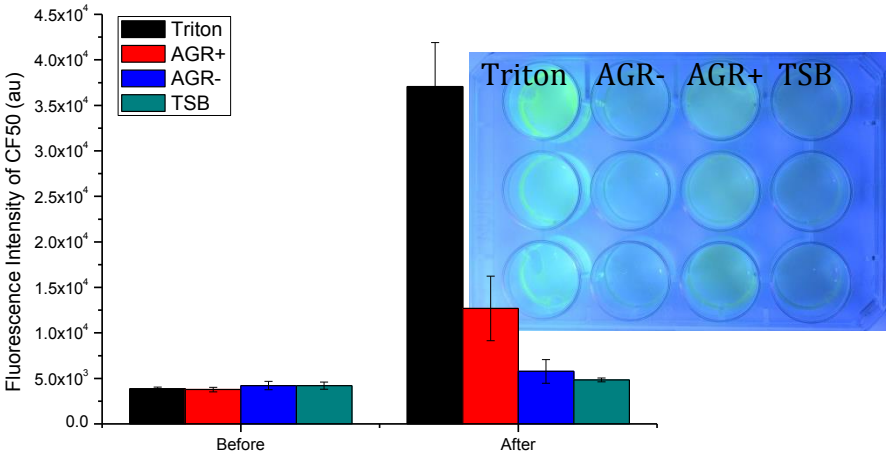

Figure 6.15: Average well scans before addition of overnight bacterial culture and after 18hr of overnight incubation with shaking at 37°C. Vesicles show both fluorescence increase and visible colour change following incubation with AGR+ stain of S. aureus.

6.3.5. Summary of gel-coated fabric system

Various hydrogels were used to create the gel-coated fabric system. Stability and response of the systems were studied. Results show that all systems showed response and stability when incubated with bacterial supernatant overnight. The hypromellose/agarose system showed promising results, however reproducibility of a uniform distribution of the initial gel mixture was low, therefore this system was not selected for further development. The hypromellose system also indicated desirable stability and sensitivity; however, the viscosity of the gel prevented the gel from being bound to the fabric. This required further improvement for physical attachment; as a result, this system was not selected for further studies. The agarose system was selected for further development as this system demonstrated the desirable stability, sensitivity, physical properties and reproducibility results as well as the desirable characteristics for dressing fabrication.

6.4. First Generation Prototype (FGP) wound dressing

The agarose gel coated non-woven polypropylene with 15% TCDA–DS vesicles immobilised system showed most promising results when the data from Chapter 4 and the data presented in this chapter were combined and analysed. As a result, this system was proposed as 'the first generation wound dressing'. The response of this dressing on addition of bacterial supernatants is shown in figure 6.16.

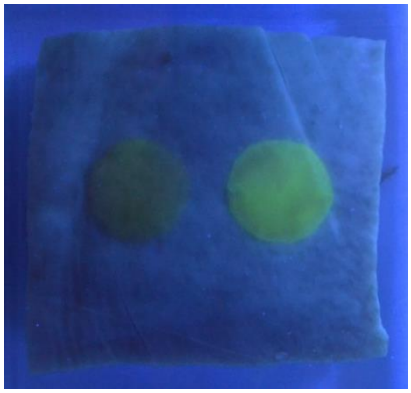

Figure 6.16: Image of prototype dressing with addition of AGR +/- *S. aureus* supernatant on porcine skin

6.4.1. Improving visual response

In order to improve the visual response of the agarose dressing, a higher concentration of vesicle was used to make the initial gel/vesicle mixture. The normal concentration of vesicle solution is approximately $1x10^{12}$ particles mL^{-1}; the higher concentration of the vesicle is approximately $1x10^{36}$ particles/mL. This resulted in the use of a triple concentrated solution, thus translating into three times the number of particles to be lysed within a dressing (figure 6.17).

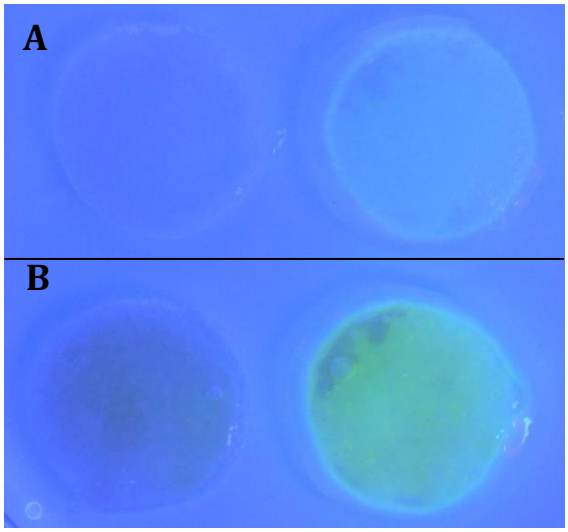

Figure 6.17: A: agarose coated dressing with lower concentration of vesicles, approximately $1x10^{12}$. **B:** agarose coated dressing with higher concentration of vesicles, approximately $1x10^{36}$ (first generation prototype dressing). HEPES buffer was added to the dressings on the left and Triton X-100 to the dressings on the right.

In order to validate the stability and response of the dressings containing the higher concentration of vesicles, an overnight assay was conducted using bacterial supernatant (figure 6.18). Results display a similar pattern of stability and response compared to previous studies involving lower concentration of vesicles. Therefore the higher concentration of vesicles was used in the proceeding studies.

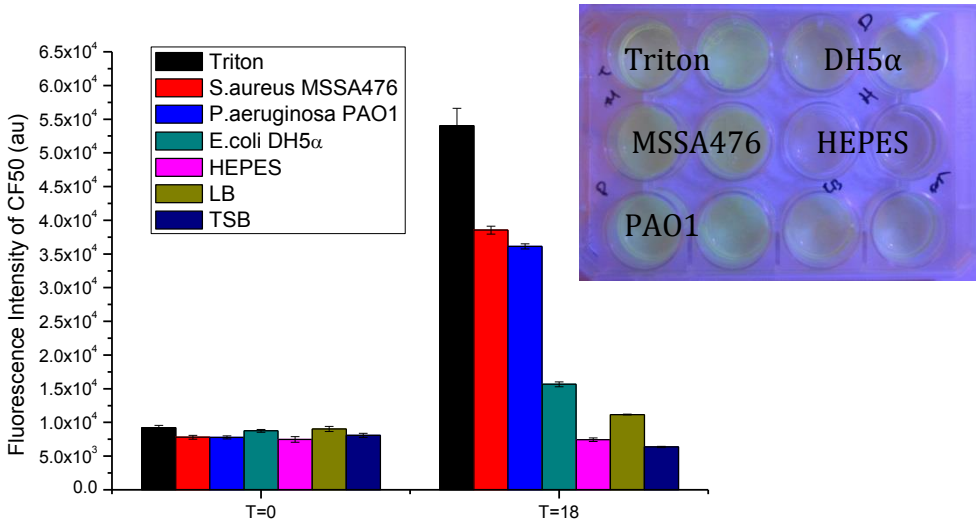

Figure 6.18: Average of well scan following overnight incubation with bacterial culture. Results show responsive and stable vesicles even when a higher concentration of vesicles was incorporated.

6.4.2. Studying the stability of FGP for storage

The stability for storage purposes was tested over a period of 21 days at 4°C. On the 21st day of the study, Triton X100 was added to ensure sensitivity of vesicles following storage. This is shown in figure 6.19, with an SR-parameter value of 13 obtained following 21 day stability assessment at 4°C.

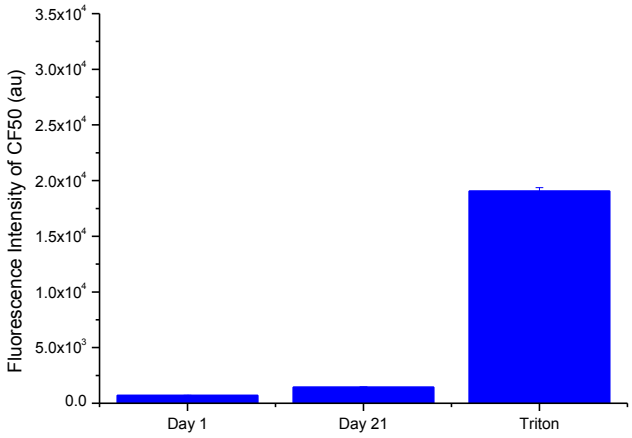

Figure 6.19: Average of well scans on Day 1, Day 21 and following addition of Triton X100 on Day 21. SR-parameter of 13.2 ±0.222

6.4.3. FGP on *ex vivo* skin model

The response and stability of the prototype dressing on skin was tested on porcine as well as human skin obtained from the Bond McIndoe Reseach Foundation.

6.4.3.1. Response of FGP on Porcine skin

Response of FGP dressings on infected porcine tissue was assessed. Two methods were used to conduct this analysis. First, an overnight bacterial culture was directly injected into the tissue sample, without cutting the top layer of the skin; the dressings were placed on top of the skin and incubated overnight. The second method used an opened layer of the tissue sample, where the top epidermal layer was removed, exposing the dermal layer. Overnight cultures were injected into the opened dermal layer; dressings were placed on the surface, and incubated overnight. Both methods showed lysis of vesicles on incubation of *S. aureus* MSSA476 and *P. aeruginosa* PAO1 and stability to controls. Figure 6.19, shows images taken before incubation and after 20 h incubation, displaying fluorescent dressings on tissue samples infected with pathogenic bacteria, and absence of fluorescence on the control. This demonstrates that lysis of vesicles was caused by the pathogenic bacteria and that vesicles in the dressing are stable on porcine tissue over a period of 20 h at 37°C.

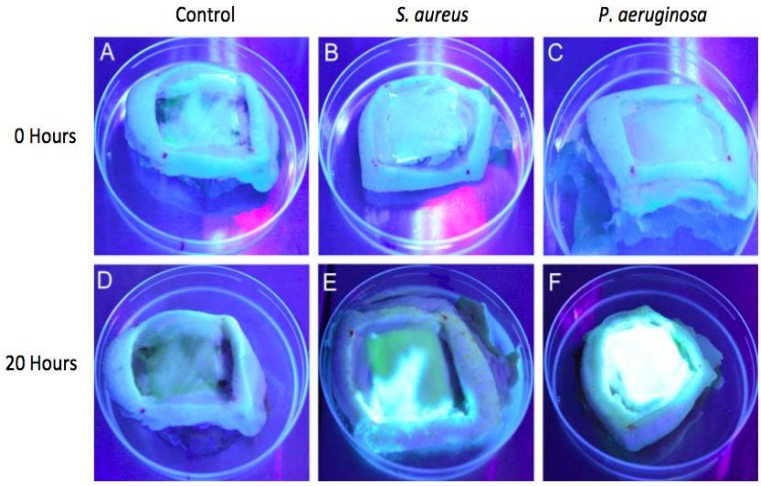

Figure 6.20: image of before incubation and after incubation of FGP dressing on tissue injected with overnight bacterial culture. Acknowledgment: W.D. Jamieson and Maisem Labbei, University of Bath.

6.4.3.2. Response of FGP on Human skin

Fresh human skin, obtained following elective procedures in surgical wards, was used for this study. The skin was washed in 70% ethanol and cut to obtain desired size. The overnight culture was washed in PSB buffer and 500µl of washed culture was injected into the tissue to obtain approximately $5x10^5$ $CFUmL^{-1}$. The FGP dressings were placed on top of the injected tissue and incubated over 20 h at 37°C.

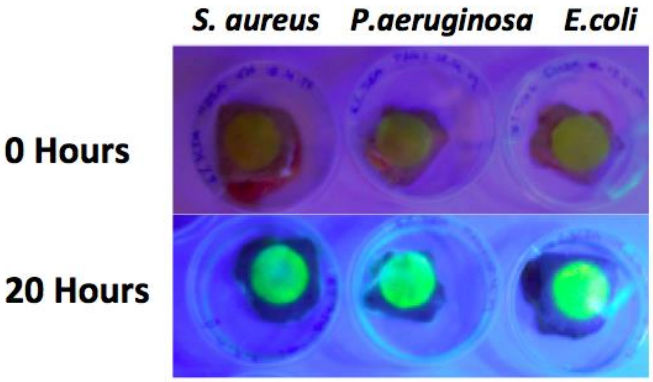

Figure 6.21: image of before incubation and after incubation of FGP dressing on tissue injected with overnight bacterial culture.

The verification of response of the FGP dressing was unsuccessful, as vesicles had lysed on all tissue samples, including non-toxin producing DH5α lysed over the period of 20 h. The instability of vesicles could be due to a number of different reasons; vesicle instability to the proteins present in the tissue sample, contamination of sample with antimicrobials and antiseptic residues left on the skin from the original procedure conducted.

The studies involving animal skin were disregarded for further analysis due to lack consistency of sample collection from the organisation.

6.4.3.3. Estimating the CFU mL^{-1} required for lysis of vesicles

In an attempt to approximate the number of colony forming units required to indicate a change in fluorescence of the prototype dressing, animal skin and flesh samples were used. The prototype dressings were placed on top of pre-infected porcine skin and beef steak models with the three standard bacterial models, *S. aureus* MSSA476, *P. aeruginosa* PAO1 and *E. coli* DH5α. Fluorescence measurements of the dressings were taken at 2, 4, 6 and following 20h incubation at 37°C. This work was carried out by an undergraduate student as part of a final year project at the Department of Chemistry, University of Bath.

Table 6.1 displays the SR-parameter values obtained as well as the corresponding values of the CFU mL^{-1} of bacteria required. The results of the assay carried out on bovine tissue show that in order to obtain an SR-parameter of 10.5 and 12.0 by *P. aeruginosa* PAO1 and *S. aureus* MSSA476 respectably, bacterial concentration in the magnitude of 10^7 CFU mL^{-1} was required. The same assay carried out on porcine tissue showed an SR-value of 50.9 at $5.6x10^5$ CFU mL^{-1}. The results suggest that the dressings can be used to indicate the present of bacterial colonies on animal tissue.

Table 6.1: SR-values and colony forming units

Inoculation Surface	**Inoculation solution**	**SR-Parameter T=20**	**CFU** mL^{-1}
Porcine Tissue	*E. coli* DH5α	22.9	$1.6x10^4$
Porcine Tissue	*S. aureus* MSSA 476	38.3	$8.0x10^6$
Porcine Tissue	*P. aeruginosa* PAO1	50.9	$5.6x10^5$
Porcine Tissue	LB	26.0	No growth
Bovine Tissue	*E. coli* DH5α	1.55	$1.7x10^4$
Bovine Tissue	*S. aureus* MSSA 476	12.0	$4.7x10^7$
Bovine Tissue	*P. aeruginosa* PAO1	10.5	$1.7x10^7$
Bovine Tissue	LB	1.73	No growth

6.5. Second generation prototype (SGP) wound dressing

As previously mentioned in Chapter one and at the beginning of this Chapter, the wound healing property of a dressing is a desirable characteristic, especially for a burn wound. As a result, the FGP dressing was further embellished by addition of a cell growth-enhancing layer to give rise to a second generation prototype wound dressing (SGP).

6.5.1. Collagen based biological dressing

The advantages of using collagen based biological dressings in the management of burns have been shown by previous studies[5,6]. Collagen is an essential component in cellular adhesion and migration within the natural wound healing process.

Collagen is naturally produced by the human body as an extra cellular matrix to aid migration and binding of keratinocytes. Cells have integrin for cell to cell binding as well as cell to extra cellular matrix binding. Collagen contains numerous integrin binding sites for this to occur. As a result the collagen layer on the dressing should theoretically enhance cell migration towards the dressing, and upon migration, encourage cell binding, which in turn should promote further cell migration and thus stimulate closure of the wound by keratinocyte cells.

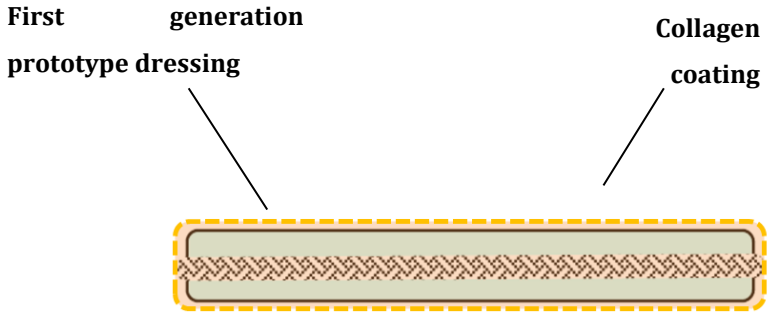

Figure 6.22: Cartoon representation of the prototype dressing

6.5.2. Proposed mechanism of wound healing enhancement by SGP

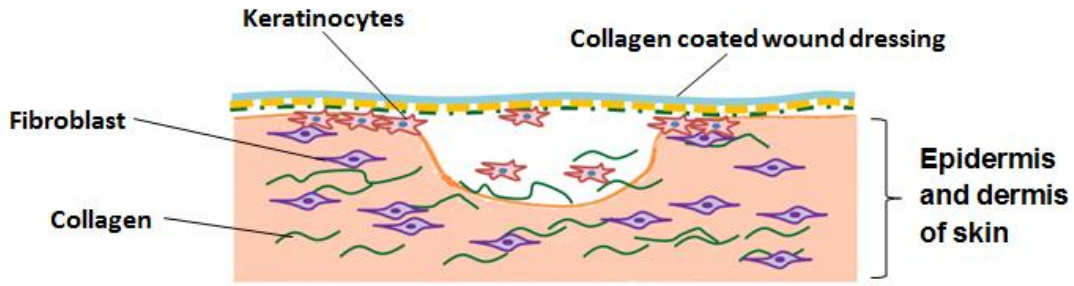

Figure 6.23: Representation of wound healing being promoted by second generation dressing (collagen dressing)

As previously discussed, wound healing occurs from the outer side of the wound site towards the middle. Thus, in larger injuries, the middle of the wound is exposed for a longer period of time hence the chances of infection is increased. The proposed wound dressing acts to enhance wound healing throughout the entire wound bed by means of a collagen coating (figure 6.23).

6.5.3. Experimental results of cell growth on SGP

The cell attachment property and growth property of the SGP dressing was studied using HaCaT and Ea.hy926 cells. The initial attachment was verified by seeding a large cell density onto the wound dressing, followed by 1h incubation and removal of the solution and washing with PBS. In order to assess the growth, media was replenished and the cells were incubated at 37°C with 5% CO_2 over 48s. Following 48h incubation, resazurin assay was used to measure cell respiration. As controls, the same procedure was carried using the FGP dressing and a blank surface (non-adherent to cells) to ensure that growth of cells was due to the collagen and to monitor healthy cell growth.

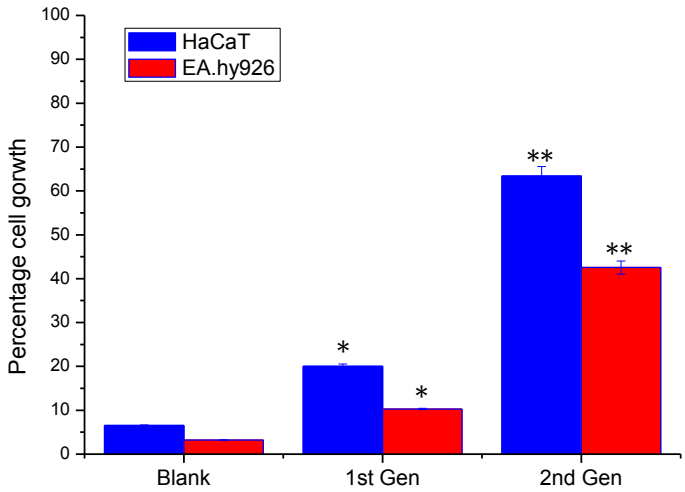

Figure 6.24: Eukaryotic cell growth on black surface (non-adherent to cells), agarose coated fabric and collagen coated agarose coated fabric normalised against maximum cell growth of tissue culture plate. Both HaCaT and Eayh926 cell lines show improved attachment on collagen coated dressing compared to simple agarose coated fabric. Statistical analysis were carried out by a Student's t-test, * P-value > 0.05, **P- value < 0.05

Figure 6.24 displays data indicating that with the additional collagen layer, there was a 65% cell growth observed for HaCaT cells and 42% growth for EA.hy926. Whereas on the FGP dressings, growth of only 20% was observed for HaCaTs, and growth of 10% was identified for EA.hy926 cells. Furthermore, the growth of both types of cells on the blank plates was negligible.

6.6. Conclusion

In this Chapter, two major types of dressing prototypes were looked at, the gel-block system and the gel-coated fabric system. The coated fabric system was favoured over the gel-block system due to the slow diffusion of lysing agents on thick gels and brittle mechanical properties of the thin gels. Out of the several gel-coated systems, the agarose gel was selected due to results showing stability and sensitivity of vesicles as well as reproducibility of these results. The visual response of the agarose-gel coated fabric was improved by the use of higher concentration of vesicles and produced the first generation prototype dressing (FGP). The *in vitro* response of FGP was assessed using infected animal skin models. Furthermore, FGP dressing was further embellished by an additional collagen coating was added, which was shown, by *in vitro* studies, to improve the cell attachment and growth property of the dressing.

6.7. References

1. Schultz, G., Molecular regulation of wound healing. Acute and chronic wounds: Nursing management. 2nd edition. St. Louis, MO: Mosby **1999**, 413-429.

2. Martin, P., Wound healing--aiming for perfect skin regeneration. Science **1997,** 276 (5309), 75-81.

3. Sai K, P.; Babu, M., Collagen based dressings—a review. Burns **2000,** 26 (1), 54-62.

4. Boateng, J. S.; Matthews, K. H.; Stevens, H. N. E.; Eccleston, G. M., Wound healing dressings and drug delivery systems: A review. Journal of Pharmaceutical Sciences **2008,** 97 (8), 2892-2923.

5. Mathangi Ramakrishnan, K.; Babu, M.; Mathivanan, J. V.; Shankar, J., Advantages of collagen based biological dressungs in the management og superficial and and superficial partial thickness burns in children, *Ann Burns Fire Disasters* **2013**, 26(2), 98-104

6. Yang HT, Y. H., Cho YS, Kim D, Hur J, Chun W, Kim JH, Seo CH, Lee BC, Koh JH, Treatment of Deep Second Degree Burn Wound using Heterogenic Type I Collagen Dressing. J Korean Burn Soc **2010,** 13 (2), 3.

Chapter Seven: Post project development

7.1. Conclusions and Future work

The initial aim of this project was to develop a pathogenic bacterial detection system to incorporate into a wound dressing with wound healing properties. This was to be used for management of paediatric burns, where bacterial infection can be lethal.

During the course of this research, a stable in various different pH and temperature ranges as well as in a eukaryotic cellular environment and sensitive to pathogenic bacteria system was developed. The system consisted of 15% TCDA,

20% cholesterol, 2% DSPE and 63% DSPC. This phospholipid based sensor was successfully immobilised and developed in an initial prototype wound dressing (FGP) consisting of a gel coated non-woven polypropylene fabric. This was then further enhanced with an additional collagen coating to yield the final SGP dressing with the potential ability to enhance cell growth, thus promote wound healing.

Although the SGP dressing have shown desirable stability and response, the thickness of the gel and the lack of transparency of the prototype remain as a weakness. As diffusion was the main difficulty involving the gel-block system, the fabric was used as a scaffold for the vesicles embedded hydrogel to increase surface area exposed to pathogenic bacterial supernatant/ toxins. However, the presence of the fabric can block the fluorescence increase, thus the dressing can be improved through the use of a fabric with larger holes, such as woven cotton fabric. Moreover, a gel-block type system can be developed using a high crosslinked hydrogel system with larger pores, allowing for faster diffusion of vesicle lysing agents.

The response of the vesicle to multiple strains of bacteria was tested by other members of the group; however, the response of entire prototype was only carried out on a limited number of pathogenic bacteria. Thus, a detailed analysis of response of the prototype to a wide range of pathogens may be beneficial. Furthermore, the cell growth assays on the SGP dressings were only carried out over a period of 48h, thus only showing the proliferation process of cell. Future work may include extended assay time, to assess the growth of cells on the dressing.

7.2. Demand for new methods to combat/prevent infections

In 2004, there were 11 million burn incidents reported globally; of this population, 153 per 100,000 occurred on children under the age of 15 with 20% TBSA[1]. Globally, approximately 19,000 children are admitted to hospitals every year for treatment of burn injuries[2], and as previously stated, the majority of these injuries are hot liquid scalds. As well as the trauma caused to the patient and their family, the cost of the treatment is tremendous if hospitalisation is required.

7.2.1. Infections and Antimicrobial resistance

As previously stated in Chapter one, one of the main concerns over a burn injury is the risk of development of an infection, which can prove fatal unless the infection is rapidly diagnosed and timely and appropriate treatment administered.

Antibiotics can be prescribed on suspicion of an infected wound; however indiscriminate use of antibiotics has been known to be one of the leading causes of development of antibiotic resistance[3]. Furthermore, the typical treatment of burn infection involves administration of broad spectrum antibiotics, which can add to the build-up of antibiotic resistance.

7.2.2. Economics of development of new antibiotics

The main theme of the World Health Day in 2011 was 'antimicrobial resistance: no action today and no cure tomorrow'[4]. Despite the high demand for new antibiotics, large Pharmaceutical industries have reduced investment into development of new classes of antibiotics due to the supposed lack of return on investment[5]. These low returns are likely caused by the legislated controlled use, in order to minimise further development of antibiotic resistance, but is also related to rapid development of resistance, causing a discontinued use of the newly developed drug[6].

7.3. Health-economics of development of a new dressing

The dressing being developed by this research will not only aid prevention of further development of antibiotic resistance, but also help towards minimising the cost involved in the treatment of burns.

7.3.1. Cost involved in treatment of burns

The South West Paediatric Burn service in Bristol conducted a survey on the cost of treatment of 144 patients admitted with scalds. The cost of treatment of minor burns, affecting less than 10% of total body surface area (TBSA), showed an average cost of £ 1850. The cost involving major scalds, affecting more than 10% TBSA, showed a cost ranging from £55,354.79 to £74,494.24, giving a mean of £63,157.22 per patient. The cost involved arises from long hospital stays, intensive care stays, visits to the operating theatre with general anaesthesia for initial assessment and scrubbing of the wound site, application of biological wound dressings, possible skin grafting, and the use of antibiotics[7]. Besides these, this data does not include the cost of posttraumatic wound and scar management and the multiple visits for physiotherapy required following a major burn[8].

Table 7.1: Shows the average breakdown of costs involved in treatment of a minor burn injury.

Treatment	***Average cost (£)***
Hospital bed	1195
Theatre visit	539
Medication used	2
Dressings used	114
Total	1850

Table 7.1 shows the average cost involved in treatment of paediatric scald as well as the breakdown of the cost. The study was limited minor to less than 10% TBSA

burns and neglected to include the cost of scar management post burn. The average total cost was found to be £1850, of which the majority of the cost involved was due to hospitalisation.[9] Demonstrating that minimising hospitalisation can reduce the cost associated with burn injuries.

7.4. The proposed solution: commercialisation of the prototype dressing

The aim of this research was to develop a novel wound dressing which can signal the presence of pathogenic bacteria by detection of lytic proteins produced by the bacteria, as well as to enhance the healing process of the wound by encouraging cell growth around the injured area. The dressing was designed with the aim to aid wound healing as a result of burns, specifically scalds.

The dressing components have been tested for their potential cytotoxic effects to eukaryotic cells, via *in vitro* analysis, which showed negligible cytotoxic effects. The assessment of stability and sensitivity of the dressing on skin was attempted in an in vitro assay using porcine skin as well as human tissue, however results were inconclusive. As a result, at present, the behaviour of the dressings on infected tissue is yet to be explored.

According to the regulations provided by the Food and Drugs Administration (FDA), a medical device is an instrument which is 'intended for use in the diagnosis of disease or other conditions' as well as affecting the function or the structure of the body. Therefore, the dressing being developed in this study can be classified as a medical device, as it is intended to use for diagnosis of burn infection, by use of bacterial toxin sensitive nanosensors, and intended to affect the structure of the injured body through enhancing the healing process by stimulating cell migration on the surface of the wound.[10]

As the prototype developed in this study can be classified as a medical device, Good Manufacturing Practices have to be followed.

7.4.1. Clinical trials

Clinical trials have to be conducted in accordance with the Helsinki agreements[11] and the FDA's requirements for protection of human subjects; clinical trials

conducted on children have additional safety requirements. Further detail can be found on the FDA information sheets provided by the agency[10,12].

In general pre-clinical studies are conducted on small and large animals prior to conducting trials on human subjects.

7.4.1.1. Pre-clinical phase studies

In order to further assess the wound healing properties of the prototype dressing, the dressings must be tested on real wounds. For this, research using animals has to be conducted prior to conducting clinical assessments on humans. The stability and sensitivity of dressings on porcine, bovine and human skin must be assessed.

7.4.1.2. Pre-clinical Phase studies on small animals

Prior to conducting clinical tests on humans, pre-clinical studies are required to be conducted though a number of different stages. Primarily, pre-clinical in-vivo studies on small animals to evaluate biocompatibility, analysis of the migratory pathways of inflammatory cells and their interaction with bacteria on infected models, and the response of the dressing to bacterial toxins in the presence of inflammatory cells. Mouse and rats are often used for conducting these studies, as they are relatively inexpensive, have a short life-cycle giving rise to collections of reproducible data[13].

7.4.1.3. Pre-clinical Phase studies on large animals

Following studies on small animals, studies on larger animals can provide evidence on safety and effectiveness of the dressing. Pigs have often been used as models to study wound healing effects of dressings. The physiological, anatomical and epidemiological factors of porcine skin have been known to resemble human skin, allowing closely relating outcomes when used as models[14,15,16]. Figure 7.1 shows the comparison of histological features of human and porcine tissue indicating similarities in the thickness of epidermal and dermal layers.

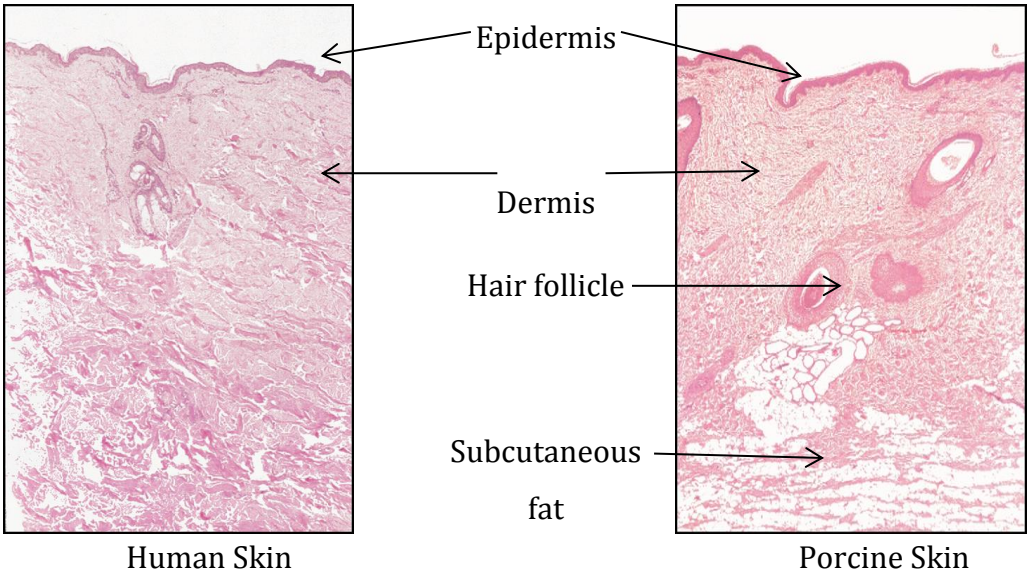

Figure 7.1: Histological features of human and porcine skin. Sections were taken through comparable portions of the dermis of both tissue samples. Images modified from article by Sullivan et al. [14]

Furthermore, Sullivan et al. presented porcine burn models for studying the effect of different methods of treatment on wound healing of burns[17].

The pre-clinical assessments on animals will provide data on biocompatibility of the dressings, data on immune response and the effects on stability and activity of the dressings, effectiveness of the dressing in detecting bacterial toxins in the presence of inflammatory cells, as well as the effectiveness of the collagen layer in aiding the wound healing process.

7.4.1.4. Clinical trials on humans

Upon successful completion of pre-clinical phase studies on animal models, clinical studies on humans can be started. In general, there are four different phases to the clinical trials, phases 1 to 4. Phase 1 investigates the safety of a particular device or drug being developed and phases 2 through to 4 generally examine the efficacy of the product, including the use of placebos for accurate evaluation of effectiveness of the device.

7.5. Summary

In summary, the dressing being developed through this research can be classified as a medical device, used as a diagnostic tool for bacterial infection as well as a material to aid the re-epithelialisation process of wounds. The dressing was initially designed for paediatric scalds; however, it has the potential to be used as a dressing for any type of skin injury with a high risk of development of a bacterial infection.

7.6. References

1. Peck, M. D., Epidemiology of burns throughout the world. Part I: Distribution and risk factors. *Burns* **2011,** *37* (7), 1087-1100.

2. Davies, M.; Maguire, S.; Okolie, C.; Watkins, W.; Kemp, A. M., How much do parents know about first aid for burns? *Burns* **2013,** *39* (6), 1083-1090.

3. Liebowitz, L. D., MRSA burden and interventions. *International journal of antimicrobial agents* **2009,** *34*, S11-S13.

4. Piddock, L. J. V., The crisis of no new antibiotics—what is the way forward? *The Lancet Infectious Diseases* **2012,** *12* (3), 249-253.

5. Nathan, C.; Goldberg, F. M., Outlook: The profit problem in antibiotic R&D. *Nature Reviews Drug Discovery* **2005,** *4* (11), 887-891.

6. White, A. R.; Blaser, M.; Carrs, O.; Cassell, G.; Fishman, N.; Guidos, R.; Levy, S.; Powers, J.; Norrby, R.; Tillotson, G.; Davies, R.; Projan, S.; Dawson, M.; Monnet, D.; Keogh-brown, M.; Hand, K.; Garner, S.; Findlay, D.; Morel, C.; Wise, R.; Bax, R.; Burke, F.; Chopra, I.; Czaplewski, L.; Finch, R.; Livermore, D.; Piddock, L. J. V.; White, T., Effective antibacterials: At what cost? The economics of antibacterial resistance and its control. *Journal of antimicrobial chemotherapy* **2011,** *66* (9), 1948-1953.

7. Pellatt, R. A. F.; Williams, A.; Wright, H.; Young, A. E. R., The cost of a major paediatric burn. *Burns* **2010,** *36* (8), 1208-1214.

8. Mirastschijski, U.; Sander, J.-T.; Weyand, B.; Rennekampff, H.-O., Rehabilitation of burn patients: An underestimated socio-economic burden. *Burns* **2013,** *39* (2), 262-268.

9. Griffiths, H. R.; Thornton, K. L.; Clements, C. M.; Burge, T. S.; Kay, A. R.; Young, A. E. R., The cost of a hot drink scald. *Burns*, 2006; 32 (3), 372-374.

10. Pisano, D. J.; Mantus, D., *FDA Regulatory Affairs: A Guide for Prescription Drugs, Medical Devices, and Biologics*.

11. Robertson, A., Helsinki Agreement and Human Rights. *Notre Dame L.* **1977,** *53*, 34.

12. FDA Regulatory Controls. http://www.fda.gov/MedicalDevices/DeviceRegulationandGuidance/Overview/GeneralandSpecialControls/default.htm (accessed 25/10/13).

13. Kistler, D.; Hafemann, B.; Schmidt, K., A model to reproduce predictable full-thickness burns in an experimental 0animal. *Burns* **1988,** *14* (4), 297-302.

14. Sullivan, T. P.; Eaglstein, W. H.; Davis, S. C.; Mertz, P., THE PIG AS A MODEL FOR HUMAN WOUND HEALING. *Wound Repair and Regeneration* **2001,** *9* (2), 66-76.

15. Meyer, W., The skin of domestic mam-mals as a model for the human skin, with special reference to the domestic pig. *Curr Probl Dermatol* **1978,** *7*, 39-52.

16. Montagna, W.; Yun, J. S., The Skin of the Domestic Pig1. *Journal of investigative dermatology* **1964,** *43* (1), 11-21.

17. Cuttle, L.; Kempf, M.; Phillips, G. E.; Mill, J.; Hayes, M. T.; Fraser, J. F.; Wang, X.-Q.; Kimble, R. M., A porcine deep dermal partial thickness burn model with hypertrophic scarring. *Burns* **2006,** *32* (7), 806-820.